EXPLORING THE FUNCTION OF THE CDK8 MODULE IN *DROSOPHILA*

A Dissertation

by

XIAO LI

Submitted to the Office of Graduate and Professional Studies of
Texas A&M University
in partial fulfillment of the requirements for the degree of

DOCTOR OF PHILOSOPHY

Chair of Committee,	Jun-Yuan Ji
Committee Members,	Vytas Bankaitis
	Sarah Bondos
	Pingwei Li
Head of Department,	Carol Vargas

December 2020

Major Subject: Medical Sciences

ABSTRACT

The Mediator complex, consisting of the head, middle, tail and CDK8 (Cyclin-Dependent Kinase 8) kinase module, is required by almost all the protein coding gene and a variety of non-coding gene transcription in eukaryotic cells. Dysregulation of subunits of the only enzymatic submodule, CKM (CDK8 kinase module), has been linked to diverse human diseases such as cancer. Thus, it is essential to understand the function of CKM in both normal development and tumorigenesis.

To identify interactors of CDK8, we performed a dominant modifier genetic screen in *Drosophila* based on the defects in vein patterning caused by specific depletion or overexpression of CDK8 or CycC in developing wing imaginal discs. We identified the genetic interactions between the CDK8-CycC and the components of the Decapentaplegic (Dpp, the *Drosophila* homolog of TGFβ) signaling pathway, where CDK8-CycC positively regulates transcription activated by Dpp signaling pathway primary transcription factor Mad (Mothers against Dpp).

To understand the roles of the four CKM subunits, we depleted different combinations of the four subunits and identified their antagonistic roles in regulating *Drosophila* eye development, that Med12-Med13 pair is essential for the eye development and depletion CDK8-CycC can partially rescue the defects caused by removal of Med12-Med13. In addition, the asymmetric interdependency of the four subunits was identified.

Finally, we further explore the negative role of CDK8-CycC in regulating SREBP (sterol regulatory element-binding protein). Mutation of CDK8 phosphorylation site on SREBP resulted in stabilized SREBP protein level, stronger binding to chromosome, hyper activation of target gene transcription, and finally more lipid accumulation *in vivo* in *Drosophila*. In addition, we

identified six amino acids from the N-terminal of SREBP is essential for the interaction between CDK8 and SREBP, which could be required by the phosphorylation.

Taken together, this work expands our knowledge of CDK8 or the CKM function *in vivo*, which advances our understanding about their roles in regulating transcriptions in different physiological or pathological contexts.

ACKNOWLEDGEMENTS

I would like to express my sincere gratitude to my committee chair, advisor, Dr. Jun-Yuan Ji, for mentoring and supporting throughout my graduate study and research. His guidance helped me to learn basic skills of fly genetics when I started my research, to learn designs of experiments when I gradually conducted my research by my own and finally to learn presentations of the results when I wrapped up my stories in talks or manuscripts. I am extremely grateful for his patient and wise guidance, which polished every single corner of my research skills.

I would also like to thank my committee members, Dr. Vytas Bankaitis for his criticisms and practical suggestions to optimize and supplement my studies, Dr. Sarah Bondos for her kind guidance on writing and critical suggestions on experimental design, and Dr. Pinwei Li for important advices and for teaching me the basis of structural biology and providing the opportunity to try a set of biochemistry experiments in his lab.

Thanks to former Ji lab members, especially Dr. Xiaojun Xie and Dr. Fu-Ning Hsu for sharing their experience on cell biology and biochemistry with me.

Thanks to my current lab mates, Rajitha Udakara Sampath Hemba Waduge, Dr. Mengmeng Liu, and Ye Niu for the support on my experiments and for the discussions which benefits my research a lot.

Thanks to the friendly fly community, especially our collaborators, Dr. Jian-Quan Ni in Tsinghua University, China and Dr. Dr. Henri-Marc Bourbon, Université de Toulouse, France, for providing us important reagents and fly lines.

Thanks also go to my friends and colleagues and the department faculty and staff in Molecular and Cellular Medicine Department for making my time at Texas A&M University a great experience.

Thanks to the Texas A&M University high performance research computing system (HPRC) for computational resources and systems administration to conduct this research.

Finally, thanks to my parents for their encouragement and to my wife for her patience, love and technical support on bioinformatic analysis.

CONTRIBUTORS AND FUNDING SOURCES

Contributors

This work was supervised by a dissertation committee consisting of Dr. Jun-Yuan Ji (chair), Dr. Vytas Bankaitis, Dr. Sarah Bondos of Molecular and Cellular Medicine Department and Dr. Pingwei Li of Biochemistry and Biophysics Department.

Part of the genetic tests in Chapter II, summarized in Fig. II.3G and H and Table B.II.1 are contributed by Dr. Qun Wang. Images in, Fig. II.3H, 3I and Fig. A.II.9 are generated by Rajitha Udakara Sampath Hemba Waduge and Dr. Mengmeng Liu. Analysis in Fig. A.II.1 was performed by Stephen H. Yu. The knocking down lines of different combinations of CKM, *Med12-EGFP* and *Med13-EGFP* are provided by Dr. Jian-Quan Ni in Tsinghua University, China.

All other work included in the dissertation was completed by the student independently.

Funding Sources

This work was supported by AHA, NIDDK, NIGMS, and NCI to the Ji lab.

TABLE OF CONTENTS

Page

Page

LIST OF FIGURES

Page

Page

LIST OF TABLES

Page

CHAPTER I

INTRODUCTION*

Composed of up to 30 conserved subunits, the Mediator complex plays critical roles in modulating RNA polymerase II (Pol II)-dependent gene expression by functioning as a molecular bridge linking transcriptional activators and the general transcription machinery in almost all eukaryotes [1-5]. Biochemical purification of the human Mediator complex has revealed the Cyclin-Dependent Kinase 8 (CDK8) module (CKM), composed of CDK8 (or its paralogue CDK19, also known as CDK8L), CycC, Med12 (or Med12L), and Med13 (or Med13L), and the small Mediator complex, composed of 26 subunits that are divided into the head, middle, and tail modules [6-9]. The CKM can inhibit the transcription through the interaction between the CKM and the small Mediator complex. In addition, the CKM can function as a kinase to phosphorylate different substrates to modulate specific transcription processes differently. Both roles of the CKM highlight its fundamental function in regulating transcription, which is the first step of gene expression, and dysregulation of the CKM subunits are correlated to a variety of human diseases, such as cancers [10-14].

I.1. Pathological relevance of the CDK8 module in human cancers

A recent cBioPortal analysis with 40199 tumor samples showed that one or multiple genes among CDK8, CDK19 or CCNC (gene encodes CycC in human) are amplified in different types of tumor samples, namely, prostate neuroendocrine cancers (19.6%), castration-resistant prostate cancers (18.6%), tubular stomach adenocarcinoma (5%), dedifferentiated liposarcoma (4.8%), bladder/urinary tract cancer (4.11%), colon adenocarcinoma (3.9%), intestinal type stomach adenocarcinoma (3.7%), rectal adenocarcinoma (3.6%), and breast invasive ductal

carcinoma (3%) [15]. Consistently, a large percentage of CDK8 amplification was identified in colon cancer from other studies based on different patient samples, 47% (N=123) in one study [16] and 70% (N=470) in another report [17]. In addition, a meta-study of Affymetrix HGU array data, based on samples from 3491 breast cancer patients, has revealed that higher CDK8 expression was correlated with shorter survival rates in breast cancer patient [18]. In the same study, the cBioPortal analysis revealed several subunits of CKM expression, CDK8 (2%), CDK19 (3%), CCNC (2%), and Med13 (11%), are amplified in 968 breast cancer samples [18].

Opposite to these amplifications of CDK8/CDK19, CCNC, or Med13 as described above, mutations (instead of amplification) of Med12 have been observed in 3% of the same 968 breast cancer samples. Furthermore, somatic MED12 mutations were identified in exon 1 and exon 2, particularly the highly conserved codon 44 in exon 2, in nearly 70% of uterine leiomyomas [19]. The prevalence of *MED12* mutations, either missense changes or in-frame indels, in uterine leiomyomas has been subsequently confirmed by many groups across countries, including Australia [20], Austria [21], Brazil [21, 22], China [23-25], Finland [26-29], France [30], Germany [31], Japan [32], Iran [33, 34], Italy [35], Netherlands [36], Rassia [37], Saudi Arabia [38], South Africa [19], South Korea [39, 40], Spain [41], and the United States [42-49]. As summarized in Table I.1, MED12 gene is mutated in approximately 62% of 3445 uterine leiomyoma samples that were analyzed, regardless of the race or ethnicity of the patient. In addition to MED12 mutations, several recurrent mutations have been revealed in uterine leiomyomas, including rearrangements of high mobility group AT-hook 1 and 2 (HMGA1 and HMGA2), biallelic inactivation of fumarate hydratase (FH), and deletions in collagen type IV α5 and type IV α6 (COL4A5-COL4A6) [29, 50, 51]. Mutations of these genes occur in a mutually exclusive manner, with the MED12 mutations representing the most frequent genetic alteration

in uterine leiomyomas [29, 50-52]. Moreover, somatic MED12 mutations were also identified in nearly 15% of 218 uterine leiomyosarcomas samples analyzed [21, 25, 28, 30, 32, 36, 44, 53, 54].

Table I.1 The prevalence of MED12 mutations in uterine leiomyomas across countries.

Author and year of publication	The nationality of the patients	Number of patients	Number of samples	# with *MED12* mutations	% with *MED12* mutations
Mäkinen et al., 2011	Finland	80	225	159	70.7
Mäkinen et al., 2011	South Africa	18	28	14	50.0
Je et al., 2012	South Korea	53	67	35	52.2
Perot et al., 2012	France	NA	9	6	66.7
McGuire et al., 2012	the United States	NA	148	100	67.6
Markowski et al., 2012	Germany	50	80	47	58.8
Matsubara et al., 2013	Japan	NA	55	39	70.9
Ravegnini et al., 2013	the United States	NA	19	3	15.8
de Graaff et al., 2013	Netherlands	NA	19	11	57.9
Heinonen et al., 2014	Finland	28	164	138	84.1
Bertsch et al., 2014	the United States	134	178	133	74.7
Schwetye et al., 2014	the United States	NA	28	15	53.6
Di Tommaso et al., 2014	Italy	NA	36	12	33.3
Zhang et al., 2014	China	NA	40	30	75.0
Halder et al., 2015	the United States	135	143	92	64.3
Shahbazi, et al., 2015	Iran	NA	23	11	47.8
Wang et al., 2015	China	NA	181	93	51.4
Sadeghi et al., 2016	Iran	NA	103	32	31.1
Mehine et al., 2016	Finland	NA	94	34	36.2
Osinovskaya et al., 2016	Rassia	NA	122	63	51.6
Liegl-Atzwanger et al., 2016	Austria	15	20	9	45.0
Wu et al., 2017	China	NA	362	158	43.6
Heinonen et al., 2017	Finland	244	763	599	78.5
Mäkinen et al., 2017	Finland	NA	65	37	56.9
Lee et al., 2018	South Korea	NA	60	40	66.7
Mello et al., 2018	Brazil	56	69	34	49.3
Galindo et al., 2018	Spain	NA	20	15	75.0
Jamaluddin et al., 2018	Australia	14	65	39	60.0
Hayden et al., 2018	the United States	NA	40	30	75.0
Park et al., 2018	the United States	76	219	121	55.3
Total		**903**	**3445**	**2149**	**62.4**

Note: Case reports with less than 5 cases or samples analyzed were not included in this Table. NA: not available.

Taken together, in different type of cancers, the CKM subunits are dysregulated differently, suggesting that the CKM subunits may play distinct roles in a variety of biological contexts.

I.2. Potential roles of CDK8 in different types of human cancers

Several studies focused on different type of cancers or cell lines suggest that CDK8 may function as an oncogene. For example, depletion of CDK8 eliminates the higher cell proliferation caused by hyperactivation of beta-catenin in colon cancer cells. On the contrary, overexpression of CDK8 can induce immortal murine fibroblasts (NIH 3T3) focus formation. These observations suggest that gain of CDK8 is sufficient to promote tumorigenesis of colorectal cancers [16].

Similarly, CDK8 also acts as an oncogene during the progression of malignant melanoma. It was reported that the histone variant macroH2A (mH2A) inhibits malignant melanoma progression and that loss of mH2A leads to increased expression of CDK8, which promotes the proliferation of the melanoma. Importantly, depletion of CDK8 in the cancer cells can suppress the effect caused by reduction of mH2A level, indicating oncogenic effects of CDK8 in melanoma. Gain of CDK8 in BxPC-3 cells, a pancreatic cancer cell line, increases the cell migratory, invasion capability and proliferation [55].

More recently, inhibition of CDK8 by selective CDK8/19 inhibitor, Senexin A, decreased transcriptional activity of ER (Estrogen receptor) in T47D-ER/Luc cells [56]. Similarly, knocking down of CDK8 in BT474-shCDK8 cells or knocking out of CDK8 in BT474-CRSIPR-CDK8 cells suppressed estrogen-dependent transcription. Furthermore, applying another CDK8/19 inhibitor, fulvestrant, or a combination of two inhibitors, fulvestrant and Senexin B, significantly reduce tumor volume in mice bearing MCF7 xenograft tumor, which suggests that

CDK8 may also act as an oncoprotein in breast cancer, and that CDK8 may be required by ER-dependent tumor growth [56].

Because of these discoveries, there is a considerable interest in developing drugs targeting the CDK8 kinase for cancer treatment in recent years [57, 58]. However, exactly how amplification of CDK8 in these cases contribute to tumorigenesis remains further addressed. Thus, it is essential to reveal the function and regulation of CDK8 activity in different developmental, physiological, and pathological contexts.

I.3. CDK8 and other CKM subunits functions

The CKM has been proposed to function in two modes. First, it can reversibly bind with the small Mediator complex to form the large Mediator complex, thereby physically blocks the interaction between the small Mediator complex and the general transcription machinery. Second, CDK8 can function as a kinase that phosphorylates different substrates, particularly transcriptional activators such as E2F1 [59, 60], N-ICD (intracellular domain of Notch) [61], p53 [62], Smad proteins [63, 64], SREBP (sterol regulatory element-binding protein) [65], and STAT1 (signal transducer and activator of transcription 1) [66].

For example, E2F1 can directly interact with CDK8 and be phosphorylated at Serine 375 by CDK8 [60]. Depletion of CDK8 reduced S375 phosphorylation level and elevated E2F1 targets, such as p73 and CTNNBIP1 expression level in both SW480 and HCT-116 cells. Conversely, ectopic expression of CDK8 in HCT116 cell line increases the phospho-S375 E2F1 and decreases p73 and CTNNBIP1 expression level. Taken together, CDK8 is not only sufficient but also required for E2F1 S375 phosphorylation and for playing as a negative regulator of E2F1 dependent transcription [67]. These results are consistent with the genetic interactions between CDK8 and E2F1 observed in *Drosophila*. Specifically, reducing CDK8 can strongly suppress the

phenotypes caused by depleting E2F1, a key transcription factor that regulates the G1 to S phase cell-cycle transition [68]. These results suggest that CDK8 can indirectly regulate cell-cycle progression by directly inhibiting E2F1-dependent transcription.

Another example is that CDK8 can also directly interact with Mastermind (MAM), which forms a transcription factor complex with Notch-ICD and CBF1 to activate target genes expression [69]. This indirect interaction between CDK8 and Notch-ICD through MAM allows CDK8 to phosphorylate Notch-ICD, resulting the degradation of Notch-ICD. This work also represent an elegant example illustrating how CDK8 serves as a negative regulator of gene transcription [69].

In addition, CDK8 phosphorylates STATs and causes different alterations of different IFN-γ induced genes. Flavopiridol treated HepG2 cells or mouse fibroblasts with depletion of CDK8 showed reduced phosphorylation of STAT1 at serine 727 and tyrosine 701. Mutating STAT1 serine 727 to alanine abolished the recruitment of STAT1 to IFN-γ target genes loci in IFN-γ treated MEFs. In addition, microarray analysis revealed that nearly half of 256 IFN-γ-induced genes were altered in mutant cells comparing with WT cells [66].

Besides these two major functions of CDK8 or CKM as a physical block or a kinase module, some of the CKM subunits were also reported to have unique functions. For example, Med12 and Med13 were reported to be required by Wnt signaling targets transcription. Somatic homozygous clones of Med12 or Med13 mutation in *Drosophila* wing imaginal discs, abolished expression of Wnt signaling target genes, such as *Dll (Distal less)* and *Sens (Senseless).* Immunoprecipitations results suggests that Med12 and Med13 may interact with Lgs/Arm/TCF complex to function as a molecular bridge between this transcription factor complex and the small Mediator complex for the target genes transcription [70].

Taken together, CDK8 or the other three CKM subunits function differently depend on different physiological or pathological context. Thus, it is important to further investigate the function of CDK8 or the CKM *in vivo* to understand how the CKM contributes to tumorigenesis.

I.4. Summary

To extend the knowledge of the CKM subunits function, it is important to identify the upstream regulators and downstream effectors of CKM. In this work, I have been using *Drosophila* as a model system for the following reason: First, the CKM subunits and many other regulation networks are highly conserved but much simpler in *Drosophila.* Second, there are a variety of genetic tools available and genetic manipulation is convenient and faster comparing with mammalian system. Third, short life cycle of *Drosophila* allows large scale tests.

To study the function and regulation of CDK8-CycC in an unbiased manner, we conceived and performed a genetic screen looking for factors that can genetically interact with CDK8-CycC *in vivo*. As described in Chapter 2, we identified components from Dpp (Decapentaplegic)/TGFβ (Transforming Growth Factor-β) signaling pathway can consistently modify the unique phenotypes caused by altering CDK8-CycC. With further cellular level tests, we concluded the positive role of the CKM subunits and four other small Mediator complex subunits in regulating Dpp downstream transcription factor, Mad (Mother against dpp) regulated transcription.

In Dpp signaling transduction, the CKM subunits all serve as positive regulator for Mad dependent transcription and may function as a complete complex. However, previous observation suggests the four subunits may play distinct roles in *Drosophila* eye, leg and thorax development [71]. In addition, it remains poorly understood how the four CKM subunits regulate each other. To understand the regulation and interplay among the four subunits of CKM, we

generated RNAi *Drosophila* lines to deplete different combinations of the CKM subunits. As summarized in Chapter3, we observed antagonistic impacts on eye development by depleting different combinations of the CKM subunits and distinct functions of pairs of the subunits CDK8-CycC and Med12-Med13 on cell proliferation. In addition to the different roles of the CKM subunits in development, the four subunits are asymmetrically interdependent to each other.

Besides the role the CKM in regulating development, CDK8-CycC was also found playing critical roles in regulating lipid metabolism [65]. In Chapter 4, I present our work analyzing the role of CDK8 in regulating lipogenesis in *Drosophila*. Previously, we have reported that CDK8 or CycC mutants increased the fat accumulation caused by increased expression of important enzymes for fatty acid synthesis, which are activated by SREBP. Further biochemistry analysis suggests that CDK8 may negatively regulate SREBP protein stability through phosphorylation of T402 [72]. As summarized in Chapter 4, this phosphorylation is likely dependent on the physical interaction between CDK8 and SREBP through N-terminal AA36-41 of SREBP. To test the *in vivo* biological consequences of this phosphorylation, I generated overexpression lines of wild type SREBP and phospho-mutant form SREBP and analyses of these two lines suggest that the phospho-mutation stabilize SREBP level, enhance its chromosome binding, target transcription and is more potent in lipid accumulation.

These characterized functions of CDK8 and the CKM highlight their fundamental roles in regulating transcription. Firstly, I have validated and extended our understanding of Mad dependent transcription *in vivo*, which suggests that several but not all of the Mediator complex subunits are required in regulating Mad-dependent gene expression, the final output for TGFβ signaling in a variety of biological and pathological contexts. Secondly, I have observed distinct

roles of the four CKM subunits in regulating *Drosophila* eye development and cell proliferation. Taken together with their asymmetric interdependency, these complicated regulations may leave insights on explanations of different amplifications or mutations of the four subunits function in different pathological contexts, especially in different types of cancers. Finally, I validated the role of CDK-CycC in negatively regulating SREBP *in vivo* and extended the knowledge of the interaction basis of the two proteins.

Taken together, the four CKM subunits are asymmetrically interdependent on each other and function differently in different biological contexts. Depletion of Med12-Med13 causes severe developmental defects and they are required by gene expressions, while CDK8-CycC modulate different transcription factors activity in different manner dependent on the phosphorylation.

CHAPTER II

THE MEDIATOR CDK8-CYCLIN C COMPLEX MODULATES WING VEIN PATTERNING IN *DROSOPHILA* BY STIMULATING MAD-DEPENDENT TRANSCRIPTION**

II.1 Introduction

Composed of up to 30 conserved subunits, the Mediator complex plays critical roles in modulating RNA polymerase II (Pol II)-dependent gene expression by functioning as a molecular bridge linking transcriptional activators and the general transcription machinery in almost all eukaryotes [1-5]. Biochemical purification of the human Mediator complex has revealed the Cyclin-Dependent Kinase 8 (CDK8) module, composed of CDK8 (or its paralogue CDK19, also known as CDK8L), CycC, Med12 (or Med12L), and Med13 (or Med13L), and the small Mediator complex, composed of 26 subunits that are divided into the head, middle, and tail modules [6-9]. CDK8 is the only Mediator subunit with enzymatic activities. The CDK8 kinase module (CKM) has been proposed to function in two modes. First, it can reversibly bind with the small Mediator complex to form the large Mediator complex, thereby physically blocking the interaction between the small Mediator complex and the general transcription machinery (notably with RNA Pol II itself). Second, CDK8 can function as a kinase that phosphorylates different substrates, particularly transcriptional activators such as E2F1 [59, 60], N-ICD (intracellular domain of Notch) [61], p53 [62], Smad proteins [63, 64], SREBP (sterol regulatory element-binding protein) [65], and STAT1 (signal transducer and activator of transcription 1) [66]. These characterized functions of CDK8 highlight fundamental roles of the CKM in regulating transcription.

Besides its roles in specific developmental and physiological contexts, the CKM subunits are dysregulated in a variety of human diseases, such as cancers [10-14]. For example, CDK8 has been reported to act as an oncoprotein in melanoma and colorectal cancers [16, 55, 59]. Moreover, CDK8 and CDK19 are overexpressed in invasive ductal carcinomas, correlating with shorter relapse-free survival in breast cancer [73]. Gain or amplification of CDK8 activity is sufficient in driving tumorigenesis in colorectal and pancreatic cancers in human, as well as in skin cancer in fish [16, 63, 74-76]. Because of these discoveries, there is a considerable interest in developing drugs targeting the CDK8 kinase for cancer treatment in recent years [57, 58]. However, exactly how CDK8 dysregulation contributes to tumorigenesis remains poorly understood. Thus, it is essential to reveal the function and regulation of CDK8 activity in different developmental, physiological, and pathological processes.

The major bottleneck for addressing these critical gaps in our knowledge is the lack of in vivo readouts for CDK8-specific activities in metazoans. We overcame this challenge by generating tissue-specific phenotypes caused by varying CDK8 activities in *Drosophila*. After validating the specificity of these phenotypes using genetic, molecular, and cell biological approaches, we performed a dominant modifier genetic screen to identify factors that interact with CDK8 in vivo based on these unique readouts for CDK8-specific activities. From the screen, we identified Dad (Daughters against dpp), which encodes an inhibitory Smad in the Dpp (Decapentaplegic)/TGFβ (Transforming Growth Factor-β) signaling pathway, as well as additional components of the Dpp signaling pathway including dpp, tkv (thickveins, encoding the type I receptor for Dpp), Mad (Mothers against dpp) and Medea (encoding the Smad1/5 and Smad4 homologs, respectively) in *Drosophila*. Consistent with the previous biochemical analyses suggesting that CDK8 may phosphorylate *Drosophila* Mad or human Smad1 [63, 64,

77], thereby regulating their transcriptional activities [63, 64, 77], our results have validated and further advanced our understanding of this conserved regulatory mechanism in vivo. Furthermore, our analyses have revealed additional Mediator subunits and protein kinases involved in regulating the Mad/Smad-dependent transcription. These results, together with previous studies, suggest that concerted recruitment of the Mediator complexes and other cofactors play a pivotal role in regulating Mad/Smad-dependent gene expression, a critical process for TGFβ signaling to function in a variety of biological and pathological contexts.

II.2 Material and methods

II.2.1 Fly strains

Flies were raised on a standard cornmeal, molasses and yeast medium, and all genetic crosses were maintained at 25˚C. The *UAS-Cdk8*$^{+}$ and *UAS-Cdk8*^{KD} lines were generated using the pUASt vector [71]. The construct allowing conditional expression of a kinase-dead CDK8 form (D173A; [78]) was generated through site-specific mutagenesis by double PCR, using the overlap extension method. The *UAS-Cdk8-RNAi* and *UAS-CycC-RNAi* lines were generated using the pVALIUM20 vector [79], and the *UAS-Cdk8-RNAi CycC-RNAi* line was generated using the pNP vector [80]. The *vgQE-lacZ* line was received from Gary Struhl [81, 82].

We obtained the following strains from the Bloomington *Drosophila* Stock Center: *ap-Gal4* (BL-3041), *nub-Gal4* (BL-25754), *sal-lacZ* (BL-11340), *UAS-Cdk7-RNAi* (BL-57245), *UAS-Cdk9-RNAi* (BL-34982), *UAS-CycT-RNAi* (BL-32976), *UAS-dpp-RNAi* (BL-33618), *UAS-2xEGFP* (BL-6874), *UAS-erk-RNAi* (BL-34744), *UAS-Mad-RNAi* (BL-31315), *UAS-Mad-RNAi* (BL-43183), *UAS-Medea-RNAi* (BL-43961), *UAS-rl-RNAi* (BL-34855), *UAS-sgg-RNAi* (BL-38293), *UAS-yki-RNAi* (BL-34067), and all deficiency (*Df*) lines (Table B.II.1). Of the two transgenic RNAi lines targeting *Mad*, the BL-31315 line (Fig. A.II.4B/A.II.4B', Fig. II.6B)

generated stronger effects than the BL-43183 line when expressed using the *ap-Gal4* driver. In addition, we tested the following mutant alleles of the Dpp signaling pathway: *Dad^{j1E4}/TM3, Sb^{1}* (BL-10305), *Dad^{MI04922}/TM3 Sb^{1}, Ser^{1}* (BL-37913), *dpp^{d6}/CyO* (BL-2062), *dpp^{hr92}/SM6a* (BL-2069), *dpp^{s11}/CyO* (BL-2065), *Mad$^{1-2}$/CyO* (BL-7323), *Mad^{12}/CyO* (BL-58785), *Mad$^{8-2}$/CyO* (BL-7324), *Mad^{k00237}/CyO* (BL-10474), *Mad^{KG00581}/CyO* (BL-14578), *Medea^{1}/TM3 Sb^{1}, Ser^{1}* (BL-9033), *Medea^{13}/TM3 Sb^{1}* (BL-7340), *tkv^{7}/CyO* (BL-3242), and *tkv^{k16713}/CyO* (BL-11191).

The following RNAi stocks, generated by the *Drosophila* TRiP project [79], were used to deplete the subunits of the Mediator complex: *UAS-Med1-RNAi* (BL-34662), *UAS-Med4-RNAi* (BL-34697), *UAS-Med6-RNAi/TM3 Sb^{1}* (BL-33743), *UAS-Med7-RNAi* (BL-34663), *UAS-Med8-RNAi* (BL-34926), *UAS-Med9-RNAi* (BL-33678), *UAS-Med10-RNAi* (BL-34031), *UAS-Med11-RNAi/TM3 Sb^{1}* (BL-34083), *UAS-Med12-RNAi* (BL-34588), *UAS-Med13-RNAi* (BL-34630), *UAS-Med14-RNAi* (BL-34575), *UAS-Med15-RNAi* (BL-32517), *UAS-Med16-RNAi* (BL-34012), *UAS-Med17-RNAi* (BL-34664), *UAS-Med18-RNAi* (BL-42634), *UAS-Med19-RNAi* (BL-33710), *UAS-Med20-RNAi* (BL-34577), *UAS-Med21-RNAi* (BL-34731), *UAS-Med22-RNAi* (BL-34573), *UAS-Med23-RNAi* (BL-34658), *UAS-Med24-RNAi* (BL-33755), *UAS-Med25-RNAi* (BL-42501), *UAS-Med26-RNAi* (BL-28572), *UAS-Med27-RNAi* (BL-34576), *UAS-Med28-RNAi/TM3 Sb^{1}* (BL-32459), *UAS-Med29-RNAi* (BL-57259), *UAS-Med30-RNAi/TM3 Sb^{1}* (BL-36711), and *UAS-Med31-RNAi* (BL-34574).

To facilitate the dominant modifier genetic screen and the subsequent analyses, we generated the following strains using the standard *Drosophila* genetics: "*w^{1118}; nub-Gal4>UAS-Cdk8^{+}/CyO*" (i.e., "*nub>Cdk8^{+}/CyO*" line), "*w^{1118}; nub-Gal4; UAS-Cdk8-RNAi*" (i.e., "*nub>Cdk8-i*" line), "*w^{1118}; nub-Gal4; UAS-CycC-RNAi*" (i.e., "*nub>CycC-i*" line), "*w^{1118}; nub-*

Gal4; UAS-Cdk8-RNAi CycC-RNAi" (i.e., "*nub>Cdk8-i CycC-i*" line), and "w^{1118}*; ap-Gal4, sal-lacZ/T(2:3)*".

For the *Df* lines in the X chromosome, we crossed *Df* female virgins with males of with the "*nub>Cdk8*$^{+}$*/CyO*", "*nub>Cdk8-i*", "*nub>CycC-i*", or "*nub>Cdk8-i CycC-i"* stocks. For the *Df* lines in the second and third chromosomes, the *Df* males were crossed with female virgins of the afore-described stocks carrying the CDK8-specific phenotypes. The control crosses were performed using w^{1118} males and female virgins. For each of these crosses, the wing vein patterns in ~10 F1 females without any balancer chromosomes were inspected under dissecting microscopes for potential dominant modifications. With few exceptions (Table B.II.1), the wing vein phenotypes and dominant modifications are generally stereotypical with high penetrance. For instance, we crossed *Df(1)BSC531,* w^{1118}*/FM7h* female virgins with "w^{1118}*/Y; nub>Cdk8*$^{+}$*/CyO*" males, and then scored F1 females with the following genotype: "w^{1118}*, Df(1)BSC531/* w^{1118}*; nub>Cdk8*$^{+}$*/+*". Similarly, we crossed "w^{1118}*; nub-Gal4; UAS-Cdk8-RNAi*" female virgins with "*Df(2R)Exel6064/CyO*" males, and then scored F1 females with the following genotype: "w^{1118}*/+; nub-Gal4/Df(2R)Exel6064; UAS-Cdk8-RNAi/+*". *Df* lines that caused lethality in F1 were considered as the enhancers.

II.2.2 Adult Drosophila wing imaging

The wings from adult females were dissected onto slides, briefly washed using isopropanol, and then mounted in 50% Canada balsam diluted in isopropanol. Images were taken under 5X objective of a microscope (Leica DM2500) and then processed by Adobe Photoshop CS6 software.

II.2.3 Immunocytochemistry

Wing discs from third instar larvae at the late wandering stage were dissected and fixed in 5% formaldehyde at room temperature for 30 minutes. After rinsing with PBS-Triton X-100 (0.2%), the samples were blocked in PBS-Triton X-100-NGS-BSA (PBS+0.2% Triton X-100+5% Normal Goat Serum+0.2% Bovine Serum Albumin) at room temperature for one hour. For immunostaining of *Drosophila* CDK8 and CycC, we used anti-dCDK8 (1:2000) and anti-dCycC (1:2000) antibodies [83-85], diluted in PBS-Triton X-100-NGS-BSA. Expression of the *lacZ* reporter expression was detected using an anti-β-galactosidase monoclonal antibody (1:50 in PBS-Triton X-100-NGS-BSA; obtained from the Developmental Studies Hybridoma Bank, DSHB-40-1a-s). C-terminal phosphorylated Mad (equivalent sites to human Smad3 S423+S425) was detected by anti-pSmad3 (1:500 in PBS-Triton X-100-NGS-BSA; purchased from Abcam, ab118825). Wing discs were incubated with these primary antibodies overnight at 4˚C on a rotator. After rinsing with PBS-Triton X-100, the discs were then incubated with the fluorophore conjugated secondary antibodies: goat anti-guinea pig (106-545-003), goat anti-mouse (115-545-003), or goat anti-rabbit (111-545-003) (all purchased from Jackson Immunological Laboratories). These secondary antibodies were diluted 1:1000 in PBS-Triton X-100-NGS-BSA, and incubated with the samples for one hour at room temperature. Discs were then stained with 1 μM DAPI at room temperature for 10 minutes, rinsed two more times with PBS-Triton X-100, and mounted in the Vectashield mounting media (Vector Laboratories, H-1000). Confocal images were taken with a Nikon Ti Eclipse confocal microscope system, with images processed using the Adobe Photoshop CS6 software.

Quantification of anti-β-galactosidase was performed with Nikon NIS software and Microsoft Excel: a single section of the wing discs was selected for the following quantification

based on the DAPI channel, which indicates the cell nucleus are on the same focal plat. Three lines around 50μm long, 10-15μm apart, were drawn along the dorsal-ventral boundary. The line-scan profile of intensity for each line was calculated along each line (Fig. A.II.5A, A.II.5B; genotype: *ap-Gal4, sal-lacZ/+; UAS-Cdk8-i/+*). The area below the intensity index profile represents the Sal-lacZ expression levels along the line (Fig. A.II.5B). To obtain the average intensity of dorsal or ventral compartment, the dorsal or ventral compartment index area was divided by the dorsal or ventral length of the line (Fig. A.II.5C). The intensity for three lines was normalized and averaged in dorsal and ventral compartments (Fig. A.II.5C, Fig. A.II.5D). Following this approach, five wing discs for each genotype were analyzed to quantify the expression of Sal-lacZ in dorsal and ventral compartments, and statistical significance was calculated using Student's one-tailed *t*-test (Fig. A.II.5E).

To validate the afore described quantification method, we also measured the signaling intensity by selecting 20x20μm squares in the dorsal and the ventral compartments of the same wing disc using the Nikon NIS software (Fig. A.II.6A, A.II.6B; genotype: *ap-Gal4, sal-lacZ/+; UAS-Med15-i/+*). We then calculated the dorsal to ventral ratios of the signal intensities of three different discs (Fig. A.II.6B), followed by statistical analyses using the Student's one-tailed *t*-test (Fig. A.II.6C, A.II.6D). We obtained similar results to the quantification based on the line profiles as described above.

II.2.4 GST-pull down assay

Full-length CDK8 fused with a N-terminal GST tag was described previously [71]. The primers *Mad-5.1* (F: 5'-caccATGGACACCGACGATGTGGA-3') and *Mad-3.3* (F: 5'-ctaTTAGGATACCGAACTAATTG-3') were used for full-length Mad (AA1-455), *Mad-5.1* and *Mad-3.1* (F: 5'-ctaCGGGAGCACCGGACTCTCCA-3') were used for a "Mad-N1" fragment

(AA1-150) that contains MH1 domain (AA10-133), *Mad-5.1* and *Mad-3.2* (F: 5'-ctaATCCTCCGAGGGACTGTAGG-3') were used for the "Mad-N2" fragment (AA1-230) that contains the MH1 domain and part of the linker region, *Mad-5.2* (F: 5'-caccatgCCAGTACTCGTTCCTCGCCA-3') and *Mad-3.3* were used for the "Mad-C2" fragment (AA151-455) that contains the MH2 domain (AA255-455) and part of the linker region, and *Mad-5.3* (F: 5'-caccatgGGCAACTCCAACAATCCGAA-3') and *Mad-3.3* were for the "Mad-C1" fragment (AA231-455) that contains the MH2 domain. These coding sequences were amplified from a cDNA clone of the *Mad* gene (LD12679) using PrimeStar Max premix (Takara, R045A). The amplified products were inserted into the pENTR/D-TOPO vector (ThermoFisher, K240020) and recombined into the pDEST17 vector (N-terminal 6XHis tag) using the Gateway LR Clonase II Enzyme mix (ThermoFisher, 11791100) in *E. coli* strain DH5α. The constructs were transformed to *E. coli* strain Rosetta for protein expression using standard protocols.

GST or GST-CDK8 was purified with Glutathione Sepharose 4B (GE Healthcare, 17-0756-01) beads with standard purification protocol. After a final wash, the buffer was replaced by the GST pull-down buffer (20mM Tris-HCl pH 7.5, 10mM $MgCl_2$, 100mM NaCl, 1mM DTT, 0.1% NP-40). His-tagged Mad fragments were extracted from the pull-down buffer by sonication. 50μL GST or GST-CDK8 coated beads (0.5-1μg protein) was mixed with 500μL of Mad fragments cell lysate and incubated at 4˚C for 3 hours. These samples were then washed with 1mL pull-down buffer at 4˚C for 5 times, 1 minute each. The interaction was detected by Western Blot with the primary antibody, anti-His (1:3000; Sigma, H1029), and the secondary antibody, anti-mouse (1:2000; Jackson Immunological Laboratories, 115-035-174).

II.2.5 Yeast two-hybrid (Y2H) assay

Full-length CDK8 was amplified from a pBS-CDK8 cDNA clone using primers *CDK8-5.1* (F: 5'-caccATGGACTACG ATTTCAAGAT-3') and *CDK8-3.1* (F: 5'-TCAGTTGAAGCGCTGGAAGT-3'), and then inserted into the pENTR/D-TOPO vector. The Gateway LR Clonase II Enzyme mix was used to recombine CDK8 cDNA into the pGADT7-GW (prey) vector, a gift from Yuhai Cui (Addgene plasmid # 61702) [86]. The linker region of Mad was amplified with *Mad-5.2* and *Mad-3.2* primers from a cDNA clone of the *Mad* gene (LD12679) using PrimeStar Max premix and inserted into the pENTR/D-TOPO vector. All pENTR Mad fragments were recombined into the pGBKT7-GW (bait) vector, a gift from Yuhai Cui (Addgene plasmid # 61703) [86], using the Gateway LR Clonase II Enzyme mix. The Y2H assay was performed using the AH109 yeast strain, as described previously [86].

II.2.6 Statistical analysis

Standard deviation and Student's one-tailed *t*-tests were performed using Microsoft Excel. Statistical significance (* $p<0.05$; ** $p<0.01$; *** $p<0.001$) was shown in figures and all error bars indicate standard deviation.

II.3 Results

II.3.1 Wing vein patterning defects caused by varying the levels of CDK8, CycC, or both

To study the function and regulation of CDK8 and CycC *in vivo*, we have generated transgenic lines to either deplete them by RNA interference (RNAi) or conditionally overexpress the wild-type CDK8 kinase using the Gal4-UAS system [87, 88]. Normal *Drosophila* wings display stereotypical vein patterns, consisting of six longitudinal veins, dubbed L1 to L6, and

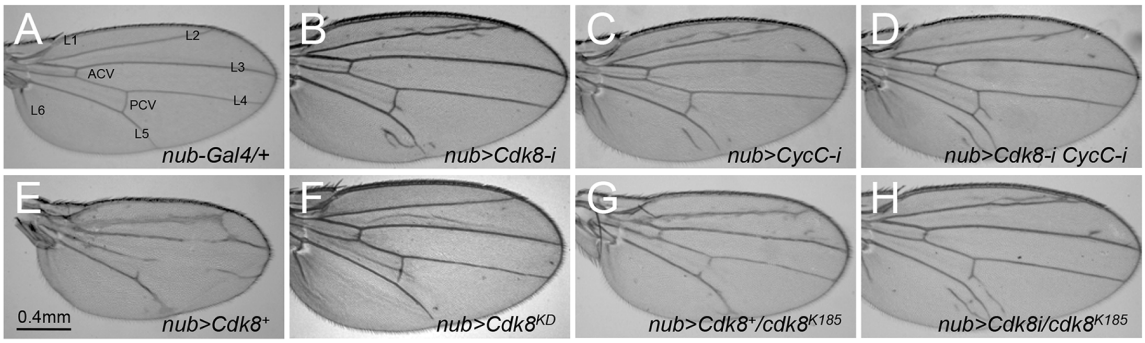

Fig. II. 1 Wing vein patterning defects caused by varying the levels of CDK8, CycC, or both. Adult female wings of (A) *nub-Gal4/+* (control), note the longitudinal veins L1-L6, anterior crossvein (ACV), and posterior crossvein (PCV); (B) w^{1118}*/+; nub-Gal4/+; UAS-Cdk8-RNAi/+*; (C) w^{1118}*/+; nub-Gal4/+; UAS-CycC-RNAi/+*; (D) w^{1118}*/+; nub-Gal4/+; UAS-Cdk8-RNAi CycC-RNAi/+*; (E) w^{1118}*/+; nub-Gal4>UAS-*$Cdk8^{+}$*/+*; (F) w^{1118}*/+; nub-Gal4/UAS-*$Cdk8^{KD}$; (G) w^{1118}*/+; nub-Gal4>UAS-*$Cdk8^{+}$*/+; *$cdk8^{K185}$; and (H) w^{1118}*/+; nub-Gal4/+; UAS-Cdk8-RNAi/*$cdk8^{K185}$.

two crossveins, the anterior crossvein and the posterior crossvein (Fig. II.1A). Knocking down of CDK8 using the *nubbin-Gal4* line (*nub-Gal4*) (see Materials and Methods for details), which is specifically expressed in the wing pouch area of the wing imaginal discs [89], results in the formation of ectopic veins in the intervein region, especially around L2 and L5 (Fig. II.1B). Similar phenotypes were observed with the depletion of CycC (Fig. II.1C) or both CDK8 and CycC (Fig. II.1D). In contrast, overexpression of wild-type CDK8 (*UAS-*$Cdk8^{+}$) disrupts the L3 vein, the L4 vein, and the crossveins (Fig. II.1E), opposite to the phenotypes caused by depleting CDK8, CycC, or both. However, overexpression of a kinase-dead (KD) CDK8 form (*UAS-*$Cdk8^{KD}$) using the same approach does not affect the vein patterns (Fig. II.1F), suggesting that the effects of CDK8 on vein phenotypes are dependent on the kinase activity of CDK8. These observations show that CDK8 and CycC are involved in regulating the vein patterning in *Drosophila*.

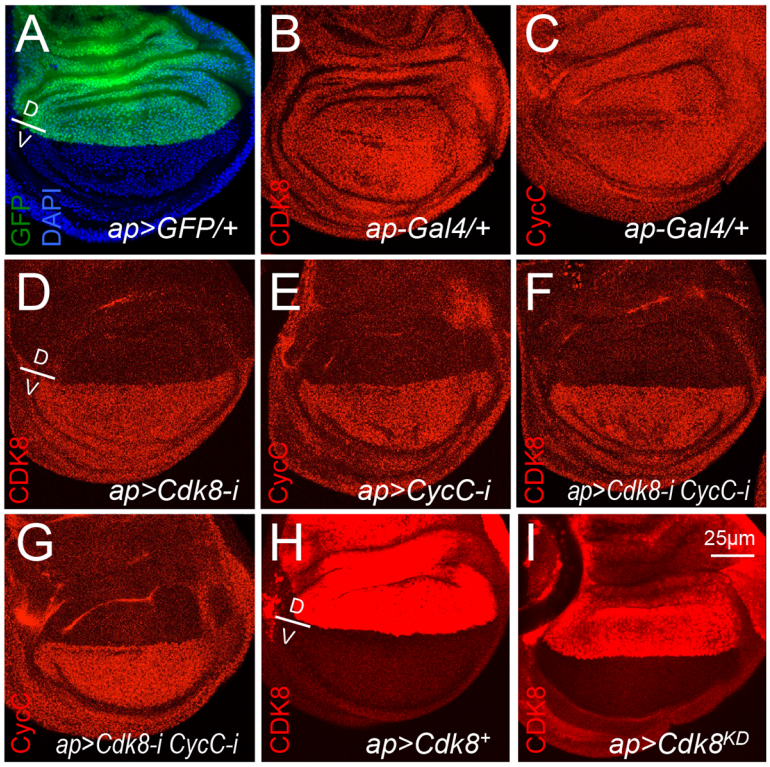

Fig. II.2 Validation of the specificity of the vein defects caused by depletion or overexpression of CDK8-CycC. Representative confocal images of the wing pouch area of a L3 wandering larval wing disc: (A) *ap-Gal4/UAS-2XGFP* with DAPI (blue) and GFP (green); (B) *ap-Gal4/+* with anti-CDK8 (red) staining; (C) *ap-Gal4/+* with anti-CycC (red) staining; (D) *ap-Gal4/+; UAS-Cdk8-RNAi/+* with anti-CDK8 (red) staining; (E) *ap-Gal4/+; UAS-CycC-RNAi/+* with anti-CycC (red) staining; (F) *ap-Gal4/+; UAS-Cdk8-RNAi CycC-RNAi/+* with anti-CDK8 (red) staining; (G) *ap-Gal4/+; UAS-Cdk8-RNAi CycC-RNAi/+* with anti-CycC (red) staining; (H) *ap-Gal4/UAS-Cdk8*$^{+}$ with anti-CDK8 (red) staining; and (I) *ap-Gal4/UAS-Cdk8*^{KD} with anti-CDK8 (red) staining. Note that the gain for confocal imaging in H and I is lower than the others to avoid over saturation of the signals. At least five wing discs were examined for each genotype. The dorsal/ventral (D/V) boundary is shown in A, D and H. Scale bar in I: 25μm.

Interestingly, depletion of CDK8 (Fig. II.1B), CycC (Fig. II.1C), or both (Fig. II.1D) increase the size of the wings, correlating to a significant increase of total cell numbers but a reduction of cell sizes (Fig. A.II.1). In contrast, overexpression of wild-type CDK8 reduces the size of wings and total cell numbers, but no obvious effects on cell size (Fig. II.1E and Fig. A.II.1). The effects of CDK8 on wing size can also be visualized using *ap-Gal4* (*apterous-Gal4*),

which is specifically expressed within the dorsal compartment of the wing discs (Fig. II.2A) [90]. *Ap-Gal4*-induced depletion of CDK8 and CycC caused the adult wing to curl downwards (Fig. A.II.2C), indicating the overgrowth of the dorsal compartment compared to the ventral compartment; while overexpression of CDK8 led to the adult wing to curve upwards (Fig. A.II.2D), suggesting reduced growth of the dorsal compartment. We have previously reported that CDK8 inhibits the transcriptional activity of E2F1, a key transcription factor that controls the expression of factors required for the G1 to S-phase transition of the cell cycle [59, 60]. Thus, the effects of CDK8 levels on wing size and cell numbers are likely through E2F1-regulated cell-cycle progression.

II.3.2 Validation of the specificity of the vein defects caused by depletion or overexpression of CDK8-CycC

To verify the specificity of these phenotypes, we recombined the *nub-Gal4* line with the CDK8-RNAi, CycC-RNAi, or CDK8-overexpression lines, and then tested whether these vein phenotypes could be dominantly modified by $cdk8^{K185}$, a null allele of *cdk8* [71]. As shown in Fig. II.1G, reducing CDK8 by half in a '$cdk8^{K185}$/+' heterozygous background suppresses the vein defects caused by CDK8 overexpression. However, heterozygosity of $cdk8^{K185}$ does not obviously enhance the vein phenotype caused by CDK8-RNAi (Fig. II.1H), indicating that the RNAi of CDK8 may have depleted most of the CDK8 protein pool.

To further validate the specificity of the CDK8-directed phenotypes at the cellular level, we analyzed the protein levels of CDK8 and CycC in wing discs at the third instar wandering larval stage by immunostaining with CDK8 or CycC specific antibodies. Normally, both the CDK8 (Fig. II.2B) and CycC (Fig. II.2C) proteins are niformly distributed in the nuclei of all wing disc cells. Depletion of CDK8 (Fig. II.2D), CycC (Fig. II.2E), or both (Fig. II.2F and 2G)

using the *ap-Gal4* line significantly reduced CDK8 or CycC proteins in the dorsal compartment. The ventral compartment of the same discs serves as the internal control. In contrast, overexpression of either wild-type (Fig. II.2H) or kinase-dead (Fig. II.2I) CDK8 using *ap-Gal4* specifically increased the levels of CDK8 protein in the dorsal compartment. Taken together, these genetic and cell biological analyses have validated the specificity of both the antibodies and transgenic lines, demonstrating that these vein phenotypes are caused by a specific gain or reduction of CDK8 activity *in vivo*.

II.3.3 Identification of deficiency lines that can dominantly modify the vein phenotypes caused by varying CDK8

Based on these CDK8-specific vein phenotypes, we performed a dominant modifier genetic screen to identify gene products that can functionally interact with CDK8 *in vivo*. The idea of using phenotypic modifications to identify multiple genes involved in determining a specific trait or a phenotypic endpoint was initially developed by Calvin B. Bridges, when he analyzed mutant genes that could interact with the *eosin* mutant in regulating eye color in flies [91]. This genetic modifier approach has been employed to reveal the functional and inter-molecular networks for proteins of interest in *Drosophila* (for instances, [92-96]), and to provide insights into the phenotypic and genetic variability in mammals [97, 98]. The approach posits that if a protein interacts with CDK8-CycC *in vivo* in defining the wing vein patterns, then reducing its level by half may either enhance or suppress the sensitized wing vein phenotypes caused by specific alteration of the CDK8 activities. Accordingly, we can survey through the fly genome to search for factors that interact with CDK8-CycC using single genetic crosses.

To facilitate this screen approach, we generated three stocks with the following genotypes: "*w^{1118}; nub-Gal4; UAS-Cdk8-RNAi*" (designated as "*nub>Cdk8-i*" for simplicity),

"*w*^{1118}*; nub-Gal4; UAS-CycC-RNAi*" ("*nub>CycC-i*"), and "*w*^{1118}*; nub-Gal4, UAS-Cdk8*$^{+}$*/CyO*" ("*nub>Cdk8*$^{+}$"). We then conducted a dominant modifier genetic screen by crossing these three lines in parallel with a collection of 490 deficiency (*Df*) lines (Table B.II.1), which uncovers the majority of the euchromatic genome [99, 100]. Any alteration of the wing vein patterns can be readily discerned under dissecting microscopes, allowing us to search for *Df* lines that could modify the vein phenotypes caused by specific alteration of CDK8 activities.

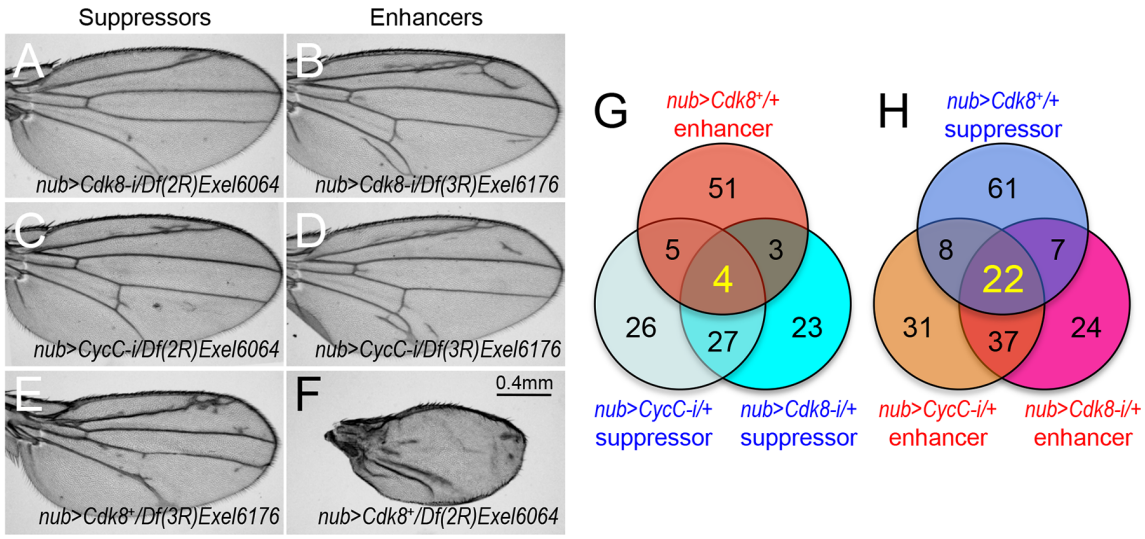

Fig. II.3 Identification of deficiency lines that can dominantly modify the vein phenotypes caused by varying CDK8. (A-F) Adult wings showing the examples of dominant modifiers. (A) *nub-Gal4/Df(2R)Exel6064; UAS-Cdk8-RNAi* (a suppressor of the CDK8-RNAi phenotype); (B) *nub-Gal4/+; UAS-Cdk8-RNAi/Df(3R)Exel6176,* (an enhancer of the CDK8-RNAi phenotype); (C) *nub-Gal4/Df(2R)Exel6064; UAS-CycC-RNAi/+* (a suppressor of the CycC-RNAi phenotype); (D) *nub-Gal4/+; UAS-CycC-RNAi/Df(3R)Exel6176* (an enhancer of the CycC-RNAi phenotype); (E) *nub-Gal4>UAS-Cdk8*$^{+}$*/+; Df(3R)Exel6176 /+* (a suppressor of the CDK8-overexpression phenotype); and (F) *nub-Gal4>UAS-Cdk8*$^{+}$*/Df(2R)Exel6064* (an enhancer of the CDK8-overexpression phenotype). Scale bar in F: 0.4mm. (G and H) The Venn diagrams summarize the numbers of suppressors and enhancers of the CDK8-specific phenotypes.

We inspected the vein patterns of the F1 females for enhancers and suppressors based on the following criteria: suppressors of the CDK8- or CycC-RNAi phenotypes are expected to display fewer or no ectopic veins (e.g., Fig. II.3A and 3C), while enhancers of the CDK8- or CycC-RNAi phenotypes show more or longer ectopic veins (e.g., Fig. II.3B and 3D). To score the strength of the modifications, we define strong suppressors as the *Df* lines that eliminate all of the ectopic veins, while the *Df* lines that only shorten the length of the ectopic veins are scored as weak suppressors. Similarly, we define strong enhancers to cause more or longer ectopic veins than CDK8- or CycC-RNAi phenotypes, while the *Df* lines causing less severe vein defects are designated as the weak enhancers. Conversely, the strong suppressors of the CDK8-overexpression phenotype are expected to have vein patterns similar to those of wild-type wings (particularly the L3/L4; e.g., Fig. II.3E, compared to the control shown in Fig. II.1E). If the *Df* lines only partially restore the missing veins, then they are scored as the weak suppressors. In contrast, the strong enhancers of the CDK8-overexpression phenotype are defined by further disrupting the vein patterns, with the entire L3 or L4 missing, often accompanied with strong disruption on other veins (e.g., Fig. II.3F); while the weaker enhancers further disrupted the vein defects compared to the CDK8-overexpression phenotype, but less severe than the strong enhancers.

From these screens, we identified 57 suppressor and 90 enhancer *Df* lines for the CDK8-RNAi phenotype, and 62 suppressor and 98 enhancer *Df* lines for the CycC-RNAi phenotype. In addition, we identified 63 enhancer and 98 suppressor *Df* lines for the CDK8-overexpression phenotype (Fig. II.3G and 3H). The results for all of these *Df* lines are summarized in Table B.II.1. Of these dominant modifier *Df* lines, four of them suppressed the CDK8-RNAi and CycC-RNAi phenotypes but enhance the CDK8-overexpression phenotype (Fig. II.3G, Table

II.1),

Table II.1. Deficiency lines that dominantly modify the CDK8- or CycC-specific phenotypes

Stock #	Deficiency lines	Cytogenetic breakpoints	*nub>CDK8+* backrgound	*nub>CDK8-RNAi* background	*nub>CycC-RNAi* background	*nub>CDK8-RNAi, CycC-RNAi* background
901	*Df(1)svr*	1A1;1B9--10	weak suppressor	strong enhancer	enhancer	lethal
25059	*Df(1)BSC531*	3C3;3E2	enhancer	strong suppressor	strong suppressor	enhancer
3196	*Df(1)Sxl-bt*	6E2;7A6	suppressor	strong enhancer	strong enhancer	strong enhancer
1581	*Df(2L)JS31*	23A3--4;23D	strong suppressor	enhancer	enhancer	enhancer
9718	*Df(2L)BSC244*	32F2;33B6	enhancer	strong suppressor	strong suppressor	strong suppressor
7512	*Df(2L)Exel6030*	33A2--33B3	suppressor	enhancer	enhancer	enhancer
7546	*Df(2R)Exel6064*	53C11;53D11	strong enhancer	suppressor	strong suppressor	suppressor
25430	*Df(2R)BSC597*	58A2;58F1	suppressor	strong enhancer	enhancer	weak enhancer
27352	*Df(2R)BSC780*	60C2;60D14	strong suppressor	strong enhancer	strong enhancer	strong enhancer
7561	*Df(2R)Exel6082*	60C4--60C7	suppressor	enhancer	enhancer	enhancer
25436	*Df(2R)BSC603*	60C7--60D1	strong suppressor	enhancer	enhancer	enhancer
24413	*Df(3L)BSC389*	66C12;66D8	suppressor	enhancer	enhancer	enhancer
27577	*Df(3L)BSC816*	66D9;66D12	weak suppressor	enhancer	strong enhancer	enhancer
26525	*Df(3L)BSC673*	67C7;67D10	suppressor	enhancer	weak enhancer	enhancer
7945	*Df(3L)Exel9011*	76B8;76B9	suppressor	weak enhancer	enhancer	enhancer
2596	*Df(3L)6B-29+Df(3R)6B-29*	81Fa;81Fa	suppressor	enhancer	enhancer	NE
7623	*Df(3R)Exel6144*	83A6-83B6	strong suppressor	enhancer	enhancer	strong enhancer
9215	*Df(3R)ED5495*	85F16;86C7	enhancer	suppressor	suppressor	weak suppressor
7965	*Df(3R)Exel7310*	86E18;87A1	suppressor	strong enhancer	enhancer	enhancer
7976	*Df(3R)Exel8159*	88A4;88B1	suppressor	enhancer	enhancer	weak enhancer
7655	*Df(3R)Exel6176*	89E11;89F1	strong suppressor	weak enhancer	weak enhancer	weak enhancer
26846	*Df(3R)BSC748*	89E5;89E11	strong suppressor	enhancer	enhancer	enhancer
7657	*Df(3R)Exel6178*	90F4;91A5	supressor	enhancer	enhancer	enhancer
2352	*Df(3R)X3F*	99D1--2;99E1	suppressor	enhancer	enhancer	lethal
2155	*Df(3R)A113*	100A;3Rt	suppressor	strong enhancer	enhancer	enhancer
7918	*Df(3R)Exel8194*	100A4;100A7	suppressor	weak enhancer	enhancer	strong enhancer

NE, no effects.

while 22 of them enhance the CDK8-RNAi and CycC-RNAi phenotypes but suppress the CDK8-overexpression phenotype (Fig. II.3H, Table II.1). To further validate this genetic approach, we generated a transgenic line that allowed us to simultaneously deplete CDK8 and CycC ("*w^{1118}; nub-Gal4; UAS-Cdk8-RNAi, CycC-RNAi*", referred to as "*nub>Cdk8-i CycC-i*")

with *nub-Gal4*, and observed identical phenotypes to the ones caused by depleting either *Cdk8* or *CycC* alone (Fig. II.1D). With the exception of one *Df* line, the rest of these 25 *Df* lines have consistently modified the ectopic vein phenotype caused by depletion of both CDK8 and CycC: four of the *Df* lines behaved as suppressors and 21 of them as enhancers (Table II.1). These results show that the CDK8-specific vein phenotypes are modifiable and can be used to identify factors that functionally interact with CDK8-CycC *in vivo*.

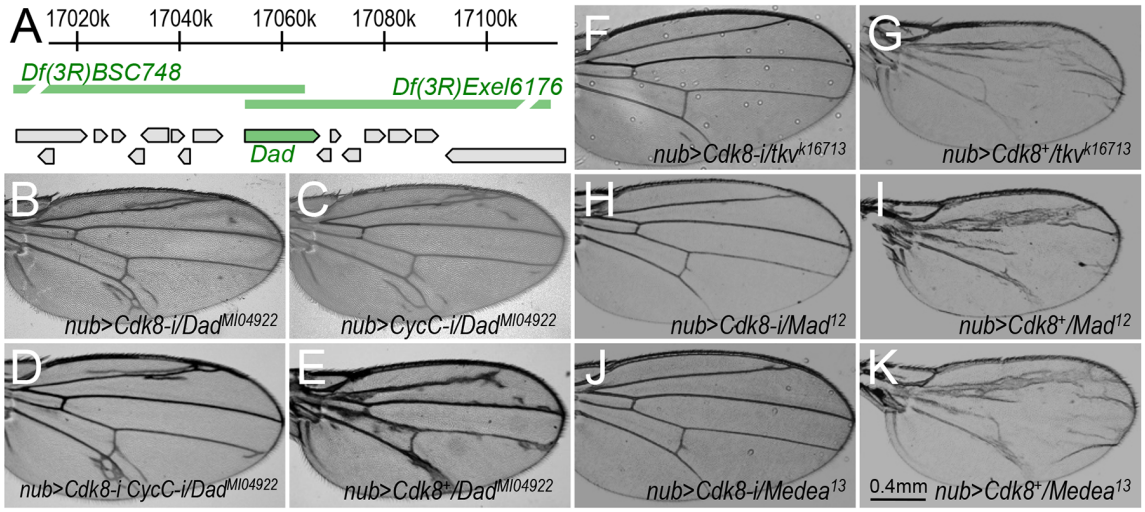

Fig. II.4 Identification of the *Dad* gene and genes encoding other components of the Dpp signaling pathway as dominant modifiers of the CDK8-specific phenotypes. (A) Schematic diagram of the genome region of *Df(3R)BSC748* and *Df(3R)Exel6176*, which uncover the gene *dad.* Adult wings with the following genotypes: (B) *nub-Gal4/+; UAS-Cdk8-RNAi/Dad^{MI04922}*; (C) *nub-Gal4/+; UAS-CycC-RNAi/Dad^{MI04922}*; (D) *nub-Gal4/+; UAS-Cdk8-RNAi CycC-RNAi/Dad^{MI04922}*; (E) *nub-Gal4>UAS-Cdk8^{+}/+; Dad^{MI04922}/+*; (F) *nub-Gal4/tkv^{k16713}; UAS-Cdk8-RNAi/+*; (G) *nub-Gal4>UAS-Cdk8^{+}/tkv^{k16713}*; (H) *nub-Gal4/Mad^{12}; UAS-Cdk8-RNAi/+*; (I) *nub-Gal4>UAS-Cdk8^{+}/Mad^{12}*; (J) *nub-Gal4/+; UAS-Cdk8-RNAi/Medea^{13}*; and (K) *nub-Gal4>UAS-Cdk8^{+}/+; Medea^{13}/+*; Scale bar in K: 0.4mm.

II.3.3 Identification of Dad as an enhancer of the nub>Cdk8-i and nub>CycC-i phenotypes but a suppressor of the Cdk8-overexpression phenotype

To identify the specific genes uncovered by these dominant modifier *Df* lines, we analyzed these 26 genome regions with partial overlapping *Df* lines (Table II.1). Interestingly, two partially overlapping *Df* lines, *Df(3R)BSC748* and *Df(3R)Exel6176*, enhanced the CDK8-RNAi and CycC-RNAi phenotypes, but suppressed the CDK8-overexpression phenotype (Fig. II.3B, 3D, and 3E; Table II.1). The overlapping region uncovers one specific gene, *Dad* (*Daughter against Dpp*), encoding the *Drosophila* homolog of Smad6/7 (Fig. II.4A). Thus, to test whether *Dad* is the specific gene that accounts for the modification of the CDK8-specific phenotypes by these two *Df* lines, we performed similar genetic tests with two mutant alleles of *Dad*: $Dad^{MI04922}$, a MiMIC (Minos Mediated Integration Cassette) insertion in an intron of the *Dad* gene [101], and Dad^{j1E4}, an insertion of the *P{lacW}* element in an intron of the *Dad* gene [102]. Indeed, both *Dad* mutant alleles dominantly enhanced the CDK8-RNAi (Fig. II.4B), CycC-RNAi (Fig. II.4C), and CDK8-RNAi plus CycC-RNAi (Fig. II.4D) phenotypes, but suppressed the CDK8-overexpression phenotype (Fig. II.4E, Table II.2). These effects on the CDK8-specific vein phenotypes are similar to those observed for *Df(3R)BSC748* and *Df(3R)Exel6176*, suggesting that *Dad* is the specific gene that genetically interacts with CDK8 *in vivo*.

Table II.2. Mutant alleles of genes encoding components of the Dpp signaling that modify the CDK8- or CycC-specific phenotypes.

Mutant alleles	*nub>Cdk8*$^{+}$	*nub>Cdk8-i*	*nub>CycC-i*	*nub>Cdk8-i CycC-i*
dpp^{d6}	NE	Suppressor	Suppressor	Suppressor
dpp^{hr92}	NE	Suppressor	Suppressor	Suppressor
dpp^{S11}	NE	Suppressor	Suppressor	Suppressor
tkv^{7}	Enhancer	NE	Suppressor	Suppressor
tkv^{k16713}	Enhancer	Suppressor	NE	Suppressor
Mad^{k00237}	Enhancer	NE	Suppressor	Suppressor
Mad$^{1-2}$	NE	Suppressor	NE	Suppressor
Mad$^{8-2}$	NE	Suppressor	NE	Suppressor
Mad^{12}	Enhancer	Suppressor	NE	NE
Mad^{KG00581}	Enhancer	NE	NE	Suppressor
Medea^{1}	Enhancer	NE	Suppressor	Suppressor
Medea^{13}	Enhancer	Suppressor	No Effect	Suppressor
Dad^{MI04922}	Suppressor	Enhancer	Enhancer	Enhancer
Dad^{j1e4}	Suppressor	Enhancer	Enhancer	Enhancer

NE, no effects.

II.3.4 Mutants of multiple components of the Dpp signaling pathway genetically interact with CDK8-CycC

The protein Dad functions as an inhibitory Smad in the Dpp/TGFβ signaling pathway, which plays critical roles in regulating cell proliferation and differentiation during the development of metazoans [103-108]. During the development of the wing discs, Dpp spreads from the anterior-posterior boundary to the anterior and posterior halves [103-105, 109]. Upon the binding of the Dpp ligand to the Tkv-Punt receptor complex on the cell membrane, the TGFβ type II receptor Punt phosphorylates and activates the type I receptor Tkv. This results in the phosphorylation of Mad by Tkv at its C-terminal SSXS motif, known as the phospho-Mad protein or pMad. Medea, the unique co-Smad protein in *Drosophila*, associates with pMad in the

cytoplasm, and then this heteromeric Smad complex translocates into the nucleus and regulates the expression of its target genes [107, 109-111].

The genetic interactions between CDK8-CycC and Dad prompted us to test whether mutant alleles of other components of the Dpp signaling pathway could also genetically interact with CDK8 and CycC. For this, we crossed multiple mutant alleles of these components with the CDK8-CycC depletion or overexpression lines. As summarized in Table II.2, mutants of multiple components of the Dpp signaling pathway could either dominantly enhance or suppress the CDK8-specific vein phenotypes. For instance, dpp^{d6}, tkv^{7}, tkv^{k16713} (Fig. II.4F), Mad^{12} (Fig. II.4H), Mad^{k00237}, $Medea^{1}$, and $Medea^{13}$ (Fig. II.4J) all dominantly suppress the ectopic vein phenotype caused by depletion of CDK8, or both CDK8 and CycC (Table II.2). However, tkv^{7}, tkv^{k16713} (Fig. II.4G), Mad^{k00237}, Mad^{12} (Fig. II.4I), $Medea^{1}$, and $Medea^{13}$ (Fig. II.4K) enhance the CDK8-overexpression phenotype (Table II.2). Testing additional mutant alleles of these genes have revealed that most of them can also dominantly modify the CDK8-specific phenotypes (Table II.2). Dpp is activated in a specific pattern in the middle part of the wing pouch area, while the *nub-Gal4* display a well-characterized pattern in the entire wing pouch area. These two patterns differ, arguing against the possibility that Dpp signaling may affect *nub-Gal4* expression pattern. In addition, reducing Mad or Dad by half has little effects on the expression of a *UAS-RFP* reporter driven by *nub-Gal4* (Fig. A.II.3), suggesting that the expression and activity of *nub-Gal4* are not affected by Dpp signaling. Taken together, these genetic interactions suggest that CDK8-CycC may affect vein patterning by modulating Dpp signaling.

II.3.5 CDK8-CycC positively regulates Mad-dependent transcription

Given that CDK8 and CycC are known subunits of the Mediator complex, which serves as a scaffold complex mediating the interactions between the RNA Pol II basal transcription

machinery and a number of gene-specific transcription activators [3, 7, 112]. Thus, the simplest model to explain the genetic interactions between Dpp signaling and CDK8-CycC is that the CDK8-CycC complex may directly regulate the transcriptional activity of Mad in the nucleus. To test this model, we analyzed the effects of CDK8-CycC depletion on the expression of *spalt major* (*salm*), a well-characterized direct target gene of Mad involved in vein differentiation [113-116]. The *sal-lacZ* (*P{PZ}salm*^{03602}) is a enhancer trap line derived from an insertion of a *P{PZ}* element in the promoter region of the *salm* gene [117, 118], and the expression of *sal-lacZ* can serve as a reporter for the transcriptional activity of Mad [119].

Because the expression of *sal-lacZ* is symmetric along the dorsal-ventral boundary of the wing pouch area of the wing discs (Fig. II.5A), we tested whether specific depletion of CDK8 or CycC within the dorsal compartment of the wing discs could affect the transcriptional activity of Mad by detecting the transcription level of *sal* using an anti-β-galactosidase (anti-β-Gal) antibody. For this, we depleted genes of interest using the *ap-Gal4* driver, and then compared the β-Gal expression between the dorsal and ventral compartments. As expected, depleting Mad with two transgenic RNAi lines (BL-43183 (Fig. II.5B) and BL-31315 (Fig. A.II.4B and A.II.4B')), Medea (Fig. II.5C), or Dpp (Fig. A.II.4A) using this approach reduced the expression of the *sal-lacZ* reporter in the dorsal compartment. Importantly, depletion of CDK8 (Fig. II.5D), CycC (Fig. II.5E), or both (Fig. II.5F), in the dorsal compartment significantly decreased the β-Gal expression level in the dorsal compartment compared with the ventral compartment of the same disc. After quantifying the line-scan profiles of the Sal-lacZ levels in the wing porch area, we calculated the relative signal intensity of dorsal to ventral Sal-lacZ levels for 5 wing discs of each genotype (Fig. A.II.5; see Materials and Methods for details), which validated the effects of

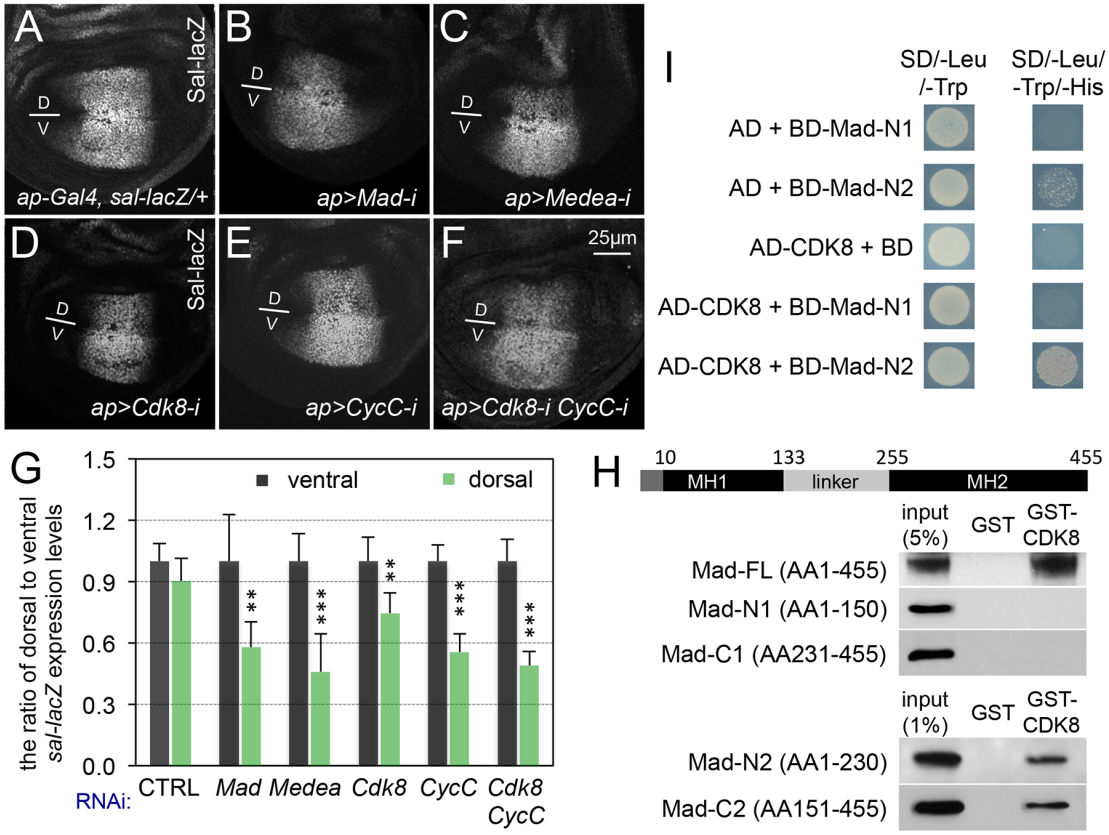

Fig. II.5 CDK8-CycC positively regulates Mad-dependent transcription. Confocal images of the wing pouch area of a L3 wandering larval wing disc of (A) *ap-Gal4, sal-lacZ/+* (control); (B) *ap-Gal4, sal-lacZ/UAS-Mad-RNAi* (BL-43183); (C) *ap-Gal4, sal-lacZ/UAS-Medea-RNAi*; (D) *ap-Gal4, sal-lacZ/+; UAS-Cdk8-RNAi/+*; (E) *ap-Gal4, sal-lacZ/+; UAS-CycC-RNAi/+*; and (F) *ap-Gal4, sal-lacZ/+; UAS-Cdk8-RNAi CycC-RNAi/+*. All signals presented were from anti-β-galactosidase staining. Scale bar in F: 25μm. Dorsal (D)-ventral (V) boundaries are marked using a short line in these images. (G) Quantification of Sal-lacZ expression. The black columns represent the average of Sal-lacZ expression in the ventral compartment of the indicated genotypes (N=5 for each genotype), and light green columns represent the measurements in the dorsal compartments. (H) Western Blots of a GST pull-down assay between GST-CDK8 and His-tagged Mad fragments. The amino acids (AA) positions of MH1 and MH2, separated by the linker region, are based on a BLAST search of *Drosophila* Mad-RA isoform (455AA). The other isoform, Mad-RB (525AA), has additional 70AA at the N-terminus. We focused on the Mad-RA isoform in this work. (I) Y2H assay showing the specific interaction between CDK8 and the linker region of Mad. SD/-Leu/-Trp and SD/-Leu/-Trp/-His are synthetic dropout (SD) media lacking "Leu and Trp", or "Leu, Trp, and His", respectively. The co-transformed yeast cultures were spotted on SD/-Leu/-Trp and SD/-Leu/-Trp/-His plates, positive interactions result in yeast growth on the SD/-Leu/-Trp/-His plate. AD, GAL4-activation domain (prey); BD, GAL4-DNA-binding domain (bait); AD- or BD-protein, AD- or BD-fusion proteins.

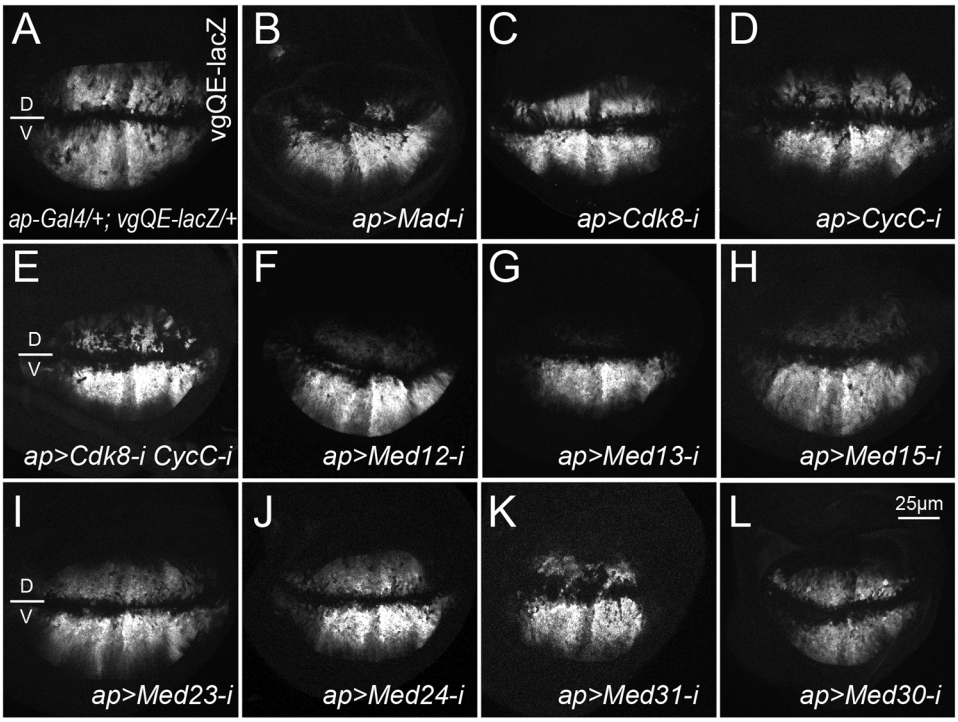

Fig. II.6 Effects of various Mediator subunits on the expression of the *vgQE-lacZ* reporter. Representative confocal images of anti-β-Gal staining of wing discs of the following genotypes: (A) *ap-Gal4/+; vgQE-lacZ/+;* (B) *ap-Gal4/+; vgQE-lacZ/UAS-Mad-RNAi* (BL-31315); (C) *ap-Gal4/+; vgQE-lacZ/UAS-Cdk8-RNAi*; (D) *ap-Gal4/+; vgQE-lacZ/UAS-CycC-RNAi*; (E) *ap-Gal4/+; vgQE-lacZ/UAS-Cdk8-RNAi, CycC-RNAi*; (F) *ap-Gal4/+; vgQE-lacZ/UAS-Med12-RNAi*; (G) *ap-Gal4/+; vgQE-lacZ/UAS-Med13-RNAi*; (H) *ap-Gal4/+; vgQE-lacZ/UAS-Med15-RNAi*; (I) *ap-Gal4/+; vgQE-lacZ/UAS-Med23-RNAi*; (J) *ap-Gal4/+; vgQE-lacZ/UAS-Med24-RNAi*; (K) *ap-Gal4/+; vgQE-lacZ/UAS-Med31-RNAi*; (L) *ap-Gal4/+; vgQE-lacZ/UAS-Med30-RNAi*. At least five wing discs were examined for each genotype. Scale bar in L: 25µm.

CDK8-CycC on *sal-lacZ* expression (Fig. II.5G). Similar observations were observed by quantifying the pixel intensities in areas in the dorsal and ventral compartments (Fig. A.II.6).

To further validate the effects of CDK8-CycC depletion on Mad-activated gene expression, we analyzed the expression of the quadrant enhancer (QE) of the selector gene *vestigial* (*vgQE-lacZ*) in wing discs. Similar to *Sal-lacZ* reporter, *vgQE-lacZ* also displays a symmetric expression pattern along the D-V boundary in the wing pouch (Fig. II.6A) [81, 82]. As expected, depleting Mad (BL-31315) using *ap-Gal4* driver significantly reduced the

expression of *vgQE-lacZ* in the dorsal compartment (Fig. II.6B). Although depleting CDK8 alone only marginally reduced the *vgQE-lacZ* expression in the dorsal compartment (Fig. II.6C), a more obvious effect was observed with the depletion of CycC (Fig. II.6D), and a stronger reduction of the reporter expression was detected with the depletion of both CDK8 and CycC (Fig. II.6E) using the same approach. We note that the interpretation of the data presented in Fig. II.6 is compounded by the fact that the transcription of the *vg* in different compartments of wing discs is controlled by Wingless (Wg) and Dpp signaling, as well as a feed-forward regulation by Vg itself [81, 82]. Nevertheless, the most parsimonious model to explain the observations based on *Sal-lacZ* and *vgQE-lacZ* reporters is that CDK8-CycC positively regulates Mad-dependent transcription.

One caveat of these analyses is that the CKM could affect *ap-Gal4* activities. As shown in Fig. A.II.7B, we observed that depleting CDK8 and CycC reduces the *ap-Gal4*-dependent expression of *UAS-GFP* in the dorsal compartment of wing discs (compared to the control shown in Fig. A.II.7A). This observation suggests that the positive effects of depletion of CDK8 and CycC on wing vein patterning are hypomorphic, representing an under-estimation of the positive effects of CDK8-CycC in regulating Mad-dependent transcription. In addition, we observed that depleting Ap protein using *ap-Gal4* has no effects on the *sal-lacZ* expression in the dorsal compartment (Fig. A.II.7C), suggesting that the expression of *sal-lacZ* is independent of the levels of Ap or Gal4.

II.3.6 Direct interactions between CDK8 and Mad

Since Mad phosphorylation at its C-terminus (pMad) by the Tkv-Punt receptor complex marks the activation of Mad, we tested whether CDK8 affects the pMad level. For this, we depleted CDK8, CycC, or both, with the *ap-Gal4* line, and then detected the levels of the

activated Mad with an anti-pMad antibody. In the wing pouch area of the control discs, the pMad protein is symmetrically distributed along the dorsal-ventral boundary (Fig. A.II.8A). However, depletion of CDK8-CycC did not affect pMad levels when comparing the dorsal compartment with the ventral compartment (Figs. A.II.8B-A.II.8D), suggesting that CDK8-CycC does not affect the phosphorylation of Mad at its carboxy terminus in the cytoplasm. These results support the idea that the CDK8-CycC complex directly regulates the transcriptional activity of Mad in the nucleus.

R-Smads are characterized by a highly conserved amino-terminal MH1 (Mad homology 1) domain that binds to DNA and a C-terminal MH2 domain that harbors the transactivation activity, separated by a serine- and proline-rich linker region (Fig. II.5H) [120]. It was previously reported that CDK8 and a few other kinases (see below) may phosphorylate Smad proteins in both *Drosophila* and mammalian cells [63, 64, 77, 109, 120], but whether and how CDK8 interacts with Smads remain unknown. To determine whether CDK8 directly interacts with Mad, we performed a GST-pulldown assay. As shown in Fig. II.5H, purified GST-CDK8 can directly bind with His-tagged full length Mad (Mad-FL, AA1-455) expressed in *E. coli*. We then mapped the specific domain of Mad that interacts with CDK8 using His-tagged fragments of the Mad protein. We observed that the "Mad-N2" fragment (AA1-230) and the "Mad-C2" fragment (AA151-455), but not the "Mad-N1" fragment (AA1-150) or the "Mad-C1" fragment (AA231-455), can interact directly with CDK8 (Fig. II.5H). We validated the interaction between CDK8 and the linker region using the yeast two-hybrid (Y2H) assay: the "Mad-N2" fragment, but not the "Mad-N1" fragment, as the bait can interact with full-length CDK8 as the prey (Fig. II.5I). It is not feasible to use this Y2H approach test with Mad-FL or Mad-C1/C2 fragments as bait, since they auto-activate as the baits; while the full-length CDK8 can also auto-activate as the bait (Fig.

A.II.9). Taken together, these results suggest that CDK8 directly interacts with part of the linker region of Mad protein (AA151-230). Implications of these physical interactions are discussed below.

II.3.7 Involvement of additional Mediator complex subunits in regulating the Mad/Smad-dependent transcription

The Med15/ARC105 subunit of the Mediator complex has been previously shown to directly interact with the transactivation MH2 domain of Smad2/3, thereby mediating the Smad2/3-Smad4-dependent transcription in *Xenopus* [121], and Med15 is required for the transcription of Dpp target genes in *Drosophila* [122]. However, whether other Mediator subunits are involved in regulating the Mad/Smad-dependent transcription remains unknown. To address this question, we depleted individual subunits of the Mediator complex upon conditional expression of interfering RNAs with *ap-Gal4*, and then analyzed the expression of the *sal-lacZ* reporter. Of the 30 Mediator subunits tested (Table II.3), we have observed that depletion of six additional Mediator subunits, Med12 (Fig. II.7B), Med13 (Fig. II.7C), Med15 (Fig. II.7D), Med23 (Fig. II.7E), Med24 (Fig. II.7F), and Med31 (Fig. II.7G), by *ap-Gal4* significantly reduced the expression of *sal-lacZ* in cells of the dorsal compartment compared with the cells in the ventral compartment of the same wing discs (Fig. II.7J); similar to depletion of CDK8 or CycC (Fig. II.5). The effects of these six Mediator subunits were further validated using the *vgQE-lacZ* reporter: their depletion using *ap-Gal4* also reduces the *vgQE-lacZ* expression in the dorsal compartment (Fig. II.6F-6K). These results suggest that these Mediator subunits are

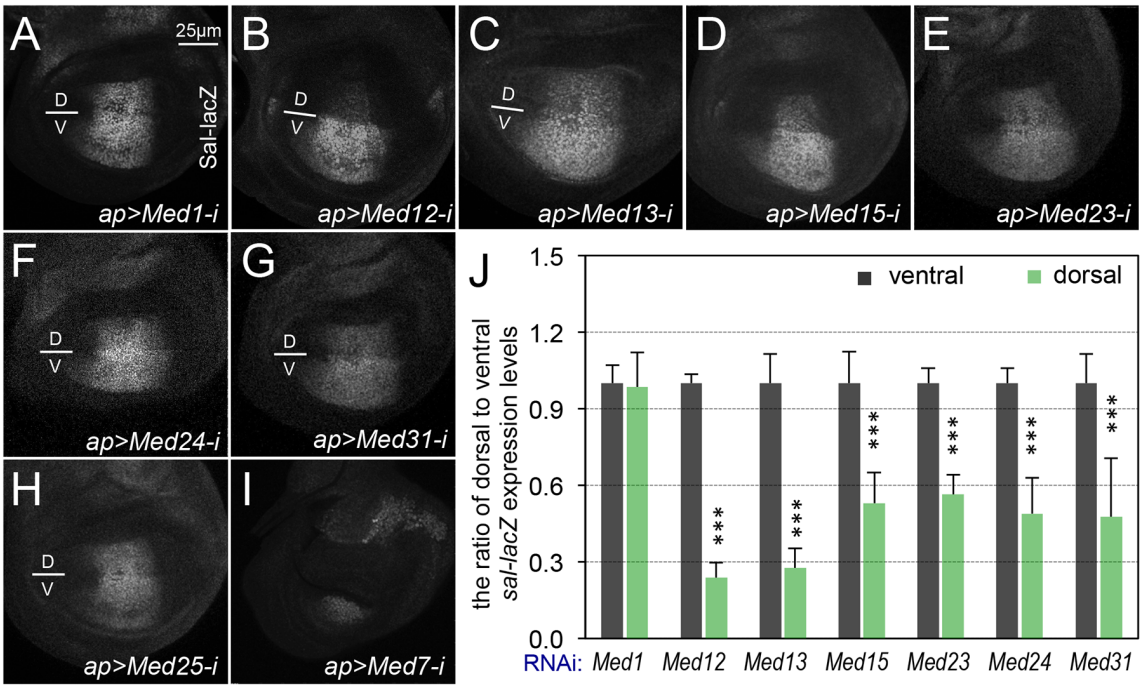

Fig. II.7 Effects of the additional Mediator subunits on the expression of the *sal-lacZ* reporter. Representative confocal images of anti-β-Gal staining of wing discs of the following genotypes: (A) *ap-Gal4, sal-lacZ/+; UAS-Med1-RNAi/+*; (B) *ap-Gal4, sal-lacZ/+; UAS-Med12-RNAi/+*; (C) *ap-Gal4, sal-lacZ/+; UAS-Med13-RNAi/+*; (D) *ap-Gal4, sal-lacZ/+; UAS-Med15-RNAi/+*; (E) *ap-Gal4, sal-lacZ/+; UAS-Med23-RNAi/+*; (F) *ap-Gal4, sal-lacZ/+; UAS-Med24-RNAi/+*; (G) in *ap-Gal4, sal-lacZ/+; UAS-Med31-RNAi/+*; (H) *ap-Gal4, sal-lacZ/UAS-Med25-RNAi*; and (I) *ap-Gal4, sal-lacZ/+; UAS-Med7-RNAi/+*. (J) Quantification of Sal-lacZ expression. The black columns represent the average of Sal-lacZ expression in the ventral compartment of five wing discs of the indicated genotypes (N=5 for each genotype), and light green columns represent the measurements in the dorsal compartments. Scale bar in A: 25μm. For (H) and (I), at least five wing discs were examined for each genotype.

required for the Mad-activated gene expression. However, RNAi depletion of the remaining 15 Mediator subunits using *ap-Gal4* driver did not significantly affect *sal-lacZ* expression (Table II.3), as β-Gal expression remained symmetric along the dorsal-ventral boundary as exemplified for depletion of Med1 (Fig. II.7A, and 7J) and Med25 (Fig. II.7H) on *sal-lacZ* expression. Similarly, depletion of Med30 using *ap-Gal4* does not obviously affect the expression of *sal-*

lacZ and *vgQE-lacZ* reporters, which remains symmetric along the dorsal-ventral boundary (Fig. II.6L, Table II.3).

Table II.3. The effects of depleting different Mediator subunits on the expression of the *Sal-lacZ* and *vgQE-lacZ* reporters in wing discs during the third instar larval stage, as well as the wing and eye phenotypes in adult flies.

Mediator subunit	Effect on *sal-lacZ* expression	Effect on vgQE-*lacZ* expression	Phenotypes using the *nub-Gal4* driver	Phenotypes using the *ey-Gal4* driver	Terriente-Felix et al. (2010) (*nub-Gal*4)
CDK8	decrease	decrease	ectopic vein	NE	ND
CycC	decrease	decrease	ectopic vein	NE	ND
CDK8&CycC	decrease	decrease	ectopic vein	NE	ND
Med12	decrease	decrease	pupal lethal	small eye	small wing
Med13	decrease	decrease	pupal lethal	small eye	ND
Med15	decrease	decrease	cell death	small eye	ND
Med23	decrease	decrease	vein defects	NE	ND
Med24	decrease	decrease	NE	small eye	ND
Med31	decrease	decrease	cell death	pupal lethal	ND
Med7	deformed	ND	wingless	pupal lethal	ND
Med8	deformed	ND	pupal lethal	pupal lethal	ND
Med14	deformed	ND	wingless	pupal lethal	ND
Med16	deformed	ND	pupal lethal	small eye	small wing
Med17	deformed	ND	wingless	pupal lethal	ND
Med21	deformed	deformed	pupal lethal	pupal lethal	ND
Med22	deformed	ND	cell death	eyeless	ND
Med1	NE	ND	cell death	NE	ND
Med4	NE	ND	vein defects	NE	ND
Med6	NE	ND	larval lethal	small eye	ND
Med9	NE	ND	NE	NE	ND
Med10	NE	ND	NE	NE	small wing
Med11	NE	ND	cell death	eyeless	ND
Med18	NE	ND	NE	NE	ND
Med19	NE	ND	ectopic vein	NE	ND
Med20	NE	ND	vein defects	small eye	cell death
Med25	NE	ND	small wing	NE	small wing
Med26	NE	ND	NE	small eye	ND
Med27	NE	ND	cell death	eyeless	small wing
Med28	NE	ND	cell death	small eye	ND
Med29	NE	ND	NE	NE	ND
Med30	NE	NE	cell death	small eye	cell death

NE, no effects.

ND, not determined.

Furthermore, depleting the remaining Mediator subunits, including Med7 (Fig. II.7I), Med8 (Fig. A.II.10A), Med14 (Fig. A.II.10B), Med16 (Fig. A.II.10C), Med17 (Fig. A.II.10D), Med21 (Fig. A.II.10E), and Med22 (Fig. A.II.10F), severely disrupted the morphology of the wing discs, making it difficult to determine their roles in regulating *sal* transcription. Taken together, these observations suggest that multiple Mediator subunits, but apparently not all of them, are required for Mad-dependent transcription in *Drosophila*.

II.3.8 CDK9 and Yorkie also positively regulate the Mad/Smad-dependent transcription

Besides CDK8, several other kinases, such as CDK7, CDK9, GSK3 (*Glycogen synthase kinase 3*), and MAPKs (mitogen-activated protein kinases) such as ERK (extracellular signal-regulated kinase) and ERK2, have been implicated to phosphorylate and regulate the transcriptional activity of Smads [63, 64, 120, 123] (Fig. II.8A, see below). The four phosphorylation sites (Ser or Thr residues) within the linker region of Smads appear to be conserved from *Drosophila* to mammals (Fig. II.8B; see Discussion). The phosphorylation of Smads within the linker region may facilitate the subsequent binding with transcription co-factors, such as YAP (Yes-associated protein) [63]. However, it is still unclear whether all of these kinases regulate Smads activity *in vivo*. With the exception of YAP (Yorkie or Yki, in *Drosophila*), it is also unclear whether these regulatory mechanisms are conserved during evolution.

To validate the relevance of these kinases in regulating Mad-dependent gene expression, we depleted the *Drosophila* orthologs of CDK7, CDK9, Shaggy (Sgg, the GSK3 homolog in *Drosophila*), Rolled, and dERK2 (MAPK/ERK homologs in *Drosophila*), in the dorsal compartment of wing discs (using *ap*-Gal4 as above), and then analyzed *sal-lacZ* expression in

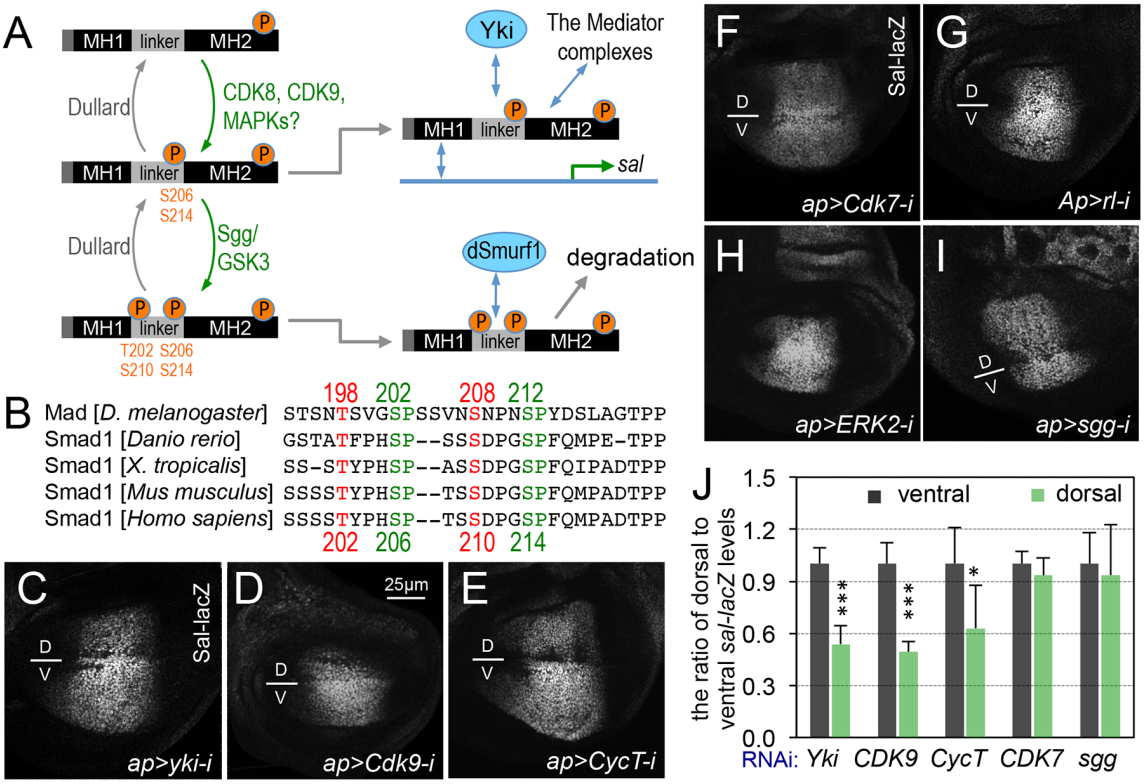

Fig. II.8 Validation of additional transcriptional cofactors for their roles in regulating Mad-dependent transcription. (A) Model: linker region of pMad may be phosphorylated by CDK8, CDK9, or MAPKs as priming kinase recruiting Yki/YAP binding to pMad to drive target gene, such as *sal* transcription; and further phosphorylation by Sgg/GSK3 at the linker region may switch the binding to dSmuf1 and causes pMad degradation. (B) Sequence alignment of part of the Mad/Smad1 linker region from different species showing the conservation of the potential phosphorylation sites by CDKs, MAPKs, and GSK3. Representative confocal images of anti-β-Gal staining of wing discs of the following genotypes: (C) *ap-Gal4, sal-lacZ/+; UAS-yki-RNAi/+*; (D) *ap-Gal4, sal-lacZ/UAS-Cdk9-RNAi*; (E) *ap-Gal4, sal-lacZ/+; UAS-CycT-RNAi/+*; (F) *ap-Gal4, sal-lacZ/UAS-Cdk7-RNAi*; (G) *ap-Gal4, sal-lacZ/+; UAS-rl-RNAi/+*; (H) *ap-Gal4, sal-lacZ/+; UAS-ERK2-RNAi/+*; and (I) *ap-Gal4, sal-lacZ/UAS-sgg-RNAi.* Scale bar in D: 25μm. (J) Quantification of Sal-lacZ expression. The grey columns represent the average of Sal-lacZ expression in the ventral compartment of the indicated genotypes, and light green columns represent the measurements in the corresponding dorsal compartments. N=5 for the quantification of *sal-lacZ* expression after depleting Yki, Cdk9, or CycT in the dorsal compartment; N=3 for the quantification of *sal-lacZ* expression after depleting Cdk7 or Sgg in the dorsal compartment. At least five wing discs were examined for depletion of Rl (G) and ERK2 (H), and the represented images were shown.

the wing pouch. As expected for a positive role of Yki in regulated Mad-dependent transcription [63], depletion of Yki in the dorsal cells significantly reduced the expression of *sal-lacZ* compared to the cells in the ventral compartment of the same discs (Fig. II.8C and 8J). Using the same approach, we have observed that depleting CDK9 (Fig. II.8D and 8J) and its partner Cyclin T (CycT, Fig. II.8E and 8J; [124]) also reduced *sal-lacZ* expression. These observations suggest that both Yki and CDK9-CycT are required for Mad/Smad-dependent transcription in *Drosophila*, which is consistent to the previous reports [63, 77]. However, depletion of CDK7 (Fig. II.8F and Fig. II.8J) or *Drosophila* MAPK homologs, either Rolled (Fig. II.8G) or dERK2 (Fig. II.8H), did not affect the expression of *sal-lacZ*. Although depletion of Sgg increased the size of the dorsal compartment, the intensity of anti-β-Gal staining remained similar to the ventral compartment (Fig. II.8I and 8J). We note that depleting CDK9 (Fig. A.II.7D), Med12 (Fig. A.II.7E), or Med13 (Fig. A.II.7F) have no obvious effects on the expression of UAS-GFP reporter, suggesting that their effects on *sal-lacZ* expression are independent of the Gal4 activity *per se*. Together with the previous reports [63, 120], our *in vivo* analyses have validated the conserved roles of CDK8-CycC, CDK9-CycT, and Yki/YAP on Mad/Smad-dependent transcription.

II.4 Discussion

To study the function and regulation of CDK8 *in vivo*, we have developed a genetic system that yields robust readouts for the CDK8-specific activities in developing *Drosophila* wings. These genetic tools provide a unique opportunity to perform a dominant modifier genetic screen, allowing us to identify multiple components of the Dpp/TGFβ signaling pathway that can genetically interact with the CDK8-CycC complex *in vivo*. Our subsequent genetic and cellular analyses reveal that CDK8, CycC, and six additional subunits of the Mediator complex, as well

as CDK9 and Yki are required for the Mad-dependent transcription in the wing discs. In addition, CDK8 can directly interact with the linker region of Mad. These results have extended the previous biochemical and molecular analyses on how different kinases and transcription cofactors modulate the Mad/Smad-activated gene expression in the nucleus. Further mapping of specific genes uncovered by other deficiency lines may also open up the new directions to advance our understanding of the conserved function and regulation of CDK8 during development.

II.4.1 Multiple subunits of the Mediator complex are required for Mad/Smad-dependent transcription

The Mediator complex functions as a molecular bridge between gene-specific transcription factors and the RNA Pol II general transcription apparatus, and diverse transactivators have been shown to interact directly with distinct Mediator subunits [4, 6-9, 125]. However, it is unclear whether all Mediator subunits are required by different transactivators to regulate gene expression, or whether Mediator complexes composed of fewer and different combinations of Mediator subunits exist in differentiated tissues or developmental stages. Gene-specific combinations of the Mediator subunits may be required in different transcription processes, as not all Mediator subunits are simultaneously required for all transactivation process [126]. For instance, ELK1 target gene transcription requires Med23, but lacking Med23 does not functionally affect some other ETS transcription factors, such as Ets1 and Ets2 [127]. Similarly, Med15 is required for the expression of Dpp target genes, but does not appear to affect the expression of EGFR (epidermal growth factor receptor) and Wg targets in *Drosophila* [122].

It has been previously reported that the Med15 subunit is required for the Smad2/3-Smad4 dependent transcription, as its removal from the Mediator complex abolishes the

expression of Smad-target genes and disrupts Smad2/3-regulated dorsal-ventral axis formation in *Xenopus* embryos [121]. Further biochemical analyses showed that increased Med15 enhances, while its depletion decreases, the transcription of Smad2/3 target genes, and that the Med15 subunit can directly bind to the MH2 domain of Smad2 or Smad3 [121]. In *Drosophila*, loss or reduction of Med15 reduced the expression of Dpp targets, resulting in smaller wings and disrupted vein patterning (mainly L2) [122]. We also observed that depletion of Med15 or CDK8 reduces the expression of a Mad-target gene. These observations support the idea that CDK8 and Med15 play a conserved and positive role in regulating Mad/Smad-activated gene expression.

Aside from Med15 and CDK8, it remains unclear whether other Mediator subunits are also involved in Mad/Smad-dependent transcription. We identified six additional Mediator subunits that are required for the Mad-dependent transcription, including CycC, Med12, Med13, Med23, Med24, and Med31 (Fig. II.5, Fig. II.6, Fig. II.7, and Table II.3). Interestingly, aside from Med23 and Med24 being specific to metazoans, counterparts of the other six subunits are not essential for cell viability in the budding yeast [5]. The similar effects of the four CKM subunits on Mad-activity suggest that they may function together to stimulate Mad-dependent transcription. We note that depletion of seven Mediator subunits, Med7, Med8, Med14, Med16, Med17, Med21, and Med22, severely disrupts the morphology of the wing discs (Fig. II.7I and Fig. A.II.10), making it difficult to assay their effects on the transcriptional activity of Mad *in vivo*. Consistently, all corresponding subunits, except Med16, are critical for cell viability in the budding yeast [5]. In contrast, reducing expression of the 15 remaining subunits of the *Drosophila* Mediator complex did not significantly alter the expression of a Mad-dependent reporter (Table II.3). Med1 and Med25 are loosely associated to the small Mediator complex in human cell lines [5]. A caveat for these negative results is that depleting these subunits using the

existing RNAi lines may not be sufficient to affect *sal-lacZ* expression, even though the majority of these transgenic RNAi lines can generate severe phenotypes in the eye, wing, or both (Table II.3). Further analyses are necessary to validate these negative data in the future. Taken together, our results indicate that not all Mediator subunits are required for the expression of the Mad-target genes that we tested in the developing wing discs.

Besides the specific roles of Med15, Med23, Med24 and Med31 in positively regulating Mad dependent transcription, depletion of several subunits results in different levels of developmental defects in wings or eyes (Table II.3), which suggests the small Mediator complex subunits may be required by different transcription activations differently and CDK8-CycC may function independently from the small Mediator complex in a variety of these activations.

II.4.2 Role of Yki/YAP and different kinases in regulating Mad/Smad-dependent transcription

Interestingly, Yki/YAP, which can function as a transcriptional co-factor for Mad/Smad, was also reported to associate with several subunits of the Mediator complex to drive transcription. Specifically, Med12, Med14, Med23, and Med24 were identified from a YAP IP-mass spectrometry sample in HuCCT1 cells [128]. Med23 was also reported to regulate Yki-dependent transcription of *Diap1* in wing discs [129]. In this work, we found that Yki, Med12, Med23, and Med24 were also required for Mad-dependent transcription of *sal-lacZ*.

Based on biochemical analyses of the Smad1 phosphomutants and cell biological analyses using cultured human epidermal keratinocytes (HaCaT cells), several kinases including CDK8, CDK9, and ERK2 were shown to phosphorylate serine residues (S) within the linker region of pSmad1 at S186, S195, S206, and S214, or the equivalent sites in pSmad2/3/5. These modifications were proposed to regulate positively Smad1-dependent transcriptional activity [63]. Of these sites, S206 and S214 are both conserved from *Drosophila* to humans (Fig. II.8B).

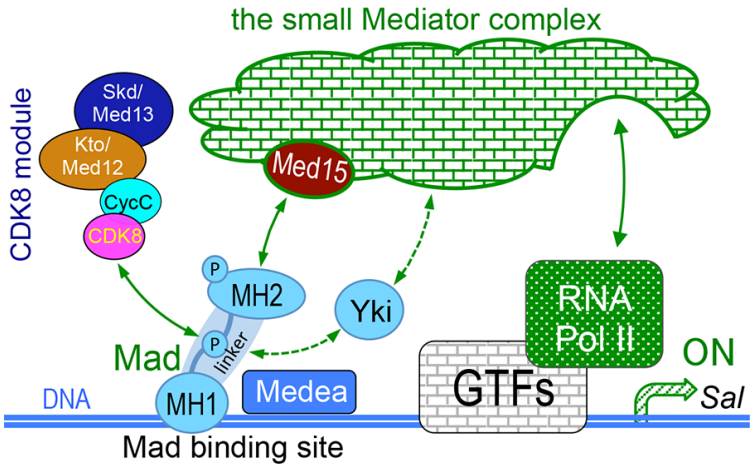

Fig. II.9 Working model. Model of Mad/Smad-dependent transcription activation through the CKM and the Mediator complex. GTFs, General Transcription Factors; MH1, Mad homology 1; MH2, Mad homology 2.

In addition, studies using *Xenopus* embryos and cultured L cells suggest that MAPKs may phosphorylate the linker region of Smad1 (including S214) and lead to its degradation [123]. Nevertheless, analyses with *Drosophila* embryos and wing discs indicate that S212 (equivalent to human pSmad1 S214) is phosphorylated by CDK8, while S204 (unique in *Drosophila*) and S208 (equivalent to human pSmad1 S210) are phosphorylated by Sgg/GSK3 [64]. These studies suggest the following model in explaining how Smads activate the expression of their target genes and how this process is turned off (Fig. II.8A, Fig. II.9): after Smads are phosphorylated at their C-termini and translocated into the nucleus, CDK8 and CDK9 (potentially also MAPKs) act as the priming kinases to further phosphorylate pSmads in the linker region at S206 and S214. This may facilitate the interaction between pSmads and transcriptional cofactors such as YAP, stimulating the expression of Smads target genes. Overexpression of Yki in *Drosophila* wing disc increases the expression of the *vgQE-lacZ* reporter [63], which validates the role of Yki/YAP in activating Mad/Smad1-dependent gene expression *in vivo*. Subsequently, pSmads

are further phosphorylated by GSK3 within the linker region at T202 and S210, which may facilitate Smad1/5 binding to E3 ubiquitin ligases such as Smurf1 and Nedd4L, causing the degradation of Smads through the ubiquitin-proteasome pathway [63, 64, 77, 109, 120].

Although this model (Fig. II.9) is still rather speculative, it serves as a conceptual framework to explain how transactivation of Smads is coupled to its degradation, similar to other transcriptional activators [130]. It is challenging to determine whether these kinases act redundantly or specifically for different phosphorylation sites, the exact orders of these phosphorylation events, as well as their biological consequences *in vivo*. Moreover, it remains unexplored whether these regulatory mechanisms are conserved during evolution. The importance of these issues is highlighted by the critical role of TGFβ signaling in regulating the normal development of metazoans and the dysregulation of this pathway in a variety of human diseases such as cancers [108, 131-133].

The precise spatiotemporal activation of the Dpp signaling pathway in the wings discs is critical for proper formation of the stereotypical vein patterns in *Drosophila* [113, 116]. This model system provides an ideal opportunity to dissect the dynamic regulation of the Mad-activated gene expression in the nucleus. Indeed, depleting CDK8 in wing discs reduces expression of the Mad-dependent *sal-lacZ* reporter, suggesting that CDK8 positively regulates Mad-dependent transcription. This is consistent with the effects of CDK8 on Smad1/5-dependent transcription in mammals [63, 134]. Depleting CDK8 does not affect the phosphorylation of Mad at its C-terminus as revealed by pMad immunostaining (Fig. A.II.8), nor does it affect the physical interaction between CDK8 and the linker region of Mad, supporting the idea that CDK8 may only affect subsequent phosphorylation of Mad, presumably within the linker region.

Besides CDK8-CycC, depleting CDK9-CycT also decreases the expression of the *sal-lacZ* reporter, supporting the notion that CDK8-CycC and CDK9-CycT may play non-redundant roles in further phosphorylating pMad in the nucleus. However, we did not observe any effects of depletion of CDK7 or MAPKs on *sal-lacZ* expression, suggesting that their role in regulating the transcriptional activity of Smads may not be conserved in *Drosophila*. Alternatively, the two MAPK/ERK homologs, Rolled and ERK2, may act redundantly in regulating Mad-dependent transcription. Lastly, depleting Sgg/GSK3 in the dorsal compartment of the wing disc increases the size of this compartment, yet the expression level of the *sal-lacZ* reporter is similar to the ventral compartment. These observations are consistent with previous reports that phosphorylations of Mad/Smad in the linker regions by CDK8-CycC and Sgg/GSK3 regulate the level and range of Mad-dependent gene expression [63, 64, 77, 109, 120].

Together with the previous reports [63, 64, 77, 109, 120, 135], our data support that CDK8-CycC and CDK9-CycT may phosphorylate pMad at the linker region, which may facilitate the binding between Yki and Mad. We speculate that this interaction may synergize the recruitment of the Mediator complex, presumably at least through the interaction between its Med15 subunit and the MH2 domain of Mad (Fig. II.9). Alternatively, Yki may also facilitate the recruitment of the whole Mediator complex through its interactions with Med12, Med23, and Med24. The synergistic interactions among Mad, Yki, the Mediator complex, and RNA Pol II may be required for the optimal transcriptional activation of the Mad-target genes (Fig. II.9).

One of the challenges is to illustrate the dynamic interactions between these factors and diverse protein complexes that couple the transactivation effects of Mad/Smads on gene transcription with their subsequent degradation at the molecular level. Smad3 phosphorylation strongly correlates with Med15 levels in breast and lung cancer tissues; together, they potentiate

metastasis of breast cancer cells [136]. Thus, it will be important to test whether additional Mediator subunits that we identified in *Drosophila* play similar roles in mammalian cells. It will also be interesting to determine whether a partial Mediator complex, composed of a subset of the Mediator subunits, exists and regulates Mad/Smad-dependent gene expression. Furthermore, detailed biochemical analyses may yield mechanistic insights into how CDK8 and Med15 act in concert in stimulating the Mad/Smad-dependent gene expression.

II.4.3 Potential role of CDK8-CycC in regulating cross-talks among different signaling pathways

Wing pouch-specific alteration of CDK8 activity results in two major phenotypes: disrupted vein patterns and altered size of wing blades. While the effects on wing size and cell numbers can be explained by the role of CDK8 in regulating cell proliferation through E2F1 [59, 60], the effects of CDK8 on vein patterning are more complex. The stereotypical wing vein patterns in adult flies are gradually defined by elaborated spatiotemporal interplays among different signaling pathways, including Dpp, EGFR, Hedgehog (Hh), Notch (N), and Wingless (Wg), in the developing wing discs [109, 113, 114, 116]. During the larval and pupal stages, these signaling pathways and their downstream transcriptional targets coordinately control the cell proliferation and differentiation of cell in different parts of the wing disc to form individual veins.

It is noteworthy that varying CDK8 activities has different effects on different veins: gain of CDK8 causes the loss of the L3 and L4 veins, but the vein patterns of L2 and L5 appear thicker and more diffusive; while the ectopic veins caused by reduction of CDK8 are mainly intertwined with the L2 and L5 veins (Fig. II.1). Our analyses on the genetic interactions between CDK8 and the components of the Dpp signaling pathway led us to discover the role of

the Mediator complex in Mad-stimulated transcription of *sal*. However, there is a gap in our understanding of how reduced expression of *sal* in wing discs is linked to the vein defects in adult wings. It is known that *salm* and *spalt-related* (*salr*), two members of the *spalt* gene family that encode zinc-finger transcriptional repressors, function downstream of the Dpp signaling pathway during development of the central part of the wing [137]. Depletion of either *salm* or *salr* alone resulted in ectopic vein formation around L2 in adult wings, yet depletion or loss of both *salm* or *salr* caused loss of vein phenotype [115, 138]. In addition, elimination of L2 in ventral-anterior and ectopic L5 in dorsal-posterior were observed in *salm/salr* clones at different region of the wing [115]. These observations suggest that the dosage of *salm* and *salr* in wing discs does not have a linear relationship with the wing vein patterning at the adult stage.

Interestingly, it is known that the CKM complex regulates the transcriptional activities of the key transcription factors of these pathways, including N-ICD downstream of N signaling [61], Mad/Smad proteins ([63, 64] and this work). In addition, Med12 (Kohtalo, or Kto in *Drosophila*) and Med13 (Skuld, or Skd in *Drosophila*) subunits of the CKM interact with Pangolin (the lymphoid-enhancing factor (LEF)/T cell factor (TCF) homolog in *Drosophila*), the key transcription factor downstream of Wg signaling, through the transcriptional cofactors such as Pygopus, Legless, and Armadillo [139]. In mammalian cells, Med12 is also known to regulate the activities of Gli proteins, the key transcription factors downstream of Hh signaling [140, 141]. Furthermore, the Mediator subunit Med23 interacts with ETS (E-twenty six transcription factor) proteins, a family of key transcription factors downstream of the EGFR signaling pathway [127]. However, whether CDK8-CycC also regulates TCF-, ETS- or Gli-dependent transcription is still not understood. Nevertheless, these studies in other biological contexts suggest that the effects of CDK8 on wing vein patterning are not likely solely through the Dpp

signaling pathway. Therefore, we speculate that the potential interactions between CDK8 and the aforementioned signaling pathways may contribute to these differential effects on distinct veins. Further analyses of these cross-talks, as well as further mapping of other *Df* lines that modify the CDK8-specific vein phenotypes, may yield the insights into the molecular and dynamic mechanisms underlying these vein phenotypes.

II.4.4 Identification of novel genomic loci that genetically interact with CDK8 in vivo

To understand how dysregulated CDK8-CycC contributes to a variety of human cancers, it is essential to elucidate the function and regulation of CDK8 *in vivo*. Given that the CDK8-CycC pair and other subunits of the Mediator complex are conserved in almost all eukaryotes [5], *Drosophila* serves as an ideal model system to identify both the upstream regulators and the downstream effectors of CDK8 activity *in vivo*. Our dominant modifier genetic screen is based on the wing vein phenotypes caused by specific alteration of CDK8 activity in the developing wing disc, which serves as a unique *in vivo* readout for the CDK8-specific activities in metazoans. This screen led us to identify 26 genomic regions that include loci whose haplo-insufficiency could consistently modify CDK8-CycC depletion or CDK8-overexpression phenotypes. Identification of *Dad* and genes encoding additional components of the Dpp signaling pathway provides a proof of principle for this approach. Since each of the chromosomal deficiencies uncovers multiple genes, further mapping of the relevant genome regions is expected to identify the specific genetic loci encoding factors that may function either upstream or downstream of CDK8 *in vivo*. It is hoped that further analyses of the underlying molecular mechanisms in both *Drosophila* and mammalian systems will advance our understanding of how dysregulation of CDK8 contributes to human diseases, thereby aiding the development of therapeutic approaches.

CHAPTER III

ASYMMETRIC INTERDEPENDENCY AMONG THE FOUR SUBUNITS OF THE CDK8 MODULE IN *DROSOPHILA*

III.1 Introduction

The multiprotein RNA polymerase II (Pol II) complex is required for the transcription of mRNAs and many non-coding RNAs in eukaryotic cells [142, 143]. Recruited by transcriptional activators, concerted actions of distinct multiprotein complexes, such as general transcription factors, Pol II, and the Mediator complex, are essential to achieve the precise control of Pol II initiation and elongation [142, 144]. Of these transcriptional complexes, the Mediator complex is the largest protein complex, composed of up to 30 conserved subunits that have been assigned to four distinct modules, the head module, the middle module , the tail module, and the CDK8 kinase module (CKM) [2, 5, 7, 142, 145].

The CKM complex is composed of four subunits, CDK8 (or its vertebrate paralog CDK19, also known as CDK8L), CycC, Med12 (or MED12L in vertebrates), and Med13 (or MED13L in vertebrates). There are two current models to explain how CKM regulates transcription: CKM can reversibly associate with the small Mediator complex, which comprises the head, middle, and tail modules, thereby blocking the interactions between the small Mediator complex and Pol II, and inhibiting the Pol II-dependent transcription [146, 147]; alternatively, the CDK8 kinase of CKM can phosphorylate a variety of transcription factors, thereby modulating their transcriptional activities in different biological contexts [59-66, 148-150].

Biochemical purification of the CKM in yeast and mammals have revealed that the four CKM subunits can be purified together, and the structure of CKM has been determined using the cryogenic electron microscopy (cryo-EM) [147, 151, 152]. In addition, both CycC and Med12

are required for the CDK8 kinase activity *in vitro* kinase assays [151], and the direct interactions between the N-terminal segment of MED12 and the T-loop of CDK8 is essential for CDK8 activation [152]. Consistent to these studies, missense mutations in exon 2 encoding part of the N-terminal segment of MED12, which have been identified in more than 62% of uterine leiomyomas across countries [52], significantly reduce the kinase activities of CDK8-CycC or CDK19-CycC [153]. These biochemical analyses suggest that the four subunits of the CKM complex function together.

Despite these elegant biochemical and structural studies, a number of genetic analyses in *Drosophila* suggest that the four subunits of CKM may have distinct functions during development. For example, null mutants of *kto* (encoding Kohtalo or *Drosophila* Med12) and *skd* (encoding Skuld of *Drosophila* Med13) are embryonic lethal, while *cdk8* and *cycC* null mutants are pupal lethal [71, 85, 154]. In addition, genetically ablating CDK8, CycC, Med12 (Kto), or Med13 (Skd) in *Drosophila* eye or leg results in distinct phenotypic consequences: tissue-specific loss of either Med12 or Med13 in eye or leg imaginal discs led to severe defects in adult eyes and legs, while tissue-specific ablation of CDK8 or CycC in eye or leg discs caused only minor defects in legs and no defects in eyes [71, 155]. The results of these genetic analyses are puzzling, considering the notion that the four subunits of CKM function together based on aforementioned biochemical analyses.

In this work, we have generated a set of transgenic *Drosophila* lines that allow us to knock down the four subunits of the CKM either alone or in all possible combinations. We have observed distinct phenotypes when these subunits are depleted in *Drosophila* eyes. At the cellular level, depleting CDK8-CycC promotes cell proliferation, while depleting Med12-Med13 does not obviously affect cell proliferation. Moreover, we have observed that the stabilities of the

four CKM subunits are asymmetrically interdependent: the stability of CDK8 is dependent on Med12 and Med13, but not CycC; the stabilities of Med12 and Med13 are interdependent to each other, while removing either CDK8 or CycC has no effects of the stabilities of MED12 and Med13. Given the reports showing that four subunits of the CKM are either mutated or amplified in a number of human cancers, cardiovascular and other diseases [10-12, 156], elucidating the specific impacts of these mutations on the function of the CKM, versus the kinase activities of CDK8 or CDK19, may advance our understanding of how mutations of these CKM subunits contribute to tumorigenesis in in different pathological contexts.

III.2 Materials and Methods

III.2.1 Fly strains

Flies were raised on a standard cornmeal, molasses and yeast medium, and all genetic crosses were maintained at 25˚C. We obtained the following strains from the Bloomington *Drosophila* Stock Center: *ap-Gal4* (BL-3041), *nub-Gal4* (BL-25754), *w1118; Kr^{If-1}/CyO, P{en1}wg^{en11}; P{Ubi-GFP.E2f1.1-230}5 P{Ubi-mRFP1.NLS.CycB.1-266}12/TM6B, Tb^{1}* (BL-55124). The following recombined lines were generated by this work: *ap-Gal4/ In (2LR), wg^{Gla}, Bc; P{Ubi-GFP.E2f1.1-230}5 P{Ubi-mRFP1.NLS.CycB.1-266}12, ap-Gal4; Cdk8-EGFP/SM6::TM6B, Tb, ap-Gal4; Med12-EGFP/SM6::TM6B, Tb, ap-Gal4; Med13-EGFP/SM6::TM6B, Tb.*

III.2.2 Generation of transgenic RNAi flies

Transgenic RNAi lines that allow us to deplete different combinations of the four CKM subunits were generated using the pNP vector (Qian HH 2018). Specifically, pairs of oligoes were synthesized for each gene (detailed information on these oligoes is included in the Table III.1). To knock down one gene at a time, the oligoes were annealed and cloned into the pNP

vector digested with EcoRI/NheI. The resulting plasmids contained one short hairpin. To simultaneously deplete two genes, one plasmid obtained from the first step was digested with SpeI, and ligated with the short hairpin fragment (300bp) released from another plasmid by SpeI/XbaI digestion. The resulting plasmids contained two short hairpins. This process is reiterated to generate the plasmids containing three or four short hairpins. Transgenic fly lines were produced by injecting these constructs into *y sc v nanos-integrase; attP2* stock by following the standard procedure [79].

III.2.3 Tagging the endogenous loci with EGFP using the CRISPR-Cas9 technique

To tag EGFP to the endogenous loci of *Cdk8*, *Med12*, and *Med13*, three constructs were designed. The pCFD3 vector was used to express two sgRNA to make two double strand breaks of *Cdk8* gene with primers gRNA-Cdk8- L-5.1, gRNA-Cdk8-L-3.1, gRNA-Cdk8-R-5.1, gRNA-Cdk8-R-3.1 as described in general protocol for pCFD3 (citing http://www.crisprflydesign.org/wp-content/uploads/2014/05/Cloning-with-pCFD3.pdf), near the 5' and 3' Untranslated Region (UTR) of *Cdk8* gene. A donor DNA was provided as a Homolog Directed Recombination (HDR) template, which contained *Cdk8* gene, EGFP inserted before the stop codon (Cdk8+EGFP-5.1 and Cdk8+EGFP-3.1), 1kb upstream of 5' break point (Homology_arm-Cdk8-L-5.1 and Homology_arm-Cdk8-L-3.1) and 1kb downstream of 3' break point (Homology_arm-Cdk8-R-5.1 and Homology_arm-Cdk8-R-3.1) as homology arm guide to align with fly genome. The Protospacer Adjacent Motif (PAM) sites were mutated to avoid unnecessary cuts, which were designed within the above primers. All the three fragments were amplified by PrimeStar Max premix (Takara, R045A) and assembled into pGEM-T easy vector (Promega, A1360) by NEBuilder HiFi DNA Assembly (NEB, E5520S). Then, all of the three constructs were co-injected together to embryo of fly strain, *nos-Cas9* by the Rainbow

Transgenic Flies, Inc (Camarillo, CA). The successful insertion was screened by genotyping with PCR (Cdk8-EGFP-test-5.1, Cdk8-EGFP-test-3.1).

III.2.4 Immunocytochemistry

Wing discs staining followed the same protocol as described before [157]. Phosphorylated Histone 3 Serine 10 signal was detected using an anti-PH3 monoclonal antibody (1:1000 in PBS-Triton X-100-NGS-BSA; obtained from the Sigma-Aldrich). Cleaved Dcp-1 (Asp216) was detected by anti-cleaved Dcp-1 (1:1000 in PBS-Triton X-100-NGS-BSA; purchased from Cell Signaling, #9578). The secondary antibodies with fluorescent were goat anti-guinea pig (106-545-003), goat anti-mouse (115-545-003), or goat anti-rabbit (111-545-003) (from Jackson Immunological Laboratories).

III.3 Results

III.3.1 Depletion of the CKM subunits distinctively impacts Drosophila development

Previous studies show that the null mutants of *Cdk8* and *CycC* are pupal lethal, while that the null mutants of *Med12* (*kto*) and *Med13* (*skd*) are embryonic lethal [71, 85, 154, 155]. To determine the specific roles of individual CKM subunits during development, it is critical, but technically difficult, to simultaneously remove these subunits in different combinations in a tissue-specific manner. To circumvent this challenge, we took the advantage of the pNP vector, which allows simultaneous expression of multiple shRNAs specifically targeting distinct genes [158]. We have generated a set of transgenic RNAi *Drosophila* lines using this pNP vector to deplete the four CKM subunits either alone or in different combinations (Table III.1). Specifically, four lines were generated to knock down each of the four subunits alone (*UAS-CDK8-RNAi, UAS-CycC-RNAi*, *UAS-Med12-RNAi*, and *UAS-Med13-RNAi*); six lines were designed to target different combinations of the two subunits of the CKM (*UAS-CDK8-i-CycC-i,*

UAS-CDK8-i-Med12-i, UAS-CDK8-i-Med13-i, UAS-CycC-i-Med12-i, UAS-CycC-i-Med13-i, UAS-Med12-i-Med13-i); one line to simultaneously deplete three subunits (*UAS-CDK8-i-CycC-i-Med12-i*); and one line to knock down all the four subunits (*UAS-CDK8-i-CycC-i-Med12-i-Med13-i* (see Materials and Methods for details). To ensure consistent expression levels of shRNAs, all these constructs were site-specifically integrated into the attP2 site on the third chromosome [159].

Table III.1. Transgenic RNAi lines to deplete the CKM subunits in different combinations

Single knock down	**Double knock down**	**Triple knock down**	**Quadruple knock down**
UAS-Cdk8-RNAi	*UAS-Cdk8-CycC-RNAi*	*UAS-Cdk8-CycC-Med12-RNAi*	*UAS-Cdk8-CycC-Med12-Med13-RNAi*
UAS-CycC-RNAi	*UAS-Cdk8-Med12-RNAi*		
UAS-Med12-RNAi	*UAS-Cdk8-Med13-RNAi*		
UAS-Med13-RNAi	*UAS-CycC-Med12-RNAi*		
	UAS-CycC-Med13-RNAi		
	UAS-Med12-Med13-RNAi		

To analyze the function of distinct CKM subunits *in vivo*, we used *eyeless-Gal4* (*ey-Gal4*) to deplete these subunits in different combinations in *Drosophila* eye. Compared to the control (Fig. III.1A), depletion of either CDK8 (Fig. III.1B) or CycC (Fig. III.1C) alone or both CDK8 and CycC (Fig. III.1D) had no obvious effects on *Drosophila* eye development, while depleting Med12 (Fig. III.1E) or Med13 (Fig. A.III.1A) severely reduced size of the adult eyes. These observations are consistent to the previous report that eye-specific removal of CDK8 or

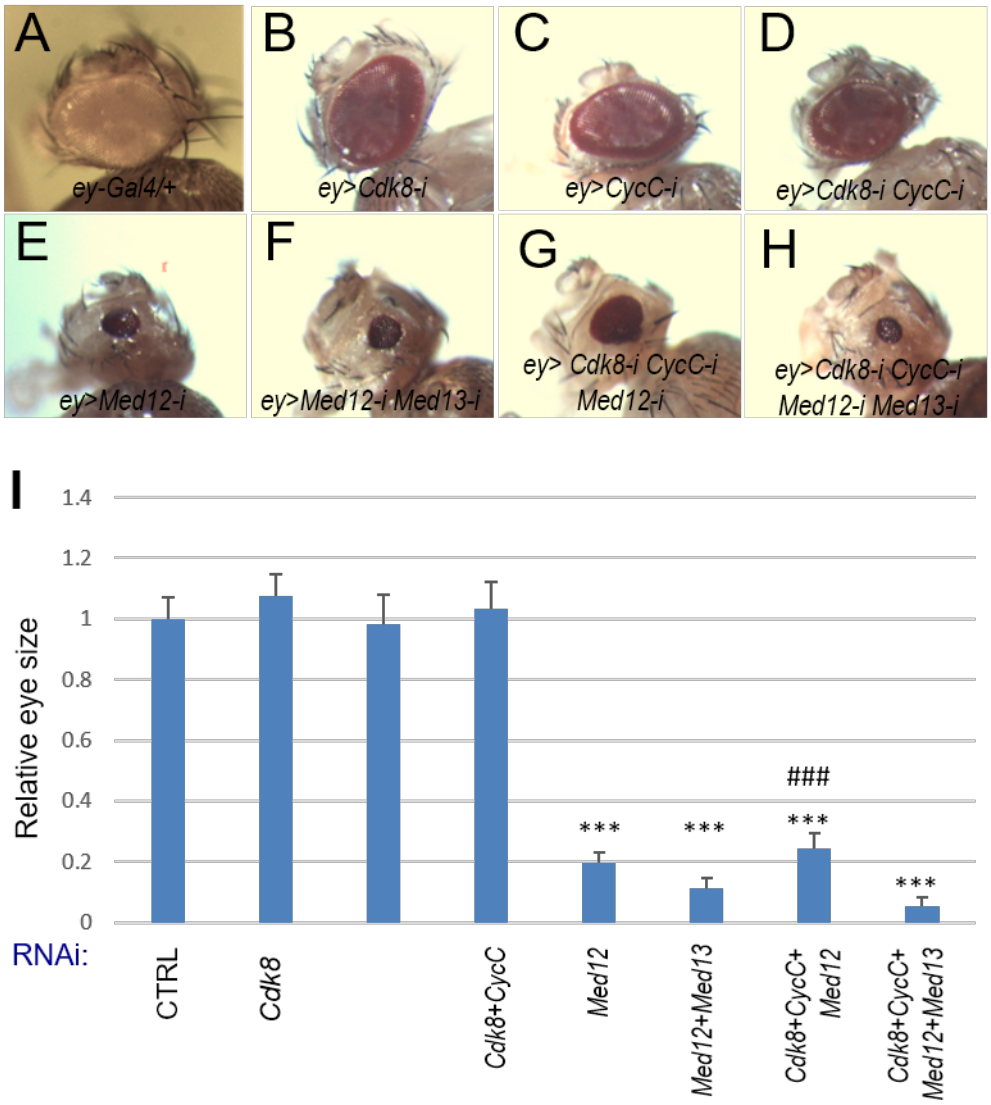

Fig. III.1. Eye defects caused by depletion of different combinations of the CKM subunits. Adult female eyes of (A) *ey-Gal4/+* (control); (B) *ey-Gal4/+; UAS-Cdk8-RNAi/+*; (C) *ey-Gal4/+; UAS-CycC-RNAi/+*; (D) *ey-Gal4/+; UAS-Cdk8-RNAi CycC-RNAi/+*; (E) *ey-Gal4/+; UAS-Med12-RNAi* (F) *ey-Gal4/+; UAS-Med12-RNAi Med13-RNAi/+*; (G) *ey-Gal4/+; UAS-Cdk8-RNAi CycC-RNAi UAS-Med12-RNAi/+*; and (H) *ey-Gal4/+; UAS-Cdk8-RNAi CycC-RNAi UAS-Med12-RNAi Med13-RNAi/+*; (I) Quantification of eye sizes.

CycC did not affect eye development, but removal of Med12 alone, or Med12 and CDK8 together, severely reduced the eye size [71]. Depletion of both Med12 and Med13 resulted in even smaller eyes than depleting either Med12 or Med13 alone, indicating that these phenotypes

are hypomorphic and modifiable (Fig. III.1F). However, depleting CDK8-Med12 (Fig. A.III.1B) had similar eye size to depleting Med12 alone, and the eye size of depleting CDK8-Med13 (Fig. A.III.1C) or CycC-Med13 (Fig. A.III.1D) were similar to depleting Med13 alone. Interestingly, simultaneous depletion of CDK8 and CycC (Fig. III.1G) or CycC (Fig. A.III.1E) alone together with Med12 led to larger eyes than knocking down Med12 alone (Fig. III.1D), although the eye size of these flies was still smaller than control. This result indicates a partial rescue of the Med12-RNAi phenotype by depleting CycC alone or CDK8 and CycC together. The partially rescue effects indicate that Med12-Med13 and CDK8-CycC may antagonize with each other during *Drosophila* eye development. Furthermore, knocking down all four CKM subunits (Fig. III.1H) led to similar effects to those caused by depleting Med12 and Med13 together (Fig. III.1F), indicating that the rescuing effects of CDK8-CycC is dependent on residual Med12-Med13. Quantification of these effects is shown in Fig. III.1I.

Quantification of the eye phenotypes using this set of transgenic RNAi lines reveals four distinct classes of the RNAi effects (Fig. III.1I): depletion of CDK8, CycC, or both CDK8 and CycC (Fig. III.1B, 1C and 1D) has no effects on eye sizes (designated as the Class I); depleting Med12 or Med13 alone (Fig. III.1D and A.III.1A) reduced the eye sizes (designated as the Class II); simultaneous depletion of one or two subunits of CDK8-CycC pair partially rescues the small eye phenotype caused by depleting Med12 alone (Fig. III.1G, A.III.1E and 1I, designated as the Class III); and finally, knocking down both Med12 and Med13 (Fig. III.1F), or all four subunits of the CKM (Fig. III.1H) resulted in the most severe small eye phenotypes compared to other combinations (designated as the Class IV). These observations suggest that the CKM, particularly Med12 and Med13, plays critical roles in eye development. These analyses also reveal an antagonistic function between the CDK8-CycC pair and the Med12-Med13 pair *in*

vivo, which is unexpected because the four subunits of the CKM can be biochemically purified as a complex and have been assumed to function together. For simplicity, we focus on the following representative lines for each class in our subsequent analyses: *UAS-Cdk8-i, CycC-i* for Class I, *UAS-Med12-i* for Class II, *UAS-Cdk8-i, CycC-i, Med12-i* for Class III, *UAS-Med12-i, Med13-i* and *UAS-Cdk8-i, CycC-i, Med12-i, Med13-i* for Class IV.

We further test the effects of depleting different subunits of the CKM in *Drosophila* wing with *apterous-Gal4* (*ap-Gal4*), which is specifically expressed in the dorsal compartment of wing discs [90]. When CDK8 and CycC were depleted, the adult wings curled downwards to the ventral side of the wing (Fig. A.III.2B), consisting with the inhibitory effects of CDK8 on cell proliferation [59, 157]. In contrast, depleting Med12 (Fig. A.III.2C) alone severely disrupted the morphology of the wing, accompanied with blisters and shrunk wing blades. Similar effects were observed when CDK8 and CycC were depleted together with Med12 (Fig. A.III.2D). Depleting Med12 and Med13 together (Fig. A.III.2E) or depleting all four subunits simultaneously (Fig. A.III.2F) resulted in stronger defects in wing and thorax development, which disable the flies from eclosing or caused pupal lethality. These wing phenotypes are difficult to quantify, thus we further analyzed the effects at the cellular level in wing discs (see below).

III.3.2 Distinct roles of the CKM subunits in regulating cell proliferation in wing discs

At the cellular level, altered organ sizes can be caused by changes in cell proliferation, cell death, or both. To examine the antagonistic effects between CDK8-CycC and Med12-Med13 at the cellular level, we first determined the potential effects of depleting subunits of the CKM on apoptosis where we used cleaved Death caspase-1 (Dcp-1, homolog of Caspas-3) antibody to mark the apoptotic cells in wing disc [160]. As shown in Fig. A.II.2A, the cleaved Dcp-1 positive cells are rarely detected in the wing pouch area of the control discs. Using *ap-Gal4* to

deplete the five representative combinations of the CKM subunits did not alter the distribution or the number of Dcp-1 marked cells (Fig. A.III.3B-F), suggesting that knocking down of the CKM subunits has little effects on apoptosis.

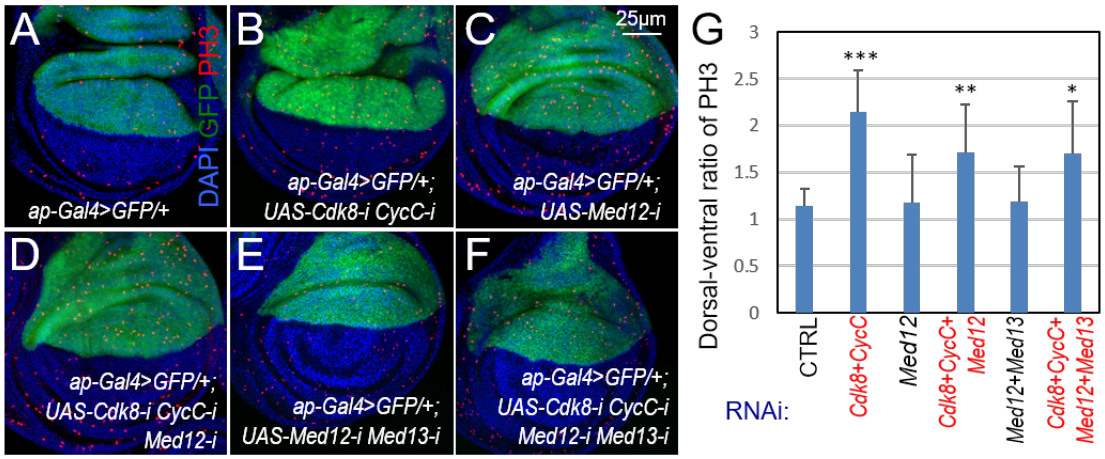

Fig. III.2. Effects of depleting different combinations of the CKM subunits on the cell proliferation. Representative confocal images of wing discs with anti-PH3 (red) staining of the following genotypes: (A) *ap-Gal4/+;* (B) *ap-Gal4/+; UAS-Cdk8-RNAi CycC-RNAi/+*; (C) *ap-Gal4/+; UAS-Med12-RNAi*; (D) *ap-Gal4/+; UAS-Cdk8-RNAi CycC-RNAi UAS-Med12-RNAi/+*; (E) *ap-Gal4/+; UAS-Med12-RNAi Med13-RNAi/+*; (F) *ap-Gal4/+; UAS-Cdk8-RNAi CycC-RNAi UAS-Med12-RNAi Med13-RNAi/+*; (G) Quantification of the PH3 signal ratio comparing Doral and Ventral compartment. At least five wing discs were examined for each genotype. Scale bar in C: 25μm.

Next, we examined the effects of depleting the CKM subunits on cell proliferation with an anti-phospho-Histone H3 on Serine 10 (PH3) antibody, which marks the mitotic cells in wing discs. In control disc, PH3-positive cells are randomly distributed throughout the wing disc, and the ratio of the mitotic cells in the dorsal compartment to them in the ventral compartment is around one (Fig. III.2A and 2G). Depleting both CDK8 and CycC (Fig. III.2B) with *ap-Gal4* significantly increased the PH3-positive cells in the dorsal compartment compared to the ventral compartment of the same wing discs. However, depletion of Med12 alone (Fig. III.2C), or both

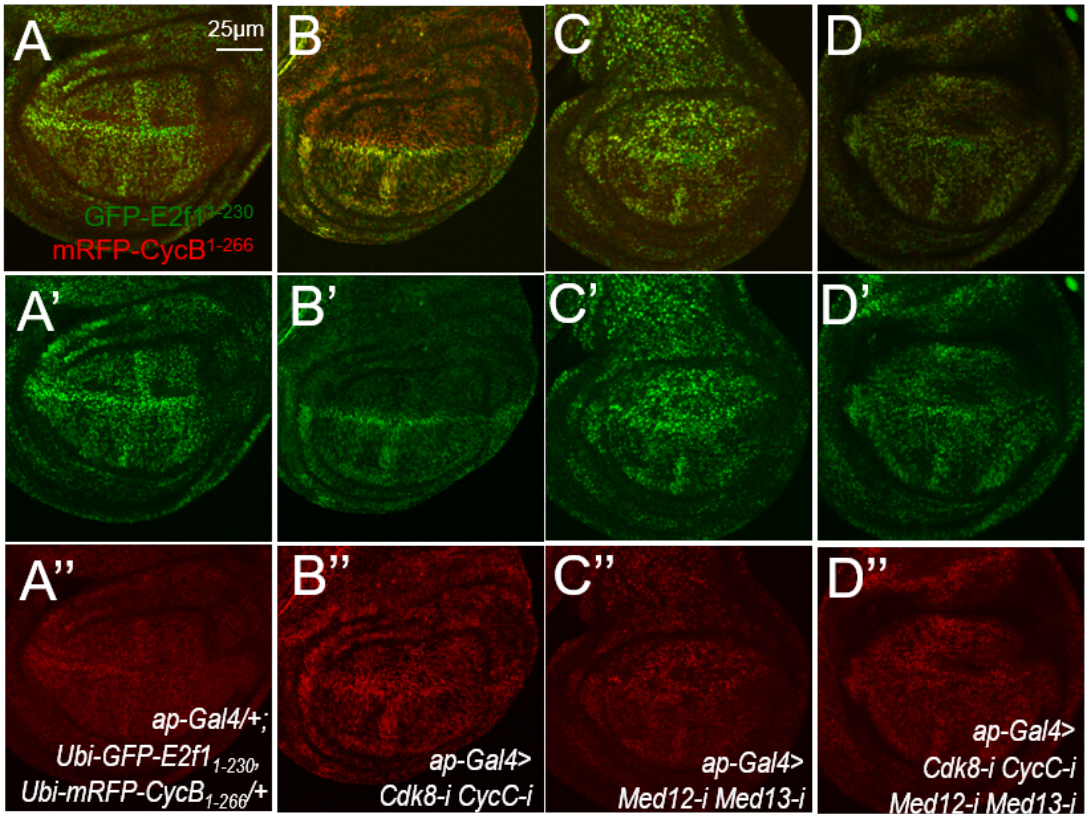

Fig. III.3. Different effects on cell cycle progression by depleting different combinations of the CKM subunits. Representative confocal images of wing discs of the following genotypes: (A) merge channel, (A') GFP-E2f1$_{1-230}$ (green) channel and (A'') mRFP-CycB$_{1-266}$ (red) channel of *ap-Gal4/+;Ubi-GFP-E2f1*$_{1-230}$, *Ubi-mRFP-CycB*$_{1-266}$*/+;* (B) merge channel, (B') GFP-E2f1$_{1-230}$ (green) channel and (B'') mRFP-CycB$_{1-266}$ (red) channel of *ap-Gal4/+;Ubi-GFP-E2f1*$_{1-230}$, *Ubi-mRFP-CycB*$_{1-266}$*/UAS-CDK8-RNAi CycC-RNAi*; (C) merge channel, (C') GFP-E2f1$_{1-230}$ (green) channel and (C'') mRFP-CycB$_{1-266}$ (red) channel of *ap-Gal4/+;Ubi-GFP-E2f1*$_{1-230}$, *Ubi-mRFP-CycB*$_{1-266}$*/UAS-Med12-RNAi Med13-RNAi;* (D) merge channel, (D') GFP-E2f1$_{1-230}$ (green) channel and (D'') mRFP-CycB$_{1-266}$ (red) channel of *ap-Gal4/+;Ubi-GFP-E2f1*$_{1-230}$, *Ubi-mRFP-CycB*$_{1-266}$*/CDK8-RNAi CycC-RNAi Med12-RNAi Med13-RNAi.* At least five wing discs were examined for each genotype. Scale bar in A: 25µm.

Med12 and Med13 (Fig. III.2E), did not affect the number of mitotic cells, as the dorsal-ventral ratios of PH3-positive cells are close to one (Fig. III.2G). Interestingly, depletion of CDK8 and

CycC in addition to Med12 significantly increased the number of PH3-positive cells in the dorsal compartment (Fig. III.2D and 2G); similar observations were made when Med12 and Med13 was depleted together with CDK8 and CycC (Fig. III.6F and 2G). These observations suggest that depletion of CDK8-CycC increases the number of cells entering mitosis, while depletion of Med12-Med13 had no obvious effects on mitosis.

To further analyze the effects of depleting the CKM subunits on cell-cycle progression, we utilized the Fluorescent Ubiquitination-based Cell Cycle Indicator (FUCCI) technology in *Drosophila*, or the Fly-FUCCI system, which provides a sophisticated *in vivo* readout of cell-cycle status of cells in complex developmental contexts [161]. In this system, combined expression of two fluorescent reporters, GFP-dE2f1$_{1\text{-}230}$ and mRFP-dCycB$_{1\text{-}266,}$ in all cells of developing tissues enables the labeling of cells in G1 phase with green fluorescence, cells in S phase are labeled in red, while the cells at the G2 phase express both probes and appear yellow [161].

In the control disc, EGFP- and RFP-labeled cells are randomly distributed in the majority part of the wing discs (Fig. III.3A), suggesting that these cells are dividing asynchronously. Depleting both CDK8 and CycC (Fig. III.3B), in dorsal compartment of wing discs with *ap-Gal4*, significantly increased red cells in the dorsal compartment, suggesting that reduction of CDK8-CycC potentiates the cells to enter into the S phase. This observation is consistent with the model that CDK8 functions as a negative regulator of E2F1, the key transcription factor that controls the G1-S phase transition [59, 60, 162]. However, compared to the cells in the ventral compartment, depletion Med12 and Med13 together, in the dorsal compartment did not cause any obvious effects on the distribution of cell-cycle phases (Fig. III.3C). Similarly, simultaneous depletion of all four subunits of the CKM (Fig. III.3D), in the dorsal compartment also did not

have any obvious impacts on the cell-cycle progression compared to the cells in the ventral compartment. Taken together, these results suggest that depletion of CDK8-CycC increases cell proliferation by promoting the entry of both S phase and mitosis, while depletion of Med12-Med13 does not.

III.3.3 Asymmetric interdependency among the CKM subunits

Previously, we have reported that CycC protein is destabilized in *cdk8* mutant larvae, but the stability of CDK8 protein is not affected in *cycC* mutants [85]. Although the underlying mechanism for this phenomenon remains unknown, we asked whether loss of one subunit of the CKM could affect the levels of other three CKM subunits. This question is difficult to address, due to limitations of the available antibodies against the CKM subunits for cell biological and biochemical assays.

To rigorously analyze the protein levels of the CKM subunits, we have tagged to the endogenous loci of *Cdk8*, *Med12* and *Med13* with an enhanced green fluorescent protein (EGFP), and the endogenous locus of *CycC* with a red fluorescent protein (RFP), using the CRISPR-Cas9 technique (see Materials and Methods for details). All these tags were added to the C-termini of the CKM subunits, designated as CDK8-EGFP, CycC-RFP, Med12-EGFP, and Med13-EGFP. The homozygous of all these EGFP- or RFP-tagged lines are fully viable and fertile, suggesting that the fluorescent protein tags do not interfere the normal function of the CKM subunits *in vivo*. The specificity of these four lines was verified by PCR, and more importantly, by the genetic and cell biological analyses as described below. These powerful genetic tools allowed us to deplete a single subunit of the CKM using *ap-Gal4*, and then analyze the potential impacts to the levels of all CKM subunits.

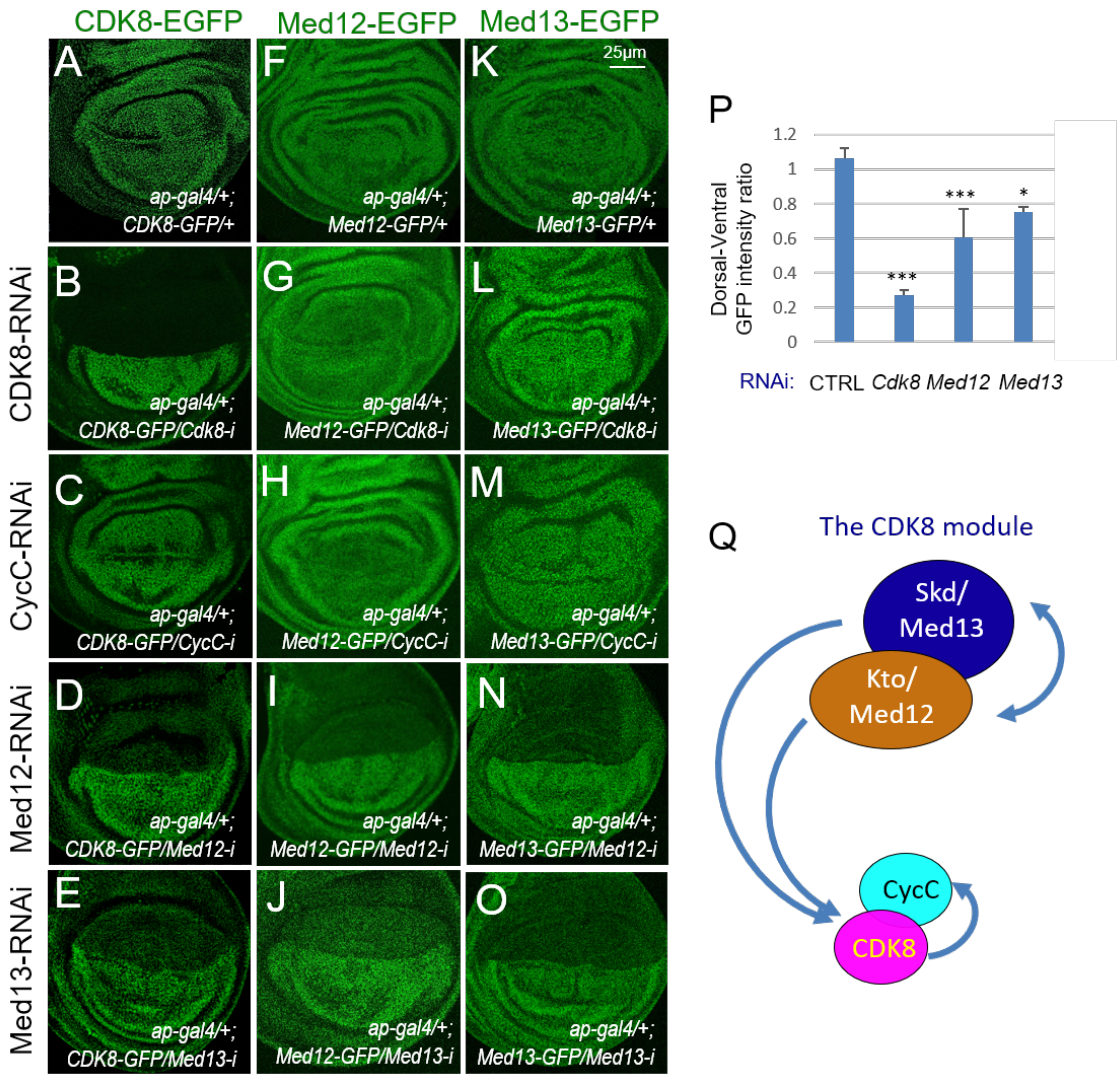

Fig III.4. Asymmetric interdependency among the four CKM subunits. Representative confocal images of wing discs with CDK8-EGFP (green) of the following genotypes: (A) *ap-Gal4/+;CDK8-EGFP/+;* (B) *ap-Gal4/+;CDK8-EGFP/UAS-CDK8-i*; (C) *ap-Gal4/+;CDK8-EGFP/UAS-CycC-i*; (D) *ap-Gal4/+;CDK8-EGFP/UAS-Med12-i*; (E) *ap-Gal4/+;CDK8-EGFP/UAS-Med13-i*; with Med12-EGFP (green) of the following genotypes: (F) *ap-Gal4/+;Med12-EGFP/+;* (G) *ap-Gal4/+;Med12-EGFP/UAS-CDK8-i*; (H) *ap-Gal4/+;Med12-EGFP/UAS-CycC-i*; (I) *ap-Gal4/+;Med12-EGFP/UAS-Med12-i*; (J) *ap-Gal4/+;Med12-EGFP/UAS-Med13-i*; with Med13-EGFP (green) of the following genotypes: (K) *ap-Gal4/+; Med13-EGFP/+;* (L) *ap-Gal4/+; Med13-EGFP/UAS-CDK8-i*; (M) *ap-Gal4/+;Med13-EGFP/UAS-CycC-i*; (N) *ap-Gal4/+; Med13-EGFP/UAS-Med12-i*; (O) *ap-Gal4/+;Med13-EGFP/UAS-Med13-i.* (P) Quantification of CDK8-EGFP signal comparing Dorsal vs Ventral compartment. (Q)Summary of the asymmetric interdependency. At least five wing discs were examined for each genotype. Scale bar in K: 25μm.

In wing discs from the third instar larvae, CDK8-EGFP (Fig. III.4A), Med12-EGFP (Fig. III.4F), and Med13-EGFP (Fig. III.4K) are even expressed in the nuclei of all cells. When CDK8 was depleted in the dorsal compartment of wing disc using *ap-Gal4*, CDK8-EGFP level was significantly reduced as expected (Fig. III.4B). Similarly, knocking down Med12 diminished Med12-EGFP levels (Fig. III.4I), and depleting Med13 ablated Med13-EGFP levels (Fig. III.4O). These results validate the specificity and efficacy of both the transgenic RNAi lines targeting the CKM subunits as well as the EGFP tagged lines for these CKM subunits.

More importantly, these genetic tools have allowed us to define the impacts of losing one subunit on the levels of other CKM subunits *in vivo*. We have observed that depletion of Med 12 (Fig. III.4D) or Med13 (Fig. III.4E) in the dorsal compartment also reduced the levels of CDK8-EGFP, which are statistically significant shown in Fig. III.4P, while depleting CycC has no effects on level of CDK8-EGFP (Fig. III.4C).

Interestingly, depletion of CDK8 or CycC in the dorsal compartment of wing discs has no effects on the levels of Med12-EGFP (Fig. III.4G and Fig. III.4H), or the levels of Med13-EGFP (Fig. III.4L and Fig. III.4M), suggesting that the levels of Med12 or Med13 are not dependent on CDK8 or CycC. However, knocking down Med13 significantly reduced the levels of Med12-EGFP (Fig. III.4J), while depleting Med12 also reduced the Med13-EGFP level (Fig. III.4N), suggesting that the levels of Med12 and Med13 are dependent on each other. These results show that the stability of CDK8 is dependent Med12 and Med13, but not on CycC; the stability of Med12 and Med13 are interdependent on each other, but not on CDK8 or CycC (Fig. III.5Q).

To test whether the subunits are degraded through 20S proteasome with ubiquitination independent manner, we predicted the potential intrinsically disordered region of the four subunits (see Discussion below). From ANCHOR2 and IUPred2 predictions, at the end of C-

terminal around 50 amino acid of CDK8 (Fig. A.III.5A), at the end C-terminal of CycC (Fig. A.III.5B), the end of C-terminal around 500 amino acid of Med12 (Fig. A.III.5C) and 500 to 1500 amino acids of Med13 are disordered (Fig. A.III.5D). These predicted intrinsically disordered region provide the structural possibility of 20S based proteasome degradation.

III.4 Discussion

To study *in vivo* functions of the four CKM subunits, we generated genetic tool that allow us to deplete these CKM subunits in different combinations in fly eyes and wings. The specific phenotypes generated by this approach suggest that loss of the different CKM subunits may result in distinct consequences during the eye or wing development. At the cellular level, the major impact of these genetic perturbations of the CKM subunits is on cell-cycle progression, but not apoptosis. Reduction of CDK8 and CycC has a clear impact in regulating the G1-S phase transition. At the molecular level, we have observed that the stabilities of the CKM subunits are asymmetrically interdependent among the four subunits. Our further analyses led us to propose that intrinsic disordered regions in the CDK8, Med12, and Med13 may facilitate their degradation in a 20S proteasome-dependent manner. Taken together, these results have revealed new layer regulatory mechanism in fine-tuning the CKM subunits *in vivo*, which may have important implications in our understanding the *in vivo* impacts of mutation or amplification of specific CKM subunits in pathological contexts.

III.4.1 The four subunits of the CKM function differently on regulating Drosophila eye and wing development

Our observation suggests that CDK8 and CycC may not be required by eye and wing development, while Med12 and Med13 may be essential for them. These results are consistent with previous report showing that eyes with $cdk8^{K185}$ and $cycC^{Y5}$ mitotic clones are normal, while

Med12^{T241} mitotic clones in eye caused strong defects on eye development [71]. In addition, depletion of CDK8 or CycC increased the wing cell number. Interestingly, depletion of different combinations had different impact on eye or wing development. The reduced eye size by depleting Med12 or Med13 can be reversed by additionally depletion of CDK8, CycC or both. However, depleting Med12 and Med13 together caused stronger defects on eye development, which cannot be rescued by additional knock down of CDK8, CycC or both. Taken the interdependency of the four subunits' results together, when Med12 or Med13 is depleted, residue subunits may be still functional. Additional depletion of CDK8 or CycC may increase E2F1 activity to promote cell proliferation and partially compliment to the eye size loss. When both Med12 and Med13 are depleted, the majority of the CKM are dissembled, the transcription activity of important genes is strongly inhibited, such as Dpp signaling targets and Wnt signaling targets, and the eyes development are further disrupted. With the strong disruption caused by depletion of both Med12 and Med13, knocking down CDK8 and CycC together with them can no longer compliment the reduction of the eye size. These results are consistent to mitotic clones with both *cdk8*^{K185} and *Med12*^{T241}. Mitotic clones of *Med12*^{T241} in eye caused strong defects on eye development, which phenotype was similar to the depletion of both Med12 and Med13. Additional mutation of *Cdk8* cannot reverse the eye size reduction [71].

These results are further dissected with wing phenotype and wing disc cellular level analyses. When CDK8 or CycC was depleted, the S phase cell population was increased, cell proliferation was promoted, and the final wing cell number was increased. These effects may be mainly through regulation of E2F1. However, depletion of Med12 or Med13 arrested cell cycle, likely at G2 stage, caused less cell proliferation and more apoptosis, and finally resulted in defects on wing development. As previous study suggested, Med12 and Med13 are required by

Wnt signaling targets transcription by bridging dTCF complex to the small Mediator complex, loss of Med12 and Med13 may cause retarded Wnt signaling or other important transcription processes [139] and resulted in the strong defects on wing development. Interestingly, when we deplete CDK8 together with Med13, we observed promoted cell proliferation based on the PH3 staining. In addition, cell cycle distribution pattern was similar to depleting Med13 alone, shown with the FUCCI system. Taken the PH3 and FUCCI results together, these observations suggest combined effects of CDK8 and Med13 on cell cycle progression. However, the adult wing showed a blistered phenotype, which is the same as depletion of Med13 alone, indicating that Med13 is more dominant in controlling wing development. This dominant role in controlling wing development of Med13 is consistent with the conclusion from eyes. One puzzle from our observation is that depletion of both CDK8 and Med13 in wing discs did not increase the apoptosis, marked by cleaved Dcp-1. However, the blistered phenotype may be caused by apoptosis happened during pupae stage. Taken together, CDK8-CycC may function independently from Med12-Med13 to act as a negative regulator of cell proliferation through E2F1, and Med12-Med13 may function independently from CDK8-CycC to be required by varieties of transcription activation, such as Wnt targets, for wing or eye development.

Notably, amplification or up-regulation of CDK8 was identified in multiple cancer types, including colorectal cancer and melanoma. In addition, its regulatory partner, CycC was also shown highly expressed in colorectal-adenocarcinoma, leukemia and lymphoma cells. Moreover, mutation of Med12 in exon 1 and exon 2 were identified in nearly 70% of uterine leiomyomas by the Lauri Aaltonen laboratory (Li et al., 2019). As different amplifications or mutations were identified in different subunits of the CKM in different diseases, the further investigation of the

molecular mechanisms underpinning these complicated relationships among the four subunits will provide new strategies to treat diseases related to the four subunits.

As vertebrates CKM is more complex, further examination or validation in mammalian system is required to understand the consequences of gain or loss of the subunits. Nevertheless, the distinct functions and asymmetric interdependency of the subunits of the CKM in eye or wing development raised novel directions to understand their roles in different biological contacts *in vivo,* especially in human diseases.

III.4.2 Asymmetric interdependency among the four subunits of CKM

Cyro-EM results suggested that CDK8 indirectly interacts with Med12 through CycC, while Med13 connected to the other subunits by direct interaction with Med12. Loss of CDK8 or Med13 did not disrupt the formation of the CKM complex of the remaining three subunits after biochemical purification. However, our observation suggested that the four subunits may affect each other's stability and may finally affect the complex formation and function *in vivo.*

With depletion of CDK8, both CDK8 and CycC protein levels are decreased, which is consistent with our previous observations that in $cdk8^{K185}$ L3 wondering larvae and white prepupae, both CDK8 and CycC are low with western blot. However, depletion of CycC only affects CycC protein level, consistent with the result of $cycC^{Y5}$ L3 wondering larvae and white prepupae western blot. Although CycC mRNA level was significantly increased with depletion of CDK8, CycC protein stability may strongly rely on the CDK8 protein level, resulting in the net effect of decrease in CycC protein level. However, while depleting either CDK8 or CycC, Med12 and Med13 protein levels are not affected obviously, although depleting CDK8 elevated Med12 and Med13 mRNA level in RT-qPCR result. As knocking down CDK8 reduced both CDK8 and CycC protein level, the kinase activity of the CKM may be lost. Similarly, depleting

CycC may disrupt the interaction between CDK8 and the other two subunits and inhibiting the kinase activity of the CKM, as CDK8 alone cannot function as a kinase, although the CDK8 protein level is not affected. In both situations, Med12-Med13 may form a sub-complex or function independently as single subunit during development.

On the other hand, depleting either Med12 or Med13 reduced all of the four subunits' protein levels, without significant impact on mRNA level of the other subunits. Loss of Med12 or Med13 may result in the dissemble of the entire complex and the abnormal function of all four subunits. However, the reduction of CDK8-EGFP level by depletion of Med12 or Med13 was not as significant as the reduction of CDK8-EGFP level by depletion of CDK8, depletion of Med12 or Med13 may not fully eliminate the CKM function. Residue partial complex may exist and still have kinase activity for some of the substrates.

III.4.3 Potential regulation of the CKM subunits degradation

Our observation indicates that the four subunits of the CKM are asymmetrically interdependent. However, the underlining mechanism of the protein destabilization of one subunit caused by depleting of other subunits remains further exploring, for example, how CDK8 is degraded upon depletion of Med12 or Med13. One theory for the degradation of subunits from protein complex is that the dissociation of protein complex will expose the intrinsically disordered region of protein monomers, be recognized and degraded by 20S proteasome [163]. Some hinds for this theory from previous works, suggest that intrinsically disordered region of p53 and ODC may be protected by large protein complex and disassembly of these complexes will release the disordered region and lead to their ubiquitin independent 20S proteasome degradation [163]. A recent structural analysis of the CKM suggested that the C-terminal of CDK8 may be wrapped and protected by Med12 [164]. Depletion of Med12 may expose this

intrinsically disordered C-terminal of CDK8 (Fig. A.III.5A) to 20S proteasome and cause CDK8 ubiquitination independent degradation. As part of the other three CKM subunits, CycC, Med12 and Med13 is also predicted to be intrinsically disordered, their degradation may follow the similar manner. However, the structural basis of CycC, Med12 and Med13 is poorly analyzed. It requires additional biochemical and genetic analysis to fully explore the regulation of the asymmetric interdependency.

CHAPTER IV

CDK8-CYCLIN C MODULATES LIPOGENESIS BY DIRECTLY INHIBITING SREBP-DEPENDENT TRANSCRIPTION IN *DROSOPHILA*

IV.1 Introduction

Lipids, such as fatty acids, triglycerides, phospholipids, and sterols, play diverse and critical roles during the normal development of multicellular organisms [165, 166]. For examples, triglycerides serve as the major energy storage molecules; while phospholipids and sterols form membranes structures that are essential for compartmentation of eukaryotic cells [167]. Moreover, cholesterol and its derivatives as well as phosphatidylinositols can also function as signaling molecules or hormones in animals and plants [167]. In metazoans, lipids or fatty acids can be obtained either directly from diets, or synthesized in cells from acetyl-CoA, a process also known as *de novo* lipogenesis. The SREBP (sterol regulatory element-binding protein) family of transcription factors play critical and conserved roles in regulating the transcription of enzymes required for *de novo* lipid and cholesterol biosynthesis [168-171]. These key lipogenic enzymes include ACC (acetyl-CoA carboxylase, the rate-limiting enzyme for lipogenesis), ACS (acetyl-CoA synthetase), and FAS (fatty acid synthase, or FASN in vertebrates) [172-175].

Given the fundamental role of SREBPs in regulating the transcription of lipogenic and cholesterogenic factors, it is not surprising that dysregulation of SREBPs has been reported in metabolism disorders and diseases such as cancer [176, 177]. In fact, elevated fatty acid biosynthesis and increased expression of lipogenic enzymes such FAS and ACC have been identified as a nearly universal feature in most human cancers [178, 179]. For example, 19 SNPs (single nucleotide polymorphism) within *SREBF1* (*Sterol Regulatory Element Binding*

Transcription Factor 1, encodes SREBP1) have been identified in 40 unrelated obese patients [180]. Many of these SNPs, especially 54G/C (rs2297508, in exon 18c), have strong correlation with obesity and type 2 diabetes with cohort studies of a French and an Austrian population [180, 181]. Significantly increased frequency SNP rs11868035 A/G in the intron region of the *SREBF1* has been observed in patients with NAFLD (non-alcoholic fatty liver disease) [182]. Aside from these metabolic disorders, elevated SREBP activity can also promote the growth or the metastasis of prostate cancer and breast cancer cells [183-189]. In contrast, downregulation of SREBPs inhibits progression of colon cancer [190, 191], endometrial cancer [192], pancreatic cancer [193], prostate cancer [194], as well as breast cancer [195]. Accordingly, therapeutic approaches have been developed to target the key lipogenic enzymes, such as ACC, FASN, and SCD (stearoyl-CoA desaturase), for cancer treatment [178, 196, 197]. Thus, understanding the function and regulation of SREBPs may provide mechanistic insights into these diseases, thereby aiding developing new approaches to treat them.

In mammals, the three SREBPs are encoded by two different genes, *SREBF1* and *SREBF2.* SREBP1a and SREBP1c are generated by alternative splicing of the *SREBF1* transcripts. SREBP1c plays a key role in regulating the transcription of lipogenic genes, while SREBP1a can regulate the expression of genes encoding both the lipogenic and cholesterogenic enzymes. SREBP2 is encoded by the *SREBF2* gene and is critical in regulating the expression of enzymes involved in cholesterol biosynthesis [198]. The full-length SREBPs are membrane proteins localized in endoplasmic reticulum. These SREBP precursors consist of a bHLH-Zip DNA binding domain at the N-terminus, a transmembrane domain, and a regulatory domain at the C-terminus [199]. At presence of sterol, these full-length SREBPs associate with the SCAP (SREBP cleavage-activating protein)-INSIG (Insulin induced gene) as a stable complex. When

the intracellular level of sterols is low, INSIG is released and SREBP-SCAP is transported to the Golgi apparatus, where the full-length SREBP precursors are cleaved by two proteases, S1P (site-1 protease) followed by S2P (site-2 protease), resulting in the release of the N-terminal fragment with bHLH-Zip DNA binding domain [200]. These N-terminal SREBP fragments enter into nucleus.and stimulate the expression of SREBP-target genes, thus they are also known as the mSREBPs (mature or nuclear form of SREBPs) [198, 201].

All of these aforementioned factors and regulations of the SREBP pathway are conserved, but much simpler, in invertebrates, such as *Drosophila* and *C. elegans*. In *Drosophila*, there is only one SREBP ortholog, in addition to single orthologs of other factors that control dSREBP processing, including dSCAP, dS1P and dS2P [168, 199, 202-204]. Instead of inhibiting by sterol, the cleavage of precursor dSREBP is regulated by the presence of palmitic acid [205], consistent to the notion that insects are auxotrophic for cholesterols due to absence of key enzymes for cholesterol biosynthesis [206, 207]. Despite this difference, dSREBP plays the conserved role in regulating *de novo* lipogenesis [168].

We have previously reported that CDK8-CycC negatively regulates lipogenesis by inhibiting the transcriptional activity of the mSREBPs in both *Drosophila* and mammals [65]. Specifically, we have observed that loss of CDK8 and CycC increases the transcription of lipogenic genes and fat accumulation in *Drosophila*, cultured mammalian cells, and mouse livers [65]. In addition, we have identified a conserved Threonine residue, Thr402 of hSREBP or Thr390 of dSREBP, as the phosphorylation site by CDK8 in *in vitro* kinase assays [65]. Moreover, depleting CDK8 or CycC in cultured human embryonic kidney 293 (HEK293) cells reduces the levels of ubiquitinated mSREBP-1a, but increases the total protein levels of mSREBP-1a, suggesting that phosphorylation of mSREBPs by CDK8 destabilizes mSREBP

through ubiquitin-dependent protein degradation [65]. However, the exact mechanisms of how CDK8 interacts with SREBP and the biological consequences of the SREBP phosphorylation by CDK8 *in vivo* are still not fully understood.

Here we report our analyses of the role of phosphomutant SREBP (mature form of *Drosophila* SREBP-Thr390Ala, designated as the dSREBP-TA mutant) in regulating its stability, DNA binding, and transcriptional activities in *Drosophila*. Our results suggest that compared to the wild-type mature dSREBP, dSREBP-TA mutant proteins are more stable, displays stronger DNA binding, and more potent in stimulating the transcription of dSREBP target genes and fat accumulation *in vivo*. In addition, we have performed *in vitro* biochemical analyses and mapped the interactions between CDK8 and dSREBP, and we have observed six amino acids at the N-terminus of dSREBP that are essential for the interactions between dSREBP and CDK8 (or Med15). Taken together, these results validate the critical roles of CDK8-meditated SREBP phosphorylation in regulating lipogenesis *in vivo*.

IV.2 Material and Methods

IV.2.1 Fly maintenance and generation of UAS-dSREBP transgenic lines

Flies were raised at 25˚C on a standard cornmeal, molasses and yeast medium. To construct the *UAS-dSREBP* transgenic lines, we first amplified the DNA sequence of the nuclear form of dSREBP using the high fidelity PrimeSTAR Max DNA polymerase (Takara, R045A) and primers SREBP-5.10 and SREBP-3.10 (Table B.IV.1). After purification, the PCR fragment was inserted into the pENTR/D-TOPO vector (ThermoFisher, K240020), and then amplified in *E. coli* strain DH5α. The T390A mutation was generated with QuikChange II Site-Directed Mutagenesis Kit (Agilent Technologies, 200523) with primers SREBP-TA-5.1 and SREBP-TA-3.1 (Table B.IV.1). After validation by sequencing, the two pENTR constructs were recombined

into the pVALIUM10-roe vector (https://plasmid.med.harvard.edu/PLASMID/GetVectorDetail.do?vectorid=495), which contains the *attB* sequence for site-specific insertion into *Drosophila* genome [208], using the Gateway LR Clonase II Enzyme mix (ThermoFisher, 11791100) following manufacturer's instructions. The amplified constructs were micro-injected into integrase expressing fly strain with *attP2* site (BL-25710: *P{y[+t7.7]=nos-phiC31\int.NLS}X, y^{1} sc^{1} v^{1} sev^{21}; P{y[+t7.7]=CaryP}attP2*) using the service provided by Rainbow Transgenic Flies (Camarillo, CA).

IV.2.2 Generation of somatic clones in larval fat body and intestines

The first instar larvae (24h after egg laying) were heat shocked at 37˚C for 5 minutes, and then raised at 25˚C until the wandering third instar larval stage. The fat body was dissected in PBS and fixed in 4% formaldehyde at room temperature for 10 minutes. For dFAS-EGFP imaging, the fat body was incubated with 1μM DAPI in PBS-Tween 20 (0.05% Tween 20) at room temperature for 10 minutes, washed by PBS-Tween 20 at room temperature for 10 minutes 3 times and mounted in the Vectashield mounting media (Vector Laboratories, H-1000). For Nile red staining, the fat body was washed with PBS-Tween 20 for 10 minutes 3 times and incubated with 100 ng/mL Nile red at room temperature for 30 minutes, followed by DAPI staining and mounting as described above for dFAS-EGFP. For immunostaining using an anti-dSREBP antiserum [209], the fixed fat body was washed with PBS-Tween 20 for 10 minutes 3 times and blocked with PBS-Tween-20-NGS-BSA (PBS+0.05% Tween 20+5% Normal Goat Serum+0.2% Bovine Serum Albumin) at room temperature for one hour. The fat body was then incubated with anti-SREBP (1:100 diluted in PBS-Tween-20-NGS-BSA) at 4˚C overnight. After rinsing with PBS-Tween 20 three times, the tissues were then incubated in a secondary antibody (Alexa Fluor 594 AffiniPure goat anti-rabbit, Jackson Immunological Laboratories, 111-585-003; 1:1000

diluted in PBS-Tween-20-NGS-BSA) at room temperature for one hour, followed by the same DAPI staining, rinsing, and mounting steps as described above.

Three-day old adult flies of specific genotypes (as described in the Results section) were heat-shocked at 37˚C for 40 minutes. These animals were then starved by being kept in vials containing 1.5% agar for four hours at 25˚C. Intestines of these animals were dissected, fixed, stained with DAPI and mounted as described above. All of the confocal images in this work were taken by Nikon Ti Eclipse confocal microscope system, processed by the Adobe Photoshop CS6 software, and representative images were shown in figures. The quantification was performed by ImageJ.

IV.2.3 Polytene spreading and immunostaining

For heat shock treatment, late third instar wandering larvae of *w1118, UAS-SREBP*$^{+}$ and *UAS-SREBP*^{T390A} were incubated at 37˚C for four hours. The slavery glands of these animals were dissected in PBS, fixed in one drop of 3.7% formaldehyde for 30 seconds and transferred to formaldehyde-acetic acid (H_2O: 37% formaldehyde: acetic acid = 4:1:5) for further fixation. Cover slide was applied and tapped to smash the slavery glands and to spread the polytene. The slides were set on dry ice before the cover slides were removed by a razor blade. The slides were then washed with PBS and blocked in 5% fat-free milk in PBS. Anti-SREBP (1:100) was diluted in 5% fat-free milk in PBS and the slides were incubated in a humid chamber overnight at 4˚C. Following three rounds of PBS washes, a secondary antibody (Alexa Fluor 594 AffiniPure goat anti-rabbit; 1:1000) was applied at room temperature for two hours. Finally, the polytene was stained with 1μM DAPI, rinsed, and then mounted in Vectashield mounting media.

IV.2.4 RNA-seq sample preparation and data analysis

The total RNA from 10 third instar larvae of w^{1118} (control), $cdk8^{K185}$, and $cycC^{Y5}$ homozygotes at the wandering stage (triplicate for each genotype) was extracted using 1.0 ml of TRIzol Regent (Invitrogen), and then purified using the RNeasy Mini Kit (Qiagen, 74104) following the manufacturer's instructions. The preparation and sequencing of the RNA libraries, as well as the quality control and adapter trimming, were performed by the Texas A&M University (TAMU) Genomics & Bioinformatics Service using the Illumina HiSeq 2500 following the standard protocols.

The processed files were uploaded to and analyzed on the TAMU High Performance Research Computing cluster Terra. RNA-seq sequences were aligned to the *Drosophila melanogaster* genome Flybase release 6.30 by STAR [210]. The gene counts were generated by featureCounts function from the Subread package [211]. Differential expression analysis was performed using DESeq2 R package [212], with adjusted p value cutoff 0.05 used to identify statistically significant differential expressed genes. The heat maps were generated by pheatmap R package [213] with normalized gene counts provided by DESeq2. The clusterProfiler R package was used to perform Gene Ontology analysis of significantly altered genes associated with Flybase gene ID [214]. The Benjamini-Hochberg multiple testing correction method was used and the output dotplot was generated by enrichplot R package [215].

IV.2.5 Protein expression and GST pull-down assay

CDK8 (AA1-262), Med15 (full length), and SREBP fragments were amplified with the PrimeSTAR Max premix (Takara, R045A), using primers listed in Table B.IV.1. These fragments were inserted into the pENTR/D-TOPO vector (ThermoFisher, K240020). The pENTR-SREBP-1-A-3 was mutated by QuikChange II Site-Directed Mutagenesis Kit (Agilent,

200523) using primers SREBP-mut-5.1 and SREBP-mut-3.1 (Table B.IV.1). The CDK8 and dMed15 fragments in pENTR vectors were recombined into the pDEST17 vector (N-terminal 6XHis tag) with Gateway LR Clonase II Enzyme mix (ThermoFisher, 11791020). Similarly, the SREBP fragments, including mutated pENTR-SREBP-1-A-3, were recombined into pDEST15 vector (N-terminal GST tag). The constructs were transformed to *E. coli* strain Rosetta for protein expression using standard protocols. Purification of GST-tagged proteins and the GST pull-down assays were performed using the same protocol as described previously [157].

IV.2.6 Sequence alignment and analyses of the intrinsically disordered regions of SRBEP proteins and sequence alignment

The AA sequences of SREBP proteins from different species were downloaded from NCBI RefSeq (National Center for Biotechnology Information Reference Sequence) database [216] and aligned using the Clustal Omega with default parameters (https://www.ebi.ac.uk/Tools/msa/clustalo/) [217]. The SREBP sequences of different species in FASTA format were individually uploaded to https://iupred2a.elte.hu/ and performed ANCHOR2 [218] and IUPred2A [219] predictions with default parameters. The heat maps were drawn by pheatmap R package [213], based on the predicted scores.

IV.3 Results

IV.3.1 Validation of the role of CDK8-CycC in regulating lipogenic gene expression using the RNA-seq analyses

Previously, we have characterized the effects of CDK8 and CycC mutations on gene expression using the microarray analyses of the $cdk8^{K185}$ and $cycC^{Y5}$ null mutant larvae [65]. However, there are a number of disadvantages of the microarray approach, such as high background owing to cross-hybridization, limited dynamic range of detection due to saturated

signals, as well as limited specificity and sensitivity, especially for low abundance transcripts [220]. To validate and extend our previous microarray analyses, we have performed transcriptome profiling of the $cdk8^{K185}$ and $cycC^{Y5}$ homozygous larvae using the RNA-seq (RNA sequencing) technique (see Materials and Methods for details). The genes that are significantly altered in $cdk8^{K185}$ and $cycC^{Y5}$ mutants comparing with the control (w^{1118}) were categorized using the GseGO (Gene Set Enrichment Analysis of Gene Ontology) function from the clusterProfiler package [214]. The top 40 Gene Ontology categories are shown as a dotplot for $cdk8^{K185}$ (Fig. IV.1A) and for $cycC^{Y5}$ (Fig. A.IV.1). Consistent to our previous reports that fatty acid biosynthesis is elevated in $cdk8^{K185}$ mutant larvae [65, 85], the fatty acid biosynthesis process is identified as one of the significantly upregulated gene categories (Fig. IV.1A).

To display the changes of genes involved in the fatty acid biosynthesis process in a higher resolution, we have used a heatmap to show all the genes within the category of all the biological triplicates of $cdk8^{K185}$, $cycC^{Y5}$, and the control (w^{1118}). As the triplicates of the same genotypes were clustered together according to the X-axis clustering (Fig. IV.1B), validating that the biological replicates were correctly sampled. Importantly, the transcription of genes encoding the key enzymes for fatty acid biosynthesis, such as FAS and ACC, are significantly elevated in $cdk8^{K185}$ or $cycC^{Y5}$ mutant larvae. The transcription of these two genes is directly activated by dSREBP, consisting with the model that the transcriptional activities of SREBP are elevated in $cdk8^{K185}$ and $cycC^{Y5}$ mutants [65].

SREBP-dependent lipogenesis is regulated by physiological conditions such as feeding and starvation. Extensive studies in the past decades have shown that the insulin/mTOR (mammalian target of rapamycin) signaling pathway is activated by dietary nutrients, such as carbohydrates and amino acids [221-225]. Interestingly, downregulation of CDK8-CycC by

insulin signaling is dependent on mTORC1 in cultured mammalian cells [226], while depleting

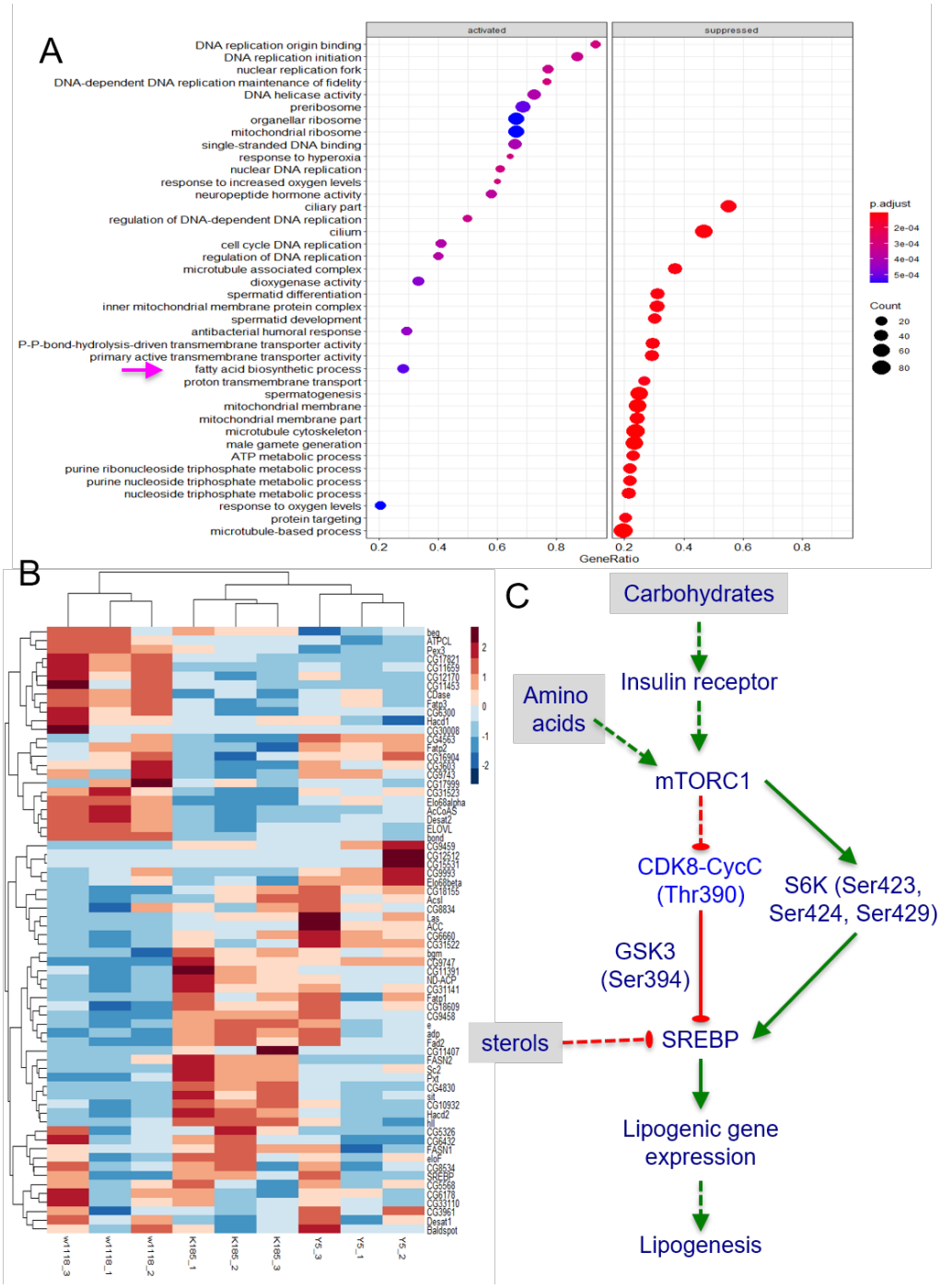

Fig. IV.1. Fatty acid biosynthetic process genes are elevated in cdk8 and cycC null mutants. (A) Dotplot of the top 40 Gene Ontology categories of significantly altered genes in cdk8K185 comparing with w1118. (B) Heatmap of genes involved in fatty acid biosynthetic process category of triplicates of w1118, cdk8K185 and cycCY5. (C) Model: The role of CDK8-CycC in the context of insulin signaling and lipogenesis.

CDK8 or CycC can potently abolish the effects of TOR activation on autophagosome formation in *Drosophila* [227]. Moreover, *cdk8* and *cycC* mutant larvae are hypersensitive to high sugar diets and higher levels of dietary amino acids that stimulate TOR in *Drosophila* [228]. These results suggest that mTORC1 functions upstream of CDK8-CycC [14]. The RNA-Seq analyses (Fig. IV.1A, Fig. IV.1B), together with our previous work [65], support the model that dietary nutrients activated insulin/mTOR signaling stimulates SREBP-dependent lipogenic gene expression and lipogenesis by inhibiting CDK8-CycC (Fig. IV.1C).

IV.3.2 Increased stability of phosphomutant dSREBP proteins in vivo

Our *in vitro* biochemical analyses suggest that CDK8 may inhibit lipogenesis by directly phosphorylating SREBP at a conserved Thr residue (Fig. IV.2A) [65]. To further determine the impacts of SREBP phosphorylation by CDK8 *in vivo*, we have tested whether mutating the phosphorylation site affects the stability, DNA-binding ability, and the transcriptional activity of SREBP in *Drosophila*. Specifically, we have generated two transgenic lines allowing us to overexpress the mature, nuclear form (AA1-451) of either the wild-type dSREBP (*UAS-dSREBP*$^{+}$) or the phosphomutant dSREBP (*UAS-dSREBP*^{T390A}). The Thr390Ala mutation was validated by sequencing (Fig. IV.2B). To reduce potential variation caused by chromatin environments of the insertion sites, we have used the *pVALIUM10-roe* vector, which flanks the expression cassettes with the *gyspy* insulators and supports site direct insertion with the *attB* integrase target sequence [208, 229]. The constructs were then specifically inserted at the same *attP2* locus of the third chromosome (see Materials and Methods).

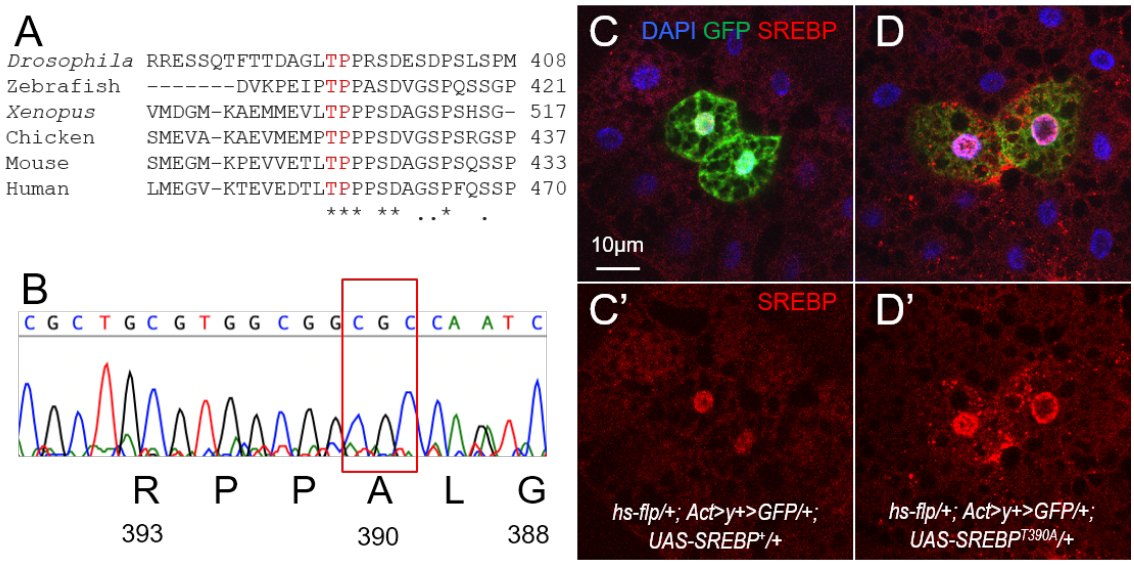

Fig IV.2. Increased stability of the phophomutant dSREBP proteins. (A) Alignment of the AA sequences of SREBP to show the conservation of Thr390Pro391 (TP) from Drosophila to humans. (B) Validation of SREBPThr390Ala mutation by sequencing. (C/D) Representative confocal images of larvae fat body stained with an anti-SREBP antibody (red), GFP (green), and the DNA dye DAPI (blue). Detailed genotypes are: (C) hs-flp/+; Act>y+>GFP/+; UAS-dSREBP+/+; (D) hs-flp/+; Act>y+>GFP/+; UAS-dSREBPT390A/+. (C'/D') The same images to C/D with only the anti-dSREBP staining (red) showed. Scale bar in C: 10μm.

To test whether the stability of dSREBP is affected in the phosphomutant proteins, we performed a clonal analysis in larval fat body using the *cis*-chromosomal recombination (FLP-out) system [230]. Specifically, we constructed the larvae with the following genotypes: *hs-flp/+; Actin>y^{+}>Gal4, UAS-GFP/+; UAS-dSREBP^{+}/+* and *hs-flp/+; Actin>y^{+}>Gal4, UAS-GFP/+; UAS-dSREBP^{T390A}/+*. GFP-labeled adipocytes overexpress either the wild-type dSREBP or dSREBP^{T390A}, and the levels of dSREBP were detected by immuno-staining using an anti-dSREBP polyclonal antibody. Compared to the cells outside of the GFP positive clones, ectopic expression of both forms of dSREBP significantly increased the dSREBP levels as expected (Fig. IV.2C and 2D). Importantly, we have observed a stronger elevation of the levels of

dSREBP^{T390A} than the wild type dSREBP (Fig. IV.2C' vs. 2D'), suggesting phosphomutant form of SREBP is more stable than wild type form of SREBP.

IV.3.3 Increased DNA-binding ability of phosphomutant dSREBP proteins in vivo

We have previously proposed a model to explain how CDK8-CycC inhibits SREBP-dependent gene expression, which posits that SREBP phosphorylation by CDK8 promotes the degradation of SREBP [65]. Consistent to this model, SREBP phosphorylation by CDK8 increased the ubiquitination and degradation of SREBP [65], and the E3 ligase SCF^{Fbw7b} is required for ubiquitination of SREBP [231]. The mSREBPs bind to the promoters of their target genes as homodimers [198], but the molecular events between CDK8 phosphorylation and SREBP degradation are still not fully understood. One likely scenario is that CDK8 phosphorylation reduces the DNA-binding ability of mSREBPs, thereby tipping the balance in favor of exporting phosphorylated mSREBPs from nucleus, aiding its subsequent degradation by the 26S proteosome.

If DNA-binding ability of SREBP is reduced by CDK8 phosphorylation, then we expect the phosphomutant dSREBP proteins have increased chromatin-binding ability than wild type dSREBP. To test this prediction, we ectopically expressed either wild-type or phosphomutant dSREBP proteins in salary glands of the third instar larvae, and then analyzed the levels of SREBP bound to the polytene chromosomes by immunostaining. There is a minimal *hsp70* core promoter between 5X UAS sequence and the multiple cloning site in the *pVALIUM10-roe* vector [208, 229], allowing us to induce SREBP expression by heat shock. Compared to the w^{1118} control (Fig. IV.3A), overexpression of either dSREBP^{+} or dSREBP^{T390A} increases SREBP binding to polytene chromosomes (Fig. IV.3B and 3C). However, compared to wild-type dSREBP (Fig. IV.3B), we have observed stronger phosphomutant SREBP-binding to polytene

chromatin (Fig. IV.3C). These observations suggest that phosphomutant SREBP increases its binding to chromatin than the wild-type SREBP proteins.

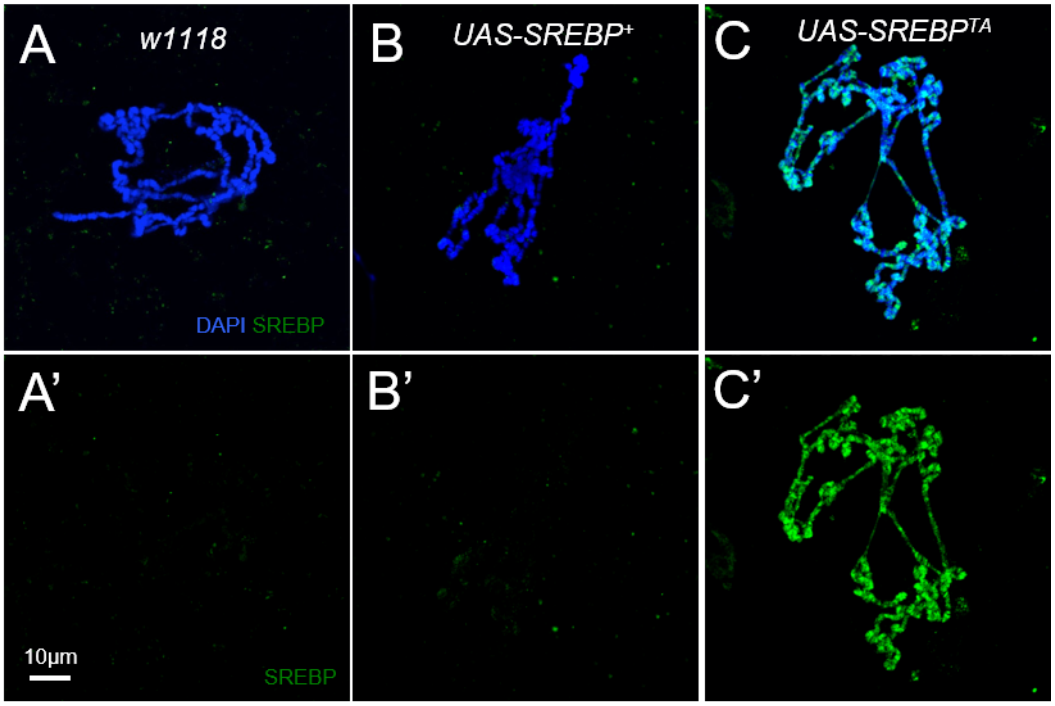

Fig. IV.3. dSREBPT390A has stronger binding to DNA. Representative confocal images of an anti-SREBP antibody immunostaining (green) and the DNA dye DAPI (blue) in of the polytene chromosomes from larval salivary glands of the following genotypes: (A) w1118, control; (B) UAS-dSREBP+; and (C) UAS-dSREBPT390A/+. Scale bar in C: 10μm.

IV.3.4 Potent effects of phosphomutant dSREBP in stimulating the lipogenic gene expression in vivo

To test whether increased DNA binding of dSREBP^{T390A} correlates with more potent transcriptional activity at the cellular level, we generated transgenic reporter line using a 4kb promoter region of the *dFAS* (*Drosophila* fatty acid synthase) gene to drive the expression of EGFP (Fig. IV.4A), designated as the *dFAS-EGFP* reporter. To determine the effects of genetic perturbation on the expression of *dFAS*, we genetically recombine this reporter with the *Actin>CD2>Gal4 UAS-RFP* "flip out" system [232] (see Materials and Methods for details).

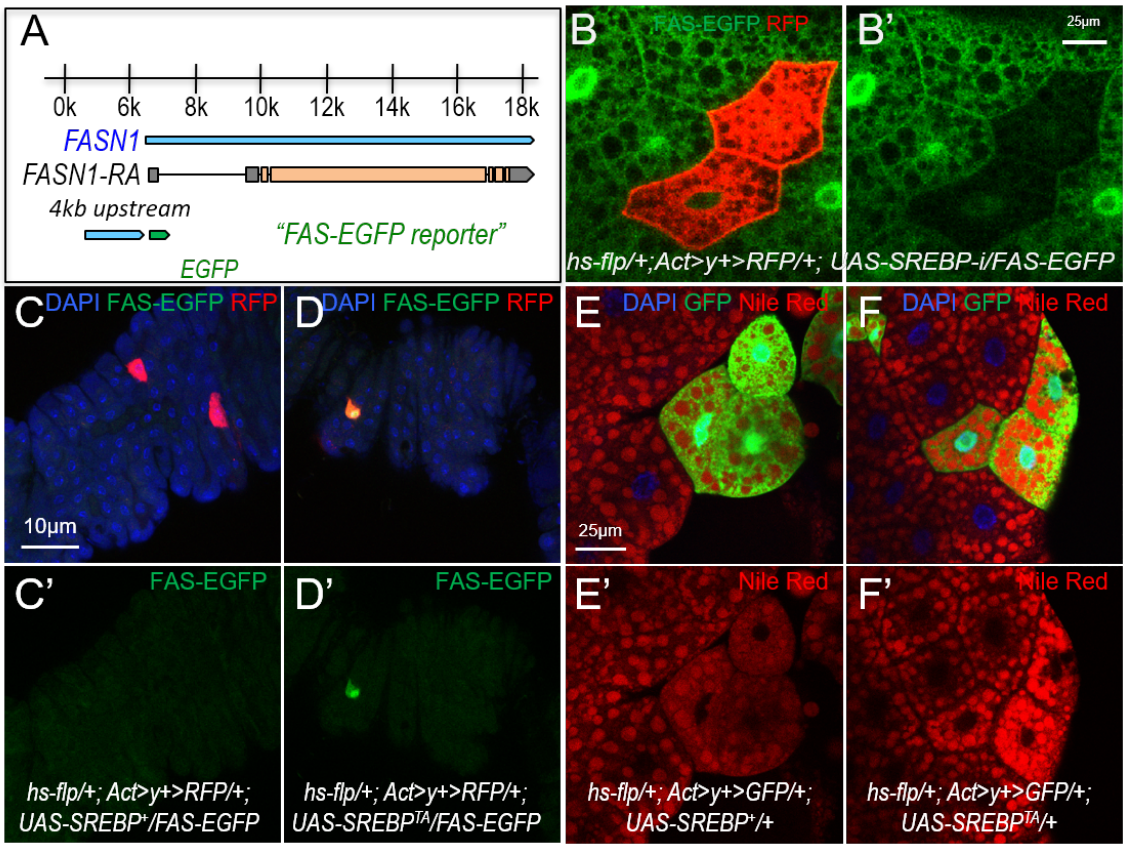

Fig IV.4. Phopho-mutant dSREBP protein is more potent in target transcription and lipid accumulation. (A) Scheme of FAS-EGFP reporter: ~ 4kb fragment upstream of the FASN1 gene from a BAC clone were used to drive the expression of an EGFP reporter. (B/B') Representative confocal images of dFAS-EGFP (green), RFP (red) and DAPI (blue) in Drosophila larvae fat body of the following genotype: hs-flp/+; Act>y+>RFP/+; UAS-dSREBP-i/dFAS-EGFP; only dFAS-EGFP (green) is shown in B'. (C/D) Representative confocal images of dFAS-EGFP (green), RFP (red) and DAPI (blue) in Drosophila adult midgut of the following genotypes: (C) hs-flp/+; Act>y+>RFP/+; UAS-dSREBP+/dFAS-EGFP; (D) hs-flp/+; Act>y+>RFP/+; UAS-dSREBPT390A/dFAS-EGFP. The signals of FAS-EGFP (green) of the same images are shown in C' and D'..(E/F) Representative confocal images of larvae fat body stained with Nile red (red), GFP (green), and DAPI (blue) of the following genotypes: (C) hs-flp/+; Act>y+>GFP/+; UAS-dSREBP+/+; (D) hs-flp/+; Act>y+>GFP/+; UAS-dSREBPT390A/+. The signals of Nile red staining (red) of the same images are shown in C' and D'. All images in this figure have the same magnification; Scale bar in B': 25μm.

To validate whether this *dFAS-EGFP* reporter is specific for SREBP activity, we deplete SREBP in the RFP marked clonal cells and observed that the clonal cells had lower EGFP level

comparing with surrounding cells (Fig. IV.4B), suggesting that *dFAS-EGFP* reporter is specific to SREBP. As shown in Fig. A.IV.2A and Fig. A.IV.2B, cells in clones marked with RFP overexpress dSREBP^{+} or m-dSREBP^{T390A} and have increased expression of dFAS-EGFP compared to the neighboring cells. Importantly, stronger effects on dFAS-EGFP expression were observed in cell overexpressing dSREBP^{T390A} than those overexpressing dSREBP^{+} (Fig. A.IV.2B).

To validate the effect of different forms of SREBP on dFAS transcription, we performed the same experiment in adult intestine with starvation. Starvation is expected to inhibit mTOR, which correlates with elevated CDK8 protein levels in *Drosophila* larvae [85]. Elevated CDK8 phosphorylates and stimulates the degradation of nuclear dSREBP^{+}, but not phosphomutant dSREBP^{T390A}, thus it is expected that only dSREBP^{T390A} can stimulate the expression of *dFAS-EGFP* reporter upon starvation (Fig. IV.4C). To test this prediction and to avoid potential positional effects in midgut for our comparison, we focused our analyses on a posterior region of midgut, near the midgut and hindgut boundary, in adult flies. The endogenous expression of dFAS in the cells within this region is low (Fig. IV.4C and 4D). When overexpressing dSREBP^{+} in the RFP labeled clone cells, the *dFAS-EGFP* expression level is low and similar to the neighboring cells (Fig. IV.4C). In contrast, when the phosphomutant dSREBP^{T390A} is overexpressed in RFP-labeled cells, the expression of *dFAS-EGFP* reporter was significantly increased than that of the neighboring cells (Fig. IV.4D). Taken together, our observations in both larval fat body and adult midgut suggest that overexpressing phosphomutant of dSREBP is more potent than the wild-type dSREBP in stimulating its target gene transcription *in vivo*.

To test whether phosphomutant dSREBP is more potent than wild-type dSREBP in promoting lipid accumulation, we used the similar FLP-out system to generate somatic clones in

larval fat body, marked by GFP, to overexpress either dSREBP^{+} or dSREBP^{T390A}, and then analyzed the lipid accumulation by Nile red. Nile red has been applied to stain neutral lipids stored in intracellular lipid droplets, including TG (Triglycerides) [233], which are increased upon SREBP activation [234]. The mature dSREBPs are presumably maximally active in adipocytes at the wandering larval stage, ectopically expressed wild-type dSREBPs are largely degraded, making it difficult to observe any obvious effects comparing to the neighboring adipocytes (Fig. IV.4E, Fig. IV.4E'). In contrast, overexpressing phosphomutant dSREBP^{T390A} led to stronger Nile red stained oil droplets in adipocytes marked with GFP, compared to the neighboring adipocytes (Fig. IV.4F, Fig. IV.4F'). These observations suggest that phosphomutant dSREBP^{T390A} proteins are more potent in stimulating lipid accumulation than the wild-type dSREBPs *in vivo*.

IV.3.5 N-terminus of dSREBP directly interacts with dCDK8

Previously, it has been reported that the N-terminus of human SREBP-1a (AA30-40) fused with GST can pull down several Mediator subunits, including CDK8, MED1, MED6, and MED15, from the HeLa cell nuclear extract, and hSREBP1a can directly interact with the KIX domain of hMED15 [235]. However, it is unclear whether CDK8 directly interacts with SREBP, or indirectly through the small Mediator complex, and whether the physical interactions between SREBP and MED15 are conserved in *Drosophila*.

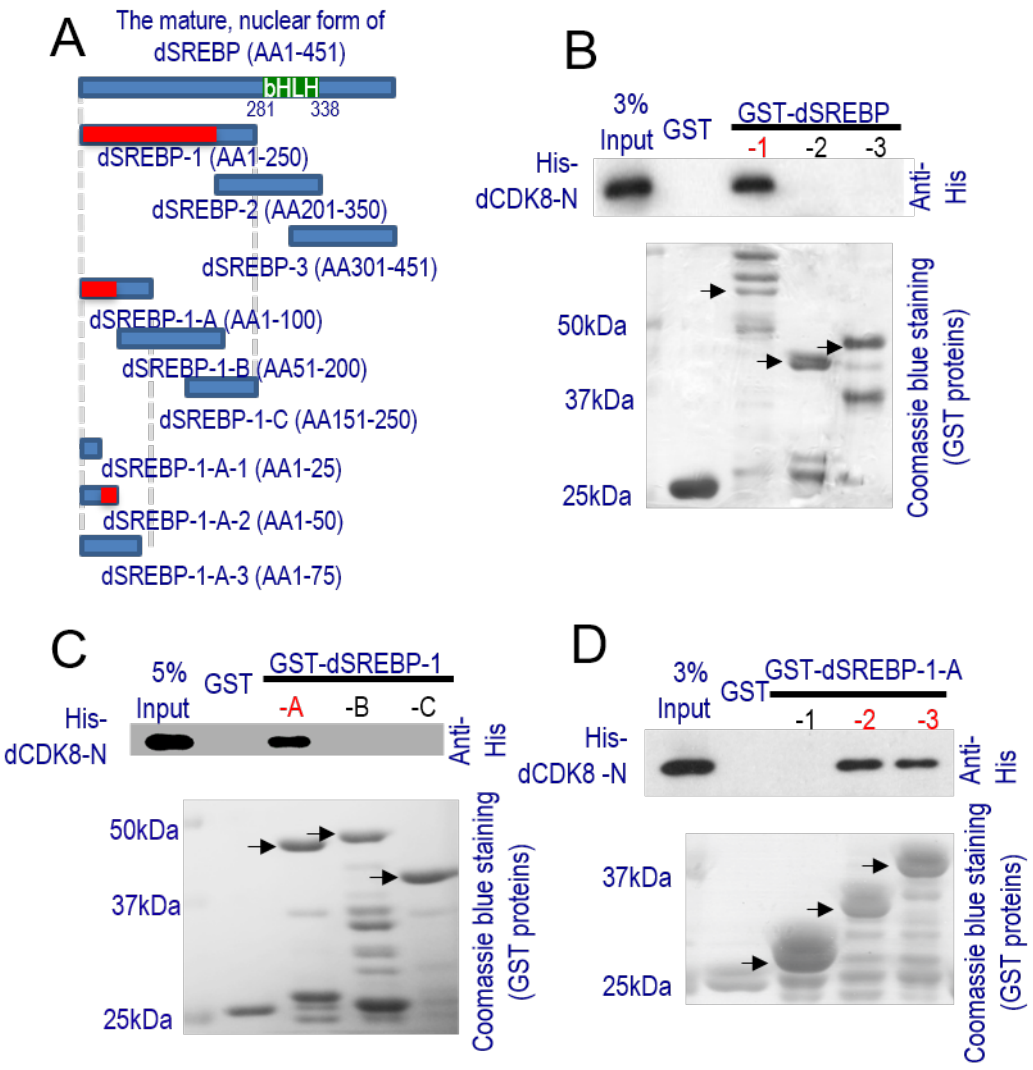

Fig IV.5. Mapping the physical interactions between dCDK8 and the mature dSREBP. (A) Scheme of the mature, nuclear form of Drosophila SREBP, containing a bHLH domain from AA381 to AA338. (B-D) Western blots showing the three rounds GST pull-down assays that allowed to further map the specific regions in dSREBP that directly interact with His-tagged dCDK8 (see the Results section for more details).

To test whether dCDK8 directly interacts with dSREBP and to further map the specific regions mediating this interaction, we have performed three rounds of GST pull-down experiments. Specifically, we generated polyhistidine (His)-tagged dCDK8 (AA1-262), containing the ATP-binding site, A-loop, CycC interface, and substrate-binding domain [236, 237]. Meanwhile, we generated GST-fusion proteins by dividing dSREBP into three partially

overlapping fragments (Fig. IV.5A), designated as GST-dSREBP-1 (AA1-250), GST-dSREBP-2 (AA201-350, containing the bHLH-Zip domain), and GST-dSREBP-3 (AA301-451), respectively. As shown in Fig. IV.5B, His-dCDK8-N (AA1-262) can interact with GST-dSREBP-1, but not GST-SREBP-2 or GST-SREBP-3, suggesting that AA1-200 of dSREBP interacts with dCDK8 *in vitro*. Next, we generated three smaller partially overlapping fragments of GST-SREBP-1 (Fig. IV.5A), and performed similar GST pull-down assays. We have observed that only GST-SREBP-1-A (AA1-100), but not GST-SREBP-1-B (AA51-200) or GST-SREBP-1-C (AA151-250), can interact with His-CDK8-N (Fig. IV.5C), suggesting that AA1-50 of dSREBP binds to dCDK8. In our third round of mapping, we have observed that GST-SREBP-1-A-2 (AA1-50) and GST-SREBP-1-A-3 (AA1-75), but not GST-SREBP-1-A-1 (AA1-25), can interact with His-dCDK8-N (Fig. IV.5A, Fig. IV.5D). These results suggest that the AA25-50 at the N-terminus of dSREBP can directly interact with dCDK8 *in vitro*.

IV.3.6 N-terminus of dSREBP directly interacts with dMed15

Because the AA30-40 region of hSREBP1a directly interacts with the KIX domain of hMED15, we have tested whether the interaction is conserved in *Drosophila*. As shown in Fig. IV.6A, GST-SREBP-1-A-3 (AA1-75) can also pull down His-tagged full-length dMed15 protein, suggesting that the interaction between the N-terminus of SREBP and MED15 is evolutionarily conserved. More importantly, the same region of dSREBP can directly interact with both dCDK8 and dMed15 (Fig. IV.5D and Fig. IV.6A), which may have important implications in our understanding of the dynamic processes that involve the small Mediator complex and the CDK8 module in SREBP-dependent gene expression (see Discussion).

Mature or nuclear dSREBP contains a structured bHLH-Zip DNA-binding domain (AA284-334), but other parts of the nuclear dSREBP are largely intrinsic disordered (Fig.

A.IV.3). As a result, only the structure of the DNA-binding domain of nuclear SREBP1a has been resolved using X-ray *crystallography* [238]. To identify the specific AAs within the N-terminus of dSREBP that are required for direct interaction with dCDK8 or dMed15, we have first analyzed the intrinsic disordered regions of the SREBP from different species using the ANCHOR2 programs [218]. ANCHOR robustly predicts protein disorder based on an energy

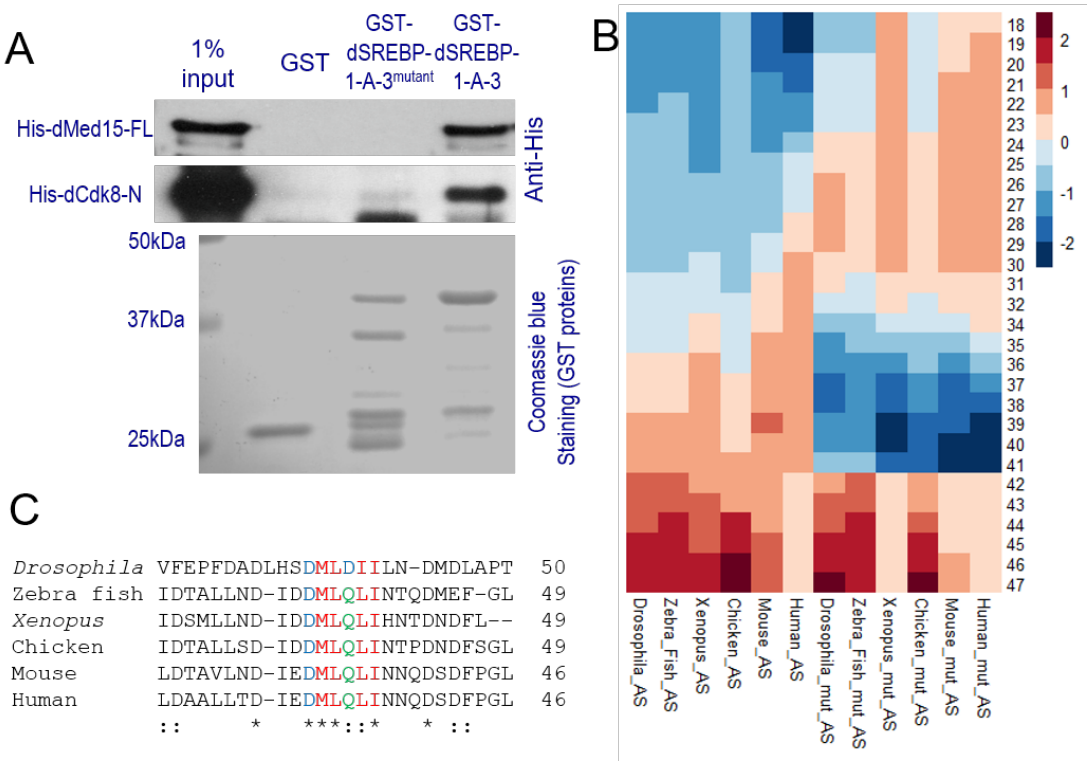

Fig IV.6. Six amino acid (AA36-41) in N-terminal of SREBP are essential for the interaction between CDK8-SREBP and Med15-SREBP. (A) Western blots of the GST pull-down assay: interactions between the wild-type or AA36-41 mutated GST-SREBP-1-A-3 and His-tagged N terminal fragment of dCDK8 or full length dMed15. (B) Heatmap of Anchor2 predication result of SREBP of different species of wild type SREBP or mutated SREBP. AS: Anchor2 Score. (C) Sequence alignment of the N-terminal of SREBP (AA25-50).

estimation approach and can also detect regions that probably gain energy by interacting with globular proteins [218]. We used heat maps to visualize the Anchor2 scores (AS) of the N-terminus of SREBP proteins from *Drosophila melanogaster*, zebrafish (*Danio rerio*, SREBP1),

frog (*Xenopus laevis*, SREBP1), chicken (*Gallus gallus*, SREBP1), mouse (*Mus musculus*, SREBP1a), and humans (*Homo sapiens*, SREBP1a) (Fig. IV.6C). Interestingly, these analyses reveal a hot spot overlapping from AA35 to AA44 across the species (Fig. IV.6B). Within this region, six amino acids, DMLDII (AA36-41) are highly conserved during evolution (Fig. IV.6C).

To test whether mutating these six AAs (DMLDII) can alter the intrinsic disorder level of the SREBP, we replaced them with six alanines from different species *in silico* and then analyzed protein disorder of these mutant SREBPs using the ANCHOR2 programs. As shown in Fig. IV.6C, the ANCHOR2 score hotspot is diminished within this region, indicating that these six conserved AAs might be important for the dSREBP, dCDK8 and dMed15 interactions. To validate this prediction experimentally, we mutated these six AAs to alanines in the GST-dSREBP-1-A-3 (AA1-75) fragment, and then performed GST pull-down assays. As shown in Fig. IV.6A, the mutation of these conserved six AAs in GST-SREBP-1-A-3 abolished its interaction with both dCDK8 and dMed15. These observations suggest that the conserved region within the N-terminus of dSREBP, particularly the highly conserved but disordered region DMLDII (AA36-41), is crucial in mediating the interactions between dSREBP and dCDK8 or dMed15.

IV.4 Discussion

Studies in the past three decades have revealed an elegant model to explain how the SREBPs control the intracellular fatty acid and cholesterol homeostasis. Major efforts have been focused on understanding the mechanisms of how the full-length SREBP precursors are processed in the cytoplasm in response to intracellular levels of sterols and fatty acids [168-171]. Another key aspect of SREBP transcriptional regulation is related to the molecular events

happening in the nucleus, i.e., how the mature SREBP proteins activate the transcription of the lipogenic and cholesterogenic genes, and how this process is turned off. Through MED15, the small Mediator complex plays a critical role in SREBP-activated gene expression [235], while our previous work suggest that CDK8-CycC plays a conserved role in turning off SREBP activities in the nucleus in *Drosophila* and mammals [65]. In this work, we analyzed the effects of CDK8 phosphorylation of dSREBP *in vivo*, and then further mapped the specific regions of dSREBP that directly interacts dCDK8 and dMed15 using *in vitro* and *in silico* approaches.

IV.4.1 Critical role of phosphorylation of SREBP Thr390 in vivo

Posttranslational modifications of SREBPs, such as acetylation and phosphorylation, play critical role in fine-tuning their activities [239, 240]. Using *in vitro* kinase assays, our previous study has identified the specific phosphorylation site of SREBP by CDK8, i.e., Thr402 of hSREBP1c, or Thr390 of dSREBP [65]. Further biochemical analyses using cultured mammalian cells have revealed that Thr402 phosphorylation regulates the stability of hSREBP1c [65]. To further validate this model *in vivo*, we have analyzed the effect of abolishing this phosphorylation in *Drosophila*, particularly on its impacts on DNA binding and stability of dSREBP, as well as the activity of dSREBP in stimulating its target gene expression and lipid accumulation. Compared to the wild-type dSREBP, phosphomutant dSREBP ($dSREBP^{T390A}$) proteins are more stable, displays stronger chromosome binding, and more potent in stimulating dSREBP target gene expression and lipid accumulation *in vivo*.

It is noteworthy that additional protein kinases have also been reported to phosphorylate multiple Thr and Ser residues of SREBP proteins, in addition to CDK8 phosphorylation of hSREBP1a at Thr402. For example, GSK-3β can phosphorylate Thr426 (equivalent to Thr402) and Ser430 (Fig. A.IV.4A), thereby promoting ubiquitination and degradation of hSREBP1a

[241]. Similarly, rat SREBP1c can be phosphorylated at Ser418, Ser419, and Ser422 residues (Fig. A.IV.4B) upon insulin treatment, and S6K (Ribosomal protein S6 kinase), a kinase downstream of insulin signaling, was shown to enhances SREBP1c precursor maturation and protects SREBP1c from proteasomal degradation [242]. These phosphorylation sites or Ser/Thr rich regions are conserved during evolution from *Drosophila* to human (Fig. A.IV.4A and A.IV.4B). Thus, it is possible that the proposed mechanisms for SREBP phosphorylation by GSK-3β and S6K may be evolutionarily conserved in *Drosophila*.

Interestingly, there are also several phosphorylation sites in SREBP that are not evolutionarily conserved. For example, rat SREBP1c Ser73 can be phosphorylated by GSK3, resulting in the dissociation of the SREBP-1c–SCAP complex and ubiquitination dependent proteasomal degradation of SREBP [243]. However, the Ser73 residue appears to be only conserved in mammalian SREBP proteins (Fig. A.IV.4C). In addition, Ser117 of hSREBP1a can be phosphorylated by stress activated MAPKs, mutating this phosphorylation site protects mice under normocaloric conditions from developing enlarged fatty livers [244], yet the Ser117 is also only conserved in mammals (Fig. A.IV.4D). Moreover, hSREBP1c Ser372 can be phosphorylated by AMPK (AMP-activated protein kinase), which suppresses SREBP-1c cleavage and nuclear translocation, thus inhibits SREBP-1c dependent transcription in hepatocytes [245]; however, the Ser372 residue of hSREBP1c is conserved in vertebrates only (Fig. A.IV.4E). Therefore, these analyses have revealed potential variations in the detailed molecular mechanisms of how insulin signaling stimulates SREBP-dependent lipogenic gene expression and promotes *de novo* lipogenesis in metazoans. To our knowledge, the role of GSK3 and S6K in regulating SREBP activity has not be tested in *Drosophila*. However, based on AA sequence conservation of SREBPs, phosphorylation of SREBP by CDK8, GSK3 and S6K could

be a more ancient regulatory mechanism than phosphorylation of SREBP by MAPKs and AMPK. Additional kinases are involved in regulating SREBP activities, which may offer adaptive advantages in coping with more complex physiological needs that require fine-tuned control of the activities of SREBP family of transcription factors in vertebrates, or mammals, compared to invertebrates such as insects.

IV.4.2 Physiological regulation of SREBP and lipogenesis by feeding and starvation

Based on the regulation of SREBP by CDK8 concluded by our observations and previous reports about the other conserved phosphorylations by other kinases, we speculate the following model concluded in Fig. IV.1C, and the following amino acids are numbered based on the equivalent sites in *Drosophila* SREBP:

Insulin signaling and amino acids can activate mTORC1 and its downstream kinase S6K [246-249], which can downregulate CDK8 [209, 226]. On one hand, mTORC1 activates S6K, which phosphorylate the SREBP precursors at Ser423, Ser424, Ser429, protect SREBP from proteasome degradation, and promotes its processing into mature form SREBP [242](Fig. IV.1C). On the other hand, activated mTORC1 can downregulate CDK8 [209, 226], which allows mSREBP to stimulate the lipogenic gene expression [65](Fig. IV.1C). According to this model, under feeding conditions, CDK8 can no longer inhibit SREBP, thus gain of either wild-type SREBP or SREBP-Thr390Ala mutant can equally stimulate the expression of SREBP-target genes and lipogenesis.

Conversely, we have previously reported that the level of CDK8 proteins is significantly elevated upon starvation, which occurs concurrently with the reduction of the mSREBP proteins in *Drosophila* larvae [209]. This elevation of CDK8 level may be through mTORC1[226]. In addition, it has been reported that starvation or overexpression of TSC1/TSC2 can reduced the

activity of mTORC1 and S6K [246, 250]. On one hand, as S6K activity is low, Ser423, Ser424, Ser429 of SREBP are not phosphorylated by S6K and unphosphorylated SREBP may be easily degraded [242](Fig. IV.1C). On the other hand, increased CDK8 will phosphorylate SREBP at Thr390 [65], which may subsequently phosphorylate by GSK3 at Ser394 [241], resulting in SREBP degradation [65, 241] (Fig. IV.1C). Thus, overexpressed wild type SREBP can be quickly eliminated at starvation condition, suggested by the unchanged dFAS reporter signal (Fig. IV.4C). However, the reduction of SREBP activity can be impacted by the phosphomutation, as overexpressing phosphomutant form of SREBP can activate target transcription even with starvation (Fig. IV.4D).

Therefore, CDK8 may play a more important role in inhibiting SREBP-dependent lipogenesis during starvation, while this mechanism is repressed by downregulating CDK8 protein through mTORC1 under the feeding condition (Fig. IV.1C). Given that both CDK8 and GSK3 are shown to phosphorylate Thr390 of SREBP, it will be important to further investigate to how these different kinases may coordinate with each other in phosphorylating SREBP and lipogenesis in different biological contexts *in vivo*.

IV.4.3 Physical interactions between SREBP and CDK8 or Med15

Our biochemical analyses suggest that both dCDK8 and dMed15 can physically interact with a small fragment within the N-terminus of dSREBP. Mutation of six amino acids (DMLDII, AA36-41) dSREBP abolished its interaction with both dCDK8 and dMed15, suggesting that these six AAs are essential for mediating these physical interactions. These results further extend the previous report that SREBP in *C. elegans* can interact with Med15 in both *C. elegans* and mammalian cells, and that MED15 is required for SREBP-activated gene expression [235].

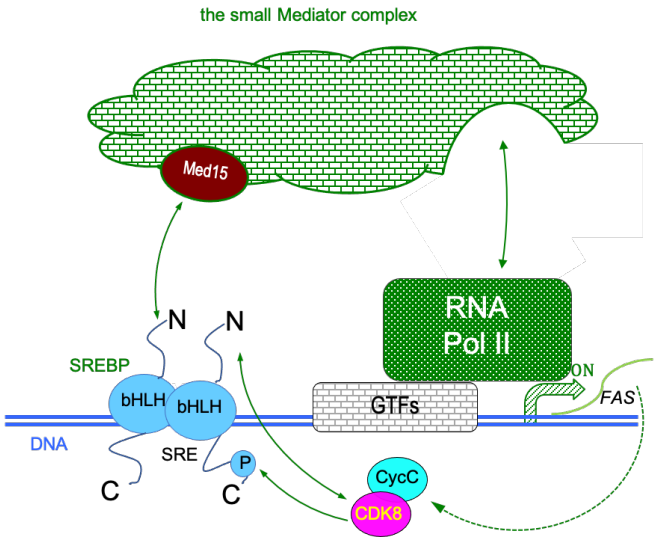

Fig. IV.7 Working model for SREBP dependent transcription. Model of SREBP-dependent transcription activation through Med15 and the small Mediator complex, which can be turned off through phosphorylation by CDK8. GTFs, General Transcription Factors.

There are several scenarios to explain the interplay among SREBP, CDK8, and MED15. Given the current understanding of the role of Mediator complexes and how the CDK8 module regulates the transcription of a number of transactivators, the most parsimonious model is that the mature SREBP homodimer binds to the sterol-response element of SREBP target genes, the N-terminus of SREBP directly interacts with the Med15 subunit of the small Mediator complex, which interacts with RNA Pol II and other general transcription factors, allowing the transcription initiation (Fig. IV.7). Prior studies suggest that the CDK8 module is recruited to the transcription start sites shortly after the transcription initiation, thereby limiting the subsequent rounds of transcription re-initiation [61, 144].

Although exactly how the CDK8 module is subsequently recruited to the promoter remains unclear, we speculate that the nascent mRNA transcripts might help to recruit the CDK8

module to the transcription start site, allowing the direct interactions between CDK8 and SREBP, or other transactivators (Fig. IV.7). It is also unclear whether CDK8 directly competes with Med15 in binding to the same N-terminus of SREBP or both of the N-termini of the SREBP homodimer (Fig. IV.7). Subsequently, CDK8 phosphorylates the Thr402 of hSREBP1c or Thr390 of dSREBP, thereby reducing SREBP binding to the SREs, favoring the export of phosphor-SREBPs to cytoplasm for further degradation (Fig. IV.7). In this model, Med15 subunit of the small Mediator complex plays a key role in SREBP-activated expression of lipogenic genes, while CDK8 plays a critical role in turning this process off. This model can explain the biological consequence that we observed in CDK8 and CycC mutants, as we reported previously [65]. As summarized in this work, our analyses of dSREBP-T390A mutant provide further support for the model described above.

Taken together, this work provides a better understanding of how mature SREBP activate its target gene transcription, and equally importantly, how this process is turned off. It provides yet another example of how transcription activation is coupled to its inactivation, and explains why transactivators generally have short half-life [130]. Perhaps, live imaging analyses using advanced microscopic approaches using fluorescent-tagged subunits of the Mediator complex may help to precisely define the dynamic process of how the small Mediator complex and the CDK8 module are recruited to the transcription start site in the future.

CHAPTER V

CONCLUSION AND FUTURE DIRECTIONS

V.1 The Mediator CDK8-Cyclin C complex modulates wing vein patterning in *Drosophila* by stimulating Mad-dependent transcription

Using our unique phenotypic readouts of the CDK8-specific activities in *Drosophila* adult wing, we have identified components of the Dpp signaling pathway that can genetically interact with CDK8-CycC. In addition, our biochemical analyses have revealed that CDK8 can directly interact with Mad in its linker region. Moreover, our developmental genetic analyses have revealed that CDK8-CycC may phosphorylate Mad at linker region and promotes Mad, Medea and Yki forming a transcriptional complex to drive the target genes, such as *sal* or *vg* expression. Furthermore, our analyses of all subunits of the Mediator complex have led us to discover that Med12, Med13, Med15, Med23, Med24, and Med31 are also required for Mad-dependent transcription. These observations support the model that the Mediator complex functions as a molecular bridge between Mad-containing transcriptional complex and the general transcription machinery.

From this dominant modifier genetic screen, only two of the partially overlapping deficiency lines were utilized to identify the Dpp component, *dad.* There are 24 additional deficiency lines that also uncover genes that can dominantly modify the wing phenotypes caused by alteration of CDK8-CycC. It will be important to further analyze these specific genetic loci in the future. In addition, we note that there are hundreds of deficiency alleles, that can modify one or two but not all of the wing phenotypes caused by altering CDK8 or CycC. Although the complexities underlying these “inconsistent” results, are still unknown, these alleles could also encode factors that functionally interact with CDK8 *in vivo*. Characterization of other upstream

regulators or downstream effectors of CDK8 is essential for a better understanding of CDK8 function.

Considering other potential genetic components and complexity of the venation regulation of *Drosophila* wing, it remains unclear exactly how CDK8 regulates vein formation during development. Although CDK8 was reported to have varieties of substrates in different species, whose homologs are also known to involve in venation of *Drosophila* wing, exactly how CDK8 regulates vein patterning during wing development is still not clear. In addition, several other signaling pathways, such as the Hh signaling pathway and the EGFR signaling pathway, coordinate together with Dpp signaling pathway finely during the vein cell-fate determination and differentiation. Coordinated interplay among these signaling pathways and downstream transcription factors are essential for precise spatiotemporal regulation of cell proliferation and differentiation to generate stereotypical vein patterns [114, 116, 251]. To provide insights to resolve the complexity of the signaling pathways coordination during normal development and diseases progression, it is important to investigate how these signaling pathways crosstalk with each other and how CDK8 plays any role in these complicated networks.

Another interesting question related to this part of our study on CDK8 and Dpp signaling is that how CDK8 modulates the Dpp and Wnt signaling pathways in regulating *vg* transcription. The second and fourth intron of *vg* locus are the known to contain the regulatory elements that control the specific expression pattern of *vg* in wing discs [252], and the fourth intron was reported to be regulated by both Dpp and Wnt signaling pathways [81, 253, 254]. Additional work with more specific reporters for the transcriptional activities of Dpp or Wnt signaling is necessary to distinguish the potentially distinct effects of CDK8 on the expression of the target genes of these two important signaling pathways in the future. Further study of *vg* transcription

regulation may provide a powerful biological context to address this important but challenging problem.

V.2 Distinct role of CDK8 module subunits and their asymmetric interdependency

Depletion of the CKM subunits in *Drosophila* eye and wing in different combinations led us to make some unexpected observations. In general, CDK8 and CycC are not required for eye development, and depletion of CDK8-CycC increased the wing cell number and affect vein patterning. In contrast, depletion of Med12-Med13 strongly disrupted the development of both *Drosophila* eye and wing. Additional developmental genetic analyses suggest that CDK8-CycC and Med12-Med13 have independent functions on cell proliferation and cell survival to each other pair of the subunits. Depletion of CDK8-CycC promotes cell proliferation, likely through their negative regulation on E2F1 [60, 68]. However, depletion of Med12-Med13 does not affect cell proliferation significantly, but may influence differentiation of eye or wing cells through Hh or Wg signaling pathways [139, 255].

To systemically understand the potential distinct roles of two pairs of the CKM subunits, CDK8-CycC and Med12-Med13, in regulating transcription to determine animal development, it is important to perform transcriptome analysis, such as RNA-seq or scRNA-seq (single cell RNA-seq). From the transcriptome analyses of samples from depleting different combinations of the four subunits, we will be able to distinguish several groups of genes that are affected differently by perturbations of the CKM subunits. We speculate several possibilities: genes are affected by all the four subunits in the same trend, such as *sal* or *vg* described in Chapter II, which requires all four subunits; transcriptions are regulated by CDK8-CycC only, but not Med12-Med13, where one possibility is E2F1 target; genes are influenced by Med12-Med13 depletion, but not CDK8-CycC, including Wg targets; genes are changed oppositely by altering

CDK8-CycC or Med12-Med13; and a group of gene is not affected by altering any of the four subunits. Further validation of transcriptional activity reporters from each group *in vivo* may significantly advance our knowledge of how the four CKM subunits function distinctly.

Finally, we observed that the stability of the four subunits of the CKM are asymmetrically interdependent on each other, which is unexpected: Depletion of Med12 or Med13, but not CycC, can reduce the level of CDK8 protein; the stability of CycC is dependent on CDK8 [85], the stability of Med12 and Med13 are dependent on each other, but not affected by depletion of CDK8 or CycC.

There are two major mechanisms for protein degradation in eukaryotic cells, lysosome dependent degradation and proteasome dependent degradation [256]. MED13 or MED13L was reported to be ubiquitinated by SCF–Fbw7 ligase and degraded through 26S proteasome [257]. However, it remains unclear whether this mechanism is conserved during evolution, whether MED13/MED13L is consistently degraded or promoted by unknown condition and whether loss of other CKM subunits trigger the degradation of MED13/MED13L through this mechanism. Moreover, the mechanisms that control the stability of the other three CKM subunits are unexplored to date. Understanding of the mechanism of asymmetric interdependency is important to understand how the four subunits affects each other stability in different type of cancers, when one of the subunits is amplified or mutated.

To address this problem, it is important to distinguish whether the subunits are degraded through lysosome or proteasome. If they are degraded through proteasome, whether it is 20S proteasome dependent or 26S proteasome dependent. One potential explanation for the protein complex subunits degradation is that dissociation of the protein complex may expose intrinsically disordered region of the subunits, which will be recognized by 20S proteasome and

be degraded ubiquitination independently [163]. As described in Chapter III, all the four subunits have intrinsically disordered region to support the 20S proteasome dependent degradation. However, further genetic and biochemistry tests are required to address exactly how the other CKM subunits are degraded upon removal of one of the subunits.

V.3 CDK8-Cyclin C modulates lipogenesis by directly inhibiting SREBP-dependent transcription in *Drosophila*

The third major part of my work focuses on analyzing the role of CDK8 in regulating lipogenesis in *Drosophila*. Previously, we have reported that phosphorylation of SREBP by CDK8 promotes the degradation of SREBP by 26S proteasome [258]. However, several questions remain unanswered. The first question is what the biological consequences of this phosphorylation *in vivo.* To address these questions, we have generated two overexpression lines to overexpression wild type mature form of SREBP or phospho-mutant form of SREBP. The observations indicate that the mutation of the phosphorylation site of nucleus form of SREBP stabilize the SREBP protein in larval fat body, increase chromosome binding of SREBP, further stimulate SREBP transcriptional target, FAS transcription in both larval fat body and adult intestine, and enhance the accumulation of lipid in larval fat body.

Interestingly, as discussed in Chapter IV, there are several other highly conserved phosphorylation sites of SREBP by different kinases, such as GSK-3β [241] and S6K [242]. However, it remains unclear whether these phosphorylation are conserved during evolution, whether the biologically consequences observed with biochemistry approaches or in cultured cells are consistent *in vivo* and how the different kinases coordinate with each other to modulate SREBP transcriptional activity. To address these questions, it is important to test them in the similar biological context *in vivo*, for example using *Drosophila* as a model system and perform

the similar examinations described in Chapter IV. Presumably, overexpressing the phospho-mutants of other phosphorylation sites and additionally co-overexpressing different combinations of kinases will result in different effects on SREBP stability and transcriptional activity, which will extend our knowledge about how different kinases communicate and regulate SREBP with different site phosphorylations.

Nevertheless, as described in Chapter IV, our biochemical analyses led us to identify six essential amino acids (AA) of N-terminus of SREBP for interaction between SREBP and CDK8. We have observed that mutating these six amino acids abolish the interaction. Interestingly, Med15, a reported positive regulator of SREBP dependent transcription [259], also interacts with SREBP through the same amino acid sequence. Taken together with the previous report about phosphorylation of SREBP by CDK8 [258], these results suggest CDK8 may interact with nucleus form of SREBP at N-terminus of SREBP but phosphorylate it at Threonine 390 and cause SREBP degradation.

Our observation revealed the interactions between SREBP and CDK8 or Med15. However, it needs to be further studied to understand how CDK8 and Med15 coordinate with each other to interact with SREBP. There are two major possibilities that could be tested in the future: First, CDK8 and Med15 may compete with each other to bind to the same site. When CDK8 is abundant, it competes to bind with SREBP to phosphorylate it and causes SREBP degradation. When CDK8 level is low, SREBP may preferentially bind to Med15 and recruiting the rest of general transcription machinery for the expression of lipogenic genes; Second, Med15 may bind to SREBP to recruit the small Mediator complex to drive the activation of SREBP dependent transcription, which subsequently introduce the CKM binding to SREBP and turn off SREBP dependent transcription by phosphorylation and degradation.

Overall, our work validated the role of CDK8 and the Mediator complex in stimulating Mad-dependent transcription, but CDK8-CycC negatively regulates SREBP dependent transcription and lipogenesis *in vivo*, further extended the knowledge about how the Mediator complex regulates transcription in different biological contexts. In addition, we have investigated the distinct roles of the four CKM subunits in regulating *Drosophila* development and their asymmetric interdependency. These results advance the knowledge about CDK8 or the CKM function *in vivo*, highlight the potential roles of CDK8 or the CKM in different types of cancers through regulating Mad/Smads or SREBP dependent transcriptions, and implicate complicated interdependent roles among the four CKM subunits in different biological contexts.

This work also opens up new research directions, for example, identification of additional uncharacterized interactors of the CKM, and determination of the specific mechanisms that control the stabilities of the four CKM subunits. *Drosophila* provides a powerful model organism to addresses these important problems. These investigations are expected to significant advance our understandings of the role and regulation of the CKM and other subunits of the Mediator complex in different physiological or pathological conditions.

REFERENCES

1. Boube M, Joulia L, Cribbs DL, Bourbon HM: **Evidence for a mediator of RNA polymerase II transcriptional regulation conserved from yeast to man**. *Cell* 2002, **110**(2):143-151.

2. Bourbon HM, Aguilera A, Ansari AZ, Asturias FJ, Berk AJ, Bjorklund S, Blackwell TK, Borggrefe T, Carey M, Carlson M *et al*: **A unified nomenclature for protein subunits of mediator complexes linking transcriptional regulators to RNA polymerase II**. *Mol Cell* 2004, **14**(5):553-557.

3. Kornberg RD: **Mediator and the mechanism of transcriptional activation**. *Trends Biochem Sci* 2005, **30**(5):235-239.

4. Soutourina J: **Transcription regulation by the Mediator complex**. *Nature reviews Molecular cell biology* 2018, **19**(4):262-274.

5. Bourbon HM: **Comparative genomics supports a deep evolutionary origin for the large, four-module transcriptional mediator complex**. *Nucleic Acids Res* 2008, **36**(12):3993-4008.

6. Conaway RC, Conaway JW: **Function and regulation of the Mediator complex**. *Curr Opin Genet Dev* 2011, **21**(2):225-230.

7. Fondell JD: **The Mediator complex in thyroid hormone receptor action**. *Biochim Biophys Acta* 2013, **1830**(7):3867-3875.

8. Poss ZC, Ebmeier CC, Taatjes DJ: **The Mediator complex and transcription regulation**. *Crit Rev Biochem Mol Biol* 2013, **48**(6):575-608.

9. Yin JW, Wang G: **The Mediator complex: a master coordinator of transcription and cell lineage development**. *Development* 2014, **141**(5):977-987.

10. Clark AD, Oldenbroek M, Boyer TG: **Mediator kinase module and human tumorigenesis**. *Crit Rev Biochem Mol Biol* 2015, **50**(5):393-426.

11. Xu W, Ji JY: **Dysregulation of CDK8 and Cyclin C in tumorigenesis**. *J Genet Genomics* 2011, **38**(10):439-452.

12. Schiano C, Casamassimi A, Rienzo M, de Nigris F, Sommese L, Napoli C: **Involvement of Mediator complex in malignancy**. *Biochim Biophys Acta* 2014, **1845**(1):66-83.

13. Spaeth JM, Kim NH, Boyer TG: **Mediator and human disease**. *Seminars in cell & developmental biology* 2011, **22**(7):776-787.

14. Li X, Liu M, Ji JY: **Understanding Obesity as a Risk Factor for Uterine Tumors Using Drosophila**. *Advances in experimental medicine and biology* 2019, **1167**:129-155.

15. Roninson IB, Győrffy B, Mack ZT, Shtil AA, Shtutman MS, Chen M, Broude EVJC: **Identifying cancers impacted by CDK8/19**. 2019, **8**(8):821.

16. Firestein R, Bass AJ, Kim SY, Dunn IF, Silver SJ, Guney I, Freed E, Ligon AH, Vena N, Ogino S *et al*: **CDK8 is a colorectal cancer oncogene that regulates beta-catenin activity**. *Nature* 2008, **455**(7212):547-551.

17. Firestein R, Shima K, Nosho K, Irahara N, Baba Y, Bojarski E, Giovannucci EL, Hahn WC, Fuchs CS, Ogino SJIjoc: **CDK8 expression in 470 colorectal cancers in relation to β‐catenin activation, other molecular alterations and patient survival**. 2010, **126**(12):2863-2873.

18. V Broude E, Gyorffy B, A Chumanevich A, Chen M, SJ McDermott M, Shtutman M, F Catroppo J, B Roninson IJCcdt: **Expression of CDK8 and CDK8-interacting genes as potential biomarkers in breast cancer**. 2015, **15**(8):739-749.

19. Makinen N, Heinonen HR, Moore S, Tomlinson IP, van der Spuy ZM, Aaltonen LA: **MED12 exon 2 mutations are common in uterine leiomyomas from South African patients**. *Oncotarget* 2011, **2**(12):966-969.

20. Jamaluddin MFB, Ko YA, Kumar M, Brown Y, Bajwa P, Nagendra PB, Skerrett-Byrne DA, Hondermarck H, Baker MA, Dun MD *et al*: **Proteomic Profiling of Human Uterine Fibroids Reveals Upregulation of the Extracellular Matrix Protein Periostin**. *Endocrinology* 2018, **159**(2):1106-1118.

21. Liegl-Atzwanger B, Heitzer E, Flicker K, Muller S, Ulz P, Saglam O, Tavassoli F, Devouassoux-Shisheboran M, Geigl J, Moinfar F: **Exploring chromosomal abnormalities and genetic changes in uterine smooth muscle tumors**. *Modern pathology : an official journal of the United States and Canadian Academy of Pathology, Inc* 2016, **29**(10):1262-1277.

22. Mello JBH, Barros-Filho MC, Abreu FB, Cirilo PDR, Domingues MAC, Pontes A, Rogatto SR: **MicroRNAs involved in the HMGA2 deregulation and its co-occurrence with MED12 mutation in uterine leiomyoma**. *Molecular human reproduction* 2018, **24**(11):556-563.

23. Wu J, Zou Y, Luo Y, Guo JB, Liu FY, Zhou JY, Zhang ZY, Wan L, Huang OP: **Prevalence and clinical significance of mediator complex subunit 12 mutations in 362 Han Chinese samples with uterine leiomyoma**. *Oncology letters* 2017, **14**(1):47-54.

24. Wang H, Ye J, Qian H, Zhou R, Jiang J, Ye L: **High-resolution melting analysis of MED12 mutations in uterine leiomyomas in Chinese patients**. *Genetic testing and molecular biomarkers* 2015, **19**(3):162-166.

25. Zhang Q, Ubago J, Li L, Guo H, Liu Y, Qiang W, Kim JJ, Kong B, Wei JJ: **Molecular analyses of 6 different types of uterine smooth muscle tumors: Emphasis in atypical leiomyoma**. *Cancer* 2014, **120**(20):3165-3177.

26. Heinonen HR, Sarvilinna NS, Sjoberg J, Kampjarvi K, Pitkanen E, Vahteristo P, Makinen N, Aaltonen LA: **MED12 mutation frequency in unselected sporadic uterine leiomyomas**. *Fertility and sterility* 2014, **102**(4):1137-1142.

27. Heinonen HR, Pasanen A, Heikinheimo O, Tanskanen T, Palin K, Tolvanen J, Vahteristo P, Sjoberg J, Pitkanen E, Butzow R *et al*: **Multiple clinical characteristics separate MED12-mutation-positive and -negative uterine leiomyomas**. *Scientific reports* 2017, **7**(1):1015.

28. Makinen N, Kampjarvi K, Frizzell N, Butzow R, Vahteristo P: **Characterization of MED12, HMGA2, and FH alterations reveals molecular variability in uterine smooth muscle tumors**. *Molecular cancer* 2017, **16**(1):101.

29. Mehine M, Kaasinen E, Heinonen HR, Makinen N, Kampjarvi K, Sarvilinna N, Aavikko M, Vaharautio A, Pasanen A, Butzow R *et al*: **Integrated data analysis reveals uterine leiomyoma subtypes with distinct driver pathways and biomarkers**. *Proceedings of the National Academy of Sciences of the United States of America* 2016, **113**(5):1315-1320.

30. Perot G, Croce S, Ribeiro A, Lagarde P, Velasco V, Neuville A, Coindre JM, Stoeckle E, Floquet A, MacGrogan G *et al*: **MED12 alterations in both human benign and malignant uterine soft tissue tumors**. *PloS one* 2012, **7**(6):e40015.

31. Markowski DN, Bartnitzke S, Loning T, Drieschner N, Helmke BM, Bullerdiek J: **MED12 mutations in uterine fibroids--their relationship to cytogenetic subgroups**. *International journal of cancer* 2012, **131**(7):1528-1536.

32. Matsubara A, Sekine S, Yoshida M, Yoshida A, Taniguchi H, Kushima R, Tsuda H, Kanai Y: **Prevalence of MED12 mutations in uterine and extrauterine smooth muscle tumours**. *Histopathology* 2013, **62**(4):657-661.

33. Shahbazi S, Fatahi N, Amini-Moghaddam S: **Somatic mutational analysis of MED12 exon 2 in uterine leiomyomas of Iranian women**. *American journal of cancer research* 2015, **5**(8):2441-2446.

34. Sadeghi S, Khorrami M, Amin-Beidokhti M, Abbasi M, Kamalian Z, Irani S, Omrani M, Azmoodeh O, Mirfakhraie R: **The study of MED12 gene mutations in uterine leiomyomas from Iranian patients**. *Tumour biology : the journal of the International Society for Oncodevelopmental Biology and Medicine* 2016, **37**(2):1567-1571.

35. Di Tommaso S, Tinelli A, Malvasi A, Massari S: **Missense mutations in exon 2 of the MED12 gene are involved in IGF-2 overexpression in uterine leiomyoma**. *Molecular human reproduction* 2014, **20**(10):1009-1015.

36. de Graaff MA, Cleton-Jansen AM, Szuhai K, Bovee JV: **Mediator complex subunit 12 exon 2 mutation analysis in different subtypes of smooth muscle tumors confirms genetic heterogeneity**. *Human pathology* 2013, **44**(8):1597-1604.

37. Osinovskaya NS, Malysheva OV, Shved NY, Ivashchenko TE, Sultanov IY, Efimova OA, Yarmolinskaya MI, Bezhenar VF, Baranov VS: **Frequency and Spectrum of MED12 Exon 2 Mutations in Multiple Versus Solitary Uterine Leiomyomas From Russian Patients**. *International journal of gynecological pathology : official journal of the International Society of Gynecological Pathologists* 2016, **35**(6):509-515.

38. Ajabnoor GMA, Mohammed NA, Banaganapalli B, Abdullah LS, Bondagji ON, Mansouri N, Sahly NN, Vaidyanathan V, Bondagji N, Elango R *et al*: **Expanded Somatic Mutation Spectrum of MED12 Gene in Uterine Leiomyomas of Saudi Arabian Women**. *Frontiers in genetics* 2018, **9**:552.

39. Je EM, Kim MR, Min KO, Yoo NJ, Lee SH: **Mutational analysis of MED12 exon 2 in uterine leiomyoma and other common tumors**. *International journal of cancer* 2012, **131**(6):E1044-1047.

40. Lee M, Cheon K, Chae B, Hwang H, Kim HK, Chung YJ, Song JY, Cho HH, Kim JH, Kim MR: **Analysis of MED12 Mutation in Multiple Uterine Leiomyomas in South Korean patients**. *International journal of medical sciences* 2018, **15**(2):124-128.

41. Galindo LJ, Hernandez-Beeftink T, Salas A, Jung Y, Reyes R, de Oca FM, Hernandez M, Almeida TA: **HMGA2 and MED12 alterations frequently co-occur in uterine leiomyomas**. *Gynecologic oncology* 2018, **150**(3):562-568.

42. Halder SK, Laknaur A, Miller J, Layman LC, Diamond M, Al-Hendy A: **Novel MED12 gene somatic mutations in women from the Southern United States with symptomatic uterine fibroids**. *Molecular genetics and genomics : MGG* 2015, **290**(2):505-511.

43. Ravegnini G, Marino-Enriquez A, Slater J, Eilers G, Wang Y, Zhu M, Nucci MR, George S, Angelini S, Raut CP *et al*: **MED12 mutations in leiomyosarcoma and extrauterine leiomyoma**. *Modern pathology : an official journal of the United States and Canadian Academy of Pathology, Inc* 2013, **26**(5):743-749.

44. Bertsch E, Qiang W, Zhang Q, Espona-Fiedler M, Druschitz S, Liu Y, Mittal K, Kong B, Kurita T, Wei JJ: **MED12 and HMGA2 mutations: two independent genetic events in uterine leiomyoma and leiomyosarcoma**. *Modern pathology : an official journal of the United States and Canadian Academy of Pathology, Inc* 2014, **27**(8):1144-1153.

45. Schwetye KE, Pfeifer JD, Duncavage EJ: **MED12 exon 2 mutations in uterine and extrauterine smooth muscle tumors**. *Human pathology* 2014, **45**(1):65-70.

46. Yatsenko SA, Mittal P, Wood-Trageser MA, Jones MW, Surti U, Edwards RP, Sood AK, Rajkovic A: **Highly heterogeneous genomic landscape of uterine leiomyomas by whole exome sequencing and genome-wide arrays**. *Fertility and sterility* 2017, **107**(2):457-466 e459.

47. McGuire MM, Yatsenko A, Hoffner L, Jones M, Surti U, Rajkovic A: **Whole exome sequencing in a random sample of North American women with leiomyomas**

identifies MED12 mutations in majority of uterine leiomyomas. *PloS one* 2012, **7**(3):e33251.

48. Hayden MA, Ordulu Z, Gallagher CS, Quade BJ, Anchan RM, Middleton NR, Srouji SS, Stewart EA, Morton CC: **Clinical, pathologic, cytogenetic, and molecular profiling in self-identified black women with uterine leiomyomata**. *Cancer genetics* 2018, **222-223**:1-8.

49. Park MJ, Shen H, Kim NH, Gao F, Failor C, Knudtson JF, McLaughlin J, Halder SK, Heikkinen TA, Vahteristo P *et al*: **Mediator Kinase Disruption in MED12-Mutant Uterine Fibroids From Hispanic Women of South Texas**. *The Journal of clinical endocrinology and metabolism* 2018, **103**(11):4283-4292.

50. Mehine M, Makinen N, Heinonen HR, Aaltonen LA, Vahteristo P: **Genomics of uterine leiomyomas: insights from high-throughput sequencing**. *Fertility and sterility* 2014, **102**(3):621-629.

51. Mehine M, Kaasinen E, Makinen N, Katainen R, Kampjarvi K, Pitkanen E, Heinonen HR, Butzow R, Kilpivaara O, Kuosmanen A *et al*: **Characterization of uterine leiomyomas by whole-genome sequencing**. *The New England journal of medicine* 2013, **369**(1):43-53.

52. Makinen N, Mehine M, Tolvanen J, Kaasinen E, Li Y, Lehtonen HJ, Gentile M, Yan J, Enge M, Taipale M *et al*: **MED12, the mediator complex subunit 12 gene, is mutated at high frequency in uterine leiomyomas**. *Science* 2011, **334**(6053):252-255.

53. Kampjarvi K, Makinen N, Kilpivaara O, Arola J, Heinonen HR, Bohm J, Abdel-Wahab O, Lehtonen HJ, Pelttari LM, Mehine M *et al*: **Somatic MED12 mutations in uterine leiomyosarcoma and colorectal cancer**. *Br J Cancer* 2012, **107**(10):1761-1765.

54. Makinen N, Aavikko M, Heikkinen T, Taipale M, Taipale J, Koivisto-Korander R, Butzow R, Vahteristo P: **Exome Sequencing of Uterine Leiomyosarcomas Identifies Frequent Mutations in TP53, ATRX, and MED12**. *PLoS genetics* 2016, **12**(2):e1005850.

55. Kapoor A, Goldberg MS, Cumberland LK, Ratnakumar K, Segura MF, Emanuel PO, Menendez S, Vardabasso C, Leroy G, Vidal CI *et al*: **The histone variant macroH2A suppresses melanoma progression through regulation of CDK8**. *Nature* 2010, **468**(7327):1105-1109.

56. McDermott MS, Chumanevich AA, Lim C-u, Liang J, Chen M, Altilia S, Oliver D, Rae JM, Shtutman M, Kiaris HJO: **Inhibition of CDK8 mediator kinase suppresses estrogen dependent transcription and the growth of estrogen receptor positive breast cancer**. 2017, **8**(8):12558.

57. Osherovich L: **CDK8 is enough in colorectal cancer** *Science-Business eXchange* 2008, **1**(34):5-7.

58. Rzymski T, Mikula M, Wiklik K, Brzozka K: **CDK8 kinase--An emerging target in targeted cancer therapy**. *Biochim Biophys Acta* 2015, **1854**(10 Pt B):1617-1629.

59. Morris EJ, Ji JY, Yang F, Di Stefano L, Herr A, Moon NS, Kwon EJ, Haigis KM, Naar AM, Dyson NJ: **E2F1 represses beta-catenin transcription and is antagonized by both pRB and CDK8**. *Nature* 2008, **455**(7212):552-556.

60. Zhao J, Ramos R, Demma M: **CDK8 regulates E2F1 transcriptional activity through S375 phosphorylation**. *Oncogene* 2013, **32**(30):3520-3530.

61. Fryer CJ, White JB, Jones KA: **Mastermind recruits CycC:CDK8 to phosphorylate the Notch ICD and coordinate activation with turnover**. *Mol Cell* 2004, **16**(4):509-520.

62. Donner AJ, Szostek S, Hoover JM, Espinosa JM: **CDK8 is a stimulus-specific positive coregulator of p53 target genes**. *Mol Cell* 2007, **27**(1):121-133.

63. Alarcon C, Zaromytidou AI, Xi Q, Gao S, Yu J, Fujisawa S, Barlas A, Miller AN, Manova-Todorova K, Macias MJ *et al*: **Nuclear CDKs drive Smad transcriptional activation and turnover in BMP and TGF-beta pathways**. *Cell* 2009, **139**(4):757-769.

64. Aleman A, Rios M, Juarez M, Lee D, Chen A, Eivers E: **Mad linker phosphorylations control the intensity and range of the BMP-activity gradient in developing Drosophila tissues**. *Scientific reports* 2014, **4**:6927.

65. Zhao X, Feng D, Wang Q, Abdulla A, Xie XJ, Zhou J, Sun Y, Yang ES, Liu LP, Vaitheesvaran B *et al*: **Regulation of lipogenesis by cyclin-dependent kinase 8-mediated control of SREBP-1**. *The Journal of clinical investigation* 2012, **122**(7):2417-2427.

66. Bancerek J, Poss ZC, Steinparzer I, Sedlyarov V, Pfaffenwimmer T, Mikulic I, Dolken L, Strobl B, Muller M, Taatjes DJ *et al*: **CDK8 Kinase Phosphorylates Transcription Factor STAT1 to Selectively Regulate the Interferon Response**. *Immunity* 2013, **38**(2):250-262.

67. Zhao J, Ramos R, Demma MJO: **CDK8 regulates E2F1 transcriptional activity through S375 phosphorylation**. 2013, **32**(30):3520-3530.

68. Morris EJ, Ji J-Y, Yang F, Di Stefano L, Herr A, Moon N-S, Kwon E-J, Haigis KM, Näär AM, Dyson NJJN: **E2F1 represses β-catenin transcription and is antagonized by both pRB and CDK8**. 2008, **455**(7212):552-556.

69. Fryer CJ, White JB, Jones KAJMc: **Mastermind recruits CycC: CDK8 to phosphorylate the Notch ICD and coordinate activation with turnover**. 2004, **16**(4):509-520.

70. Carrera I, Janody F, Leeds N, Duveau F, Treisman JEJPotNAoS: **Pygopus activates Wingless target gene transcription through the mediator complex subunits Med12 and Med13**. 2008, **105**(18):6644-6649.

71. Loncle N, Boube M, Joulia L, Boschiero C, Werner M, Cribbs DL, Bourbon HM: **Distinct roles for Mediator Cdk8 module subunits in Drosophila development**. *EMBO J* 2007, **26**(4):1045-1054.

72. Feng D, Youn DY, Zhao X, Gao Y, Quinn 3rd WJ, Xiaoli AM, Sun Y, Birnbaum MJ, Pessin JE, Yang FJPo: **mTORC1 down-regulates cyclin-dependent kinase 8 (CDK8) and cyclin C (CycC)**. 2015, **10**(6).

73. Broude EV, Gyorffy B, Chumanevich AA, Chen M, McDermott MS, Shtutman M, Catroppo JF, Roninson IB: **Expression of CDK8 and CDK8-interacting Genes as Potential Biomarkers in Breast Cancer**. *Current cancer drug targets* 2015, **15**(8):739-749.

74. Brewster CD, Birkenheuer CH, Vogt MB, Quackenbush SL, Rovnak J: **The retroviral cyclin of walleye dermal sarcoma virus binds cyclin-dependent kinases 3 and 8**. *Virology* 2011, **409**(2):299-307.

75. Rovnak J, Quackenbush SL: **Walleye dermal sarcoma virus cyclin interacts with components of the mediator complex and the RNA polymerase II holoenzyme**. *J Virol* 2002, **76**(16):8031-8039.

76. Xu W, Wang Z, Zhang W, Qian K, Li H, Kong D, Li Y, Tang Y: **Mutated K-ras activates CDK8 to stimulate the epithelial-to-mesenchymal transition in pancreatic cancer in part via the Wnt/beta-catenin signaling pathway**. *Cancer letters* 2015, **356**(2 Pt B):613-627.

77. Aragon E, Goerner N, Zaromytidou AI, Xi Q, Escobedo A, Massague J, Macias MJ: **A Smad action turnover switch operated by WW domain readers of a phosphoserine code**. *Genes & development* 2011, **25**(12):1275-1288.

78. Akoulitchev S, Chuikov S, Reinberg D: **TFIIH is negatively regulated by cdk8-containing mediator complexes**. *Nature* 2000, **407**(6800):102-106.

79. Ni JQ, Zhou R, Czech B, Liu LP, Holderbaum L, Yang-Zhou D, Shim HS, Tao R, Handler D, Karpowicz P *et al*: **A genome-scale shRNA resource for transgenic RNAi in Drosophila**. *Nat Methods* 2011, **8**(5):405-407.

80. Qiao HH, Wang F, Xu RG, Sun J, Zhu R, Mao D, Ren X, Wang X, Jia Y, Peng P *et al*: **An efficient and multiple target transgenic RNAi technique with low toxicity in Drosophila**. *Nature communications* 2018, **9**(1):4160.

81. Zecca M, Struhl G: **Control of Drosophila wing growth by the vestigial quadrant enhancer**. *Development* 2007, **134**(16):3011-3020.

82. Zecca M, Struhl G: **Recruitment of cells into the Drosophila wing primordium by a feed-forward circuit of vestigial autoregulation**. *Development* 2007, **134**(16):3001-3010.

83. Gobert V, Osman D, Bras S, Auge B, Boube M, Bourbon HM, Horn T, Boutros M, Haenlin M, Waltzer L: **A genome-wide RNA interference screen identifies a differential role of the mediator CDK8 module subunits for GATA/ RUNX-activated transcription in drosophila**. *Mol Cell Biol* 2010, **30**(11):2837-2848.

84. Lahue EE, Smith AV, Orr-Weaver TL: **A novel cyclin gene from Drosophila complements CLN function in yeast**. *Genes & development* 1991, **5**(12A):2166-2175.

85. Xie XJ, Hsu FN, Gao X, Xu W, Ni JQ, Xing Y, Huang L, Hsiao HC, Zheng H, Wang C *et al*: **CDK8-Cyclin C Mediates Nutritional Regulation of Developmental Transitions through the Ecdysone Receptor in Drosophila**. *PLoS biology* 2015, **13**(7):e1002207.

86. Lu Q, Tang X, Tian G, Wang F, Liu K, Nguyen V, Kohalmi SE, Keller WA, Tsang EW, Harada JJ *et al*: **Arabidopsis homolog of the yeast TREX-2 mRNA export complex: components and anchoring nucleoporin**. *The Plant journal : for cell and molecular biology* 2010, **61**(2):259-270.

87. Brand AH, Perrimon N: **Targeted gene expression as a means of altering cell fates and generating dominant phenotypes**. *Development* 1993, **118**(2):401-415.

88. Duffy JB: **GAL4 system in Drosophila: a fly geneticist's Swiss army knife**. *Genesis* 2002, **34**(1-2):1-15.

89. Kambadur R, Koizumi K, Stivers C, Nagle J, Poole SJ, Odenwald WF: **Regulation of POU genes by castor and hunchback establishes layered compartments in the Drosophila CNS**. *Genes & development* 1998, **12**(2):246-260.

90. Milan M, Campuzano S, Garcia-Bellido A: **Developmental parameters of cell death in the wing disc of Drosophila**. *Proceedings of the National Academy of Sciences of the United States of America* 1997, **94**(11):5691-5696.

91. Bridges CB: **Specific modifiers of eosin eye color in Drosophila melanogaster**. *J Exp Zool* 1919, **28**:337-384.

92. St Johnston D: **The art and design of genetic screens: Drosophila melanogaster**. *Nature reviews Genetics* 2002, **3**(3):176-188.

93. Ji JY, Haghnia M, Trusty C, Goldstein LS, Schubiger G: **A genetic screen for suppressors and enhancers of the Drosophila cdk1-cyclin B identifies maternal factors that regulate microtubule and microfilament stability**. *Genetics* 2002, **162**(3):1179-1195.

94. Lee LA, Elfring LK, Bosco G, Orr-Weaver TL: **A genetic screen for suppressors and enhancers of the Drosophila PAN GU cell cycle kinase identifies cyclin B as a target**. *Genetics* 2001, **158**(4):1545-1556.

95. Kennison JA, Tamkun JW: **Dosage-dependent modifiers of polycomb and antennapedia mutations in Drosophila**. *Proceedings of the National Academy of Sciences of the United States of America* 1988, **85**(21):8136-8140.

96. Ji JY, Miles WO, Korenjak M, Zheng Y, Dyson NJ: **In vivo regulation of E2F1 by Polycomb group genes in Drosophila**. *G3* 2012, **2**(12):1651-1660.

97. Nadeau JH: **Modifier genes and protective alleles in humans and mice**. *Curr Opin Genet Dev* 2003, **13**(3):290-295.

98. Nadeau JH: **Modifier genes in mice and humans**. *Nature reviews Genetics* 2001, **2**(3):165-174.

99. Parks AL, Cook KR, Belvin M, Dompe NA, Fawcett R, Huppert K, Tan LR, Winter CG, Bogart KP, Deal JE *et al*: **Systematic generation of high-resolution deletion coverage of the Drosophila melanogaster genome**. *Nat Genet* 2004, **36**(3):288-292.

100. Cook RK, Christensen SJ, Deal JA, Coburn RA, Deal ME, Gresens JM, Kaufman TC, Cook KR: **The generation of chromosomal deletions to provide extensive coverage and subdivision of the Drosophila melanogaster genome**. *Genome biology* 2012, **13**(3):R21.

101. Nagarkar-Jaiswal S, Lee PT, Campbell ME, Chen K, Anguiano-Zarate S, Gutierrez MC, Busby T, Lin WW, He Y, Schulze KL *et al*: **A library of MiMICs allows tagging of genes and reversible, spatial and temporal knockdown of proteins in Drosophila**. *eLife* 2015, **4**.

102. Tsuneizumi K, Nakayama T, Kamoshida Y, Kornberg TB, Christian JL, Tabata T: **Daughters against dpp modulates dpp organizing activity in Drosophila wing development**. *Nature* 1997, **389**(6651):627-631.

103. Hamaratoglu F, Affolter M, Pyrowolakis G: **Dpp/BMP signaling in flies: from molecules to biology**. *Seminars in cell & developmental biology* 2014, **32**:128-136.

104. Affolter M, Basler K: **The Decapentaplegic morphogen gradient: from pattern formation to growth regulation**. *Nature reviews Genetics* 2007, **8**(9):663-674.

105. Upadhyay A, Moss-Taylor L, Kim MJ, Ghosh AC, O'Connor MB: **TGF-beta Family Signaling in Drosophila**. *Cold Spring Harbor perspectives in biology* 2017, **9**(9).

106. Massague J: **TGFbeta signalling in context**. *Nature reviews Molecular cell biology* 2012, **13**(10):616-630.

107. Raftery LA, Sutherland DJ: **TGF-beta family signal transduction in Drosophila development: from Mad to Smads**. *Developmental biology* 1999, **210**(2):251-268.

108. Santibanez JF, Krstic, J., Quintanilla, M., Bernabeu, C.: **TGF–β Signalling and Its Role in Cancer Progression and Metastasis**. *eLS* 2016.

109. Restrepo S, Zartman JJ, Basler K: **Coordination of patterning and growth by the morphogen DPP**. *Current biology : CB* 2014, **24**(6):R245-255.

110. Affolter M, Marty T, Vigano MA, Jazwinska A: **Nuclear interpretation of Dpp signaling in Drosophila**. *EMBO J* 2001, **20**(13):3298-3305.

111. Moustakas A, Souchelnytskyi S, Heldin CH: **Smad regulation in TGF-beta signal transduction**. *Journal of cell science* 2001, **114**(Pt 24):4359-4369.

112. Malik S, Roeder RG: **Dynamic regulation of pol II transcription by the mammalian Mediator complex**. *Trends Biochem Sci* 2005, **30**(5):256-263.

113. Blair SS: **Wing vein patterning in Drosophila and the analysis of intercellular signaling**. *Annual review of cell and developmental biology* 2007, **23**:293-319.

114. De Celis JF: **Pattern formation in the Drosophila wing: The development of the veins**. *BioEssays : news and reviews in molecular, cellular and developmental biology* 2003, **25**(5):443-451.

115. de Celis JF, Barrio R: **Function of the spalt/spalt-related gene complex in positioning the veins in the Drosophila wing**. *Mechanisms of development* 2000, **91**(1-2):31-41.

116. Crozatier M, Glise B, Vincent A: **Patterns in evolution: veins of the Drosophila wing**. *Trends in genetics : TIG* 2004, **20**(10):498-505.

117. Spradling AC, Stern D, Beaton A, Rhem EJ, Laverty T, Mozden N, Misra S, Rubin GM: **The Berkeley Drosophila Genome Project gene disruption project: Single P-element insertions mutating 25% of vital Drosophila genes**. *Genetics* 1999, **153**(1):135-177.

118. Treisman JE, Rubin GM: **Targets of glass regulation in the Drosophila eye disc**. *Mechanisms of development* 1996, **56**(1-2):17-24.

119. Nellen D, Burke R, Struhl G, Basler K: **Direct and long-range action of a DPP morphogen gradient**. *Cell* 1996, **85**(3):357-368.

120. Xu P, Lin X, Feng XH: **Posttranslational Regulation of Smads**. *Cold Spring Harbor perspectives in biology* 2016, **8**(12).

121. Kato Y, Habas R, Katsuyama Y, Naar AM, He X: **A component of the ARC/Mediator complex required for TGF beta/Nodal signalling**. *Nature* 2002, **418**(6898):641-646.

122. Terriente-Felix A, Lopez-Varea A, de Celis JF: **Identification of genes affecting wing patterning through a loss-of-function mutagenesis screen and characterization of med15 function during wing development**. *Genetics* 2010, **185**(2):671-684.

123. Fuentealba LC, Eivers E, Ikeda A, Hurtado C, Kuroda H, Pera EM, De Robertis EM: **Integrating patterning signals: Wnt/GSK3 regulates the duration of the BMP/Smad1 signal**. *Cell* 2007, **131**(5):980-993.

124. Bacon CW, D'Orso I: **CDK9: a signaling hub for transcriptional control**. *Transcription* 2019, **10**(2):57-75.

125. Naar AM, Lemon BD, Tjian R: **Transcriptional coactivator complexes**. *Annu Rev Biochem* 2001, **70**:475-501.

126. Allen BL, Taatjes DJ: **The Mediator complex: a central integrator of transcription**. *Nature reviews Molecular cell biology* 2015, **16**(3):155-166.

127. Stevens JL, Cantin GT, Wang G, Shevchenko A, Berk AJ: **Transcription control by E1A and MAP kinase pathway via Sur2 mediator subunit**. *Science* 2002, **296**(5568):755-758.

128. Galli GG, Carrara M, Yuan WC, Valdes-Quezada C, Gurung B, Pepe-Mooney B, Zhang T, Geeven G, Gray NS, de Laat W *et al*: **YAP Drives Growth by Controlling Transcriptional Pause Release from Dynamic Enhancers**. *Mol Cell* 2015, **60**(2):328-337.

129. Oh H, Slattery M, Ma L, Crofts A, White KP, Mann RS, Irvine KD: **Genome-wide association of Yorkie with chromatin and chromatin-remodeling complexes**. *Cell reports* 2013, **3**(2):309-318.

130. Tansey WP: **Transcriptional activation: risky business**. *Genes & development* 2001, **15**(9):1045-1050.

131. Cantelli G, Crosas-Molist E, Georgouli M, Sanz-Moreno V: **TGFBeta-induced transcription in cancer**. *Seminars in cancer biology* 2017, **42**:60-69.

132. Kahata K, Dadras MS, Moustakas A: **TGF-beta Family Signaling in Epithelial Differentiation and Epithelial-Mesenchymal Transition**. *Cold Spring Harbor perspectives in biology* 2018, **10**(1).

133. Yu Y, Feng XH: **TGF-beta signaling in cell fate control and cancer**. *Current opinion in cell biology* 2019, **61**:56-63.

134. Galbraith MD, Donner AJ, Espinosa JM: **CDK8: A positive regulator of transcription**. *Transcr* 2010, **1**(1):4-12.

135. Eivers E, Fuentealba LC, Sander V, Clemens JC, Hartnett L, De Robertis EM: **Mad is required for wingless signaling in wing development and segment patterning in Drosophila**. *PloS one* 2009, **4**(8):e6543.

136. Zhao M, Yang X, Fu Y, Wang H, Ning Y, Yan J, Chen YG, Wang G: **Mediator MED15 modulates transforming growth factor beta (TGFbeta)/Smad signaling and breast cancer cell metastasis**. *Journal of molecular cell biology* 2013, **5**(1):57-60.

137. de Celis JF, Barrio R: **Regulation and function of Spalt proteins during animal development**. *The International journal of developmental biology* 2009, **53**(8-10):1385-1398.

138. Organista MF, De Celis JF: **The Spalt transcription factors regulate cell proliferation, survival and epithelial integrity downstream of the Decapentaplegic signalling pathway**. *Biology open* 2013, **2**(1):37-48.

139. Carrera I, Janody F, Leeds N, Duveau F, Treisman JE: **Pygopus activates Wingless target gene transcription through the mediator complex subunits Med12 and Med13**. *Proceedings of the National Academy of Sciences of the United States of America* 2008, **105**(18):6644-6649.

140. Zhou H, Kim S, Ishii S, Boyer TG: **Mediator modulates Gli3-dependent Sonic hedgehog signaling**. *Mol Cell Biol* 2006, **26**(23):8667-8682.

141. Zhou H, Spaeth JM, Kim NH, Xu X, Friez MJ, Schwartz CE, Boyer TG: **MED12 mutations link intellectual disability syndromes with dysregulated GLI3-dependent Sonic Hedgehog signaling**. *Proceedings of the National Academy of Sciences of the United States of America* 2012, **109**(48):19763-19768.

142. Schier AC, Taatjes DJ: **Structure and mechanism of the RNA polymerase II transcription machinery**. *Genes & development* 2020, **34**(7-8):465-488.

143. Roeder RG: **50+ years of eukaryotic transcription: an expanding universe of factors and mechanisms**. *Nature structural & molecular biology* 2019, **26**(9):783-791.

144. Hahn S: **Structure and mechanism of the RNA polymerase II transcription machinery**. *Nature structural & molecular biology* 2004, **11**(5):394-403.

145. Malik S, Roeder RG: **The metazoan Mediator co-activator complex as an integrative hub for transcriptional regulation**. *Nature reviews Genetics* 2010, **11**(11):761-772.

146. Elmlund H, Baraznenok V, Lindahl M, Samuelsen CO, Koeck PJ, Holmberg S, Hebert H, Gustafsson CM: **The cyclin-dependent kinase 8 module sterically blocks Mediator interactions with RNA polymerase II**. *Proceedings of the National Academy of Sciences of the United States of America* 2006, **103**(43):15788-15793.

147. Tsai K-L, Sato S, Tomomori-Sato C, Conaway RC, Conaway JW, Asturias FJJNs, biology m: **A conserved Mediator–CDK8 kinase module association regulates Mediator–RNA polymerase II interaction**. 2013, **20**(5):611.

148. Nemet J, Jelicic B, Rubelj I, Sopta MJB: **The two faces of Cdk8, a positive/negative regulator of transcription**. 2014, **97**:22-27.

149. Fant CB, Taatjes DJJT: **Regulatory functions of the Mediator kinases CDK8 and CDK19**. 2019, **10**(2):76-90.

150. Dannappel MV, Sooraj D, Loh JJ, Firestein RJFic, biology d: **Molecular and in vivo functions of the CDK8 and CDK19 kinase modules**. 2019, **6**:171.

151. Knuesel MT, Meyer KD, Donner AJ, Espinosa JM, Taatjes DJ: **The human CDK8 subcomplex is a histone kinase that requires Med12 for activity and can function independently of mediator**. *Mol Cell Biol* 2009, **29**(3):650-661.

152. Klatt F, Leitner A, Kim IV, Ho-Xuan H, Schneider EV, Langhammer F, Weinmann R, Muller MR, Huber R, Meister G *et al*: **A precisely positioned MED12 activation helix stimulates CDK8 kinase activity**. *Proceedings of the National Academy of Sciences of the United States of America* 2020, **117**(6):2894-2905.

153. Turunen M, Spaeth JM, Keskitalo S, Park MJ, Kivioja T, Clark AD, Makinen N, Gao F, Palin K, Nurkkala H *et al*: **Uterine leiomyoma-linked MED12 mutations disrupt mediator-associated CDK activity**. *Cell reports* 2014, **7**(3):654-660.

154. Janody F, Martirosyan Z, Benlali A, Treisman JE: **Two subunits of the Drosophila mediator complex act together to control cell affinity**. *Development* 2003, **130**(16):3691-3701.

155. Treisman J: **Drosophila homologues of the transcriptional coactivation complex subunits TRAP240 and TRAP230 are required for identical processes in eye-antennal disc development**. *Development* 2001, **128**(4):603-615.

156. Schiano C, Casamassimi A, Vietri MT, Rienzo M, Napoli C: **The roles of mediator complex in cardiovascular diseases**. *Biochim Biophys Acta* 2014, **1839**(6):444-451.

157. Li X, Liu M, Ren X, Loncle N, Wang Q, Hemba-Waduge RU, Yu SH, Boube M, Bourbon HG, Ni JQ *et al*: **The Mediator CDK8-Cyclin C complex modulates Dpp signaling in Drosophila by stimulating Mad-dependent transcription**. *PLoS genetics* 2020, **16**(5):e1008832.

158. Qiao H-H, Wang F, Xu R-G, Sun J, Zhu R, Mao D, Ren X, Wang X, Jia Y, Peng PJNc: **An efficient and multiple target transgenic RNAi technique with low toxicity in Drosophila**. 2018, **9**(1):1-13.

159. Groth AC, Fish M, Nusse R, Calos MP: **Construction of transgenic Drosophila by using the site-specific integrase from phage phiC31**. *Genetics* 2004, **166**(4):1775-1782.

160. Song Z, McCall K, Steller HJS: **DCP-1, a Drosophila cell death protease essential for development**. 1997, **275**(5299):536-540.

161. Zielke N, Edgar BA: **FUCCI sensors: powerful new tools for analysis of cell proliferation**. *Wiley interdisciplinary reviews Developmental biology* 2015, **4**(5):469-487.

162. Ji JY, Dyson NJ: **Interplay between Cyclin-dependent Kinases and E2F-dependent Transcription**. In: *Cell Cycle Deregulation in Cancer.* Edited by Enders G: Springer Science 2010: 23-41.

163. Asher G, Reuven N, Shaul Y: **20S proteasomes and protein degradation "by default"**. *BioEssays : news and reviews in molecular, cellular and developmental biology* 2006, **28**(8):844-849.

164. Klatt F, Leitner A, Kim IV, Ho-Xuan H, Schneider EV, Langhammer F, Weinmann R, Müller MR, Huber R, Meister G: **A precisely positioned MED12 activation helix stimulates CDK8 kinase activity**. *Proceedings of the National Academy of Sciences* 2020, **117**(6):2894-2905.

165. McNaught AD, Wilkinson A: **Compendium of chemical terminology**, vol. 1669: Blackwell Science Oxford; 1997.

166. Bloor WJPotSfEB, Medicine: **Outline of a classification of the lipoids**. 1920, **17**(6):138-140.

167. Fahy E, Subramaniam S, Murphy RC, Nishijima M, Raetz CR, Shimizu T, Spener F, van Meer G, Wakelam MJ, Dennis EAJJolr: **Update of the LIPID MAPS comprehensive classification system for lipids**. 2009, **50**(Supplement):S9-S14.

168. Rawson RB: **The SREBP pathway--insights from Insigs and insects**. *Nature reviews Molecular cell biology* 2003, **4**(8):631-640.

169. Jeon TI, Osborne TF: **SREBPs: metabolic integrators in physiology and metabolism**. *Trends Endocrinol Metab* 2012, **23**(2):65-72.

170. Brown MS, Goldstein JL: **The SREBP pathway: regulation of cholesterol metabolism by proteolysis of a membrane-bound transcription factor**. *Cell* 1997, **89**(3):331-340.

171. Osborne TF, Espenshade PJ: **Evolutionary conservation and adaptation in the mechanism that regulates SREBP action: what a long, strange tRIP it's been**. *Genes & development* 2009, **23**(22):2578-2591.

172. Shimomura I, Bashmakov Y, Ikemoto S, Horton JD, Brown MS, Goldstein JLJPotNAoS: **Insulin selectively increases SREBP-1c mRNA in the livers of rats with streptozotocin-induced diabetes**. 1999, **96**(24):13656-13661.

173. Shimano H, Yahagi N, Amemiya-Kudo M, Hasty AH, Osuga J-i, Tamura Y, Shionoiri F, Iizuka Y, Ohashi K, Harada KJJoBC: **Sterol regulatory element-binding protein-1 as a key transcription factor for nutritional induction of lipogenic enzyme genes**. 1999, **274**(50):35832-35839.

174. Amemiya-Kudo M, Shimano H, Hasty AH, Yahagi N, Yoshikawa T, Matsuzaka T, Okazaki H, Tamura Y, Iizuka Y, Ohashi KJJolr: **Transcriptional activities of nuclear SREBP-1a,-1c, and-2 to different target promoters of lipogenic and cholesterogenic genes**. 2002, **43**(8):1220-1235.

175. Desvergne B, Michalik L, Wahli W: **Transcriptional regulation of metabolism**. *Physiol Rev* 2006, **86**(2):465-514.

176. Moslehi A, Hamidi-zad ZJJoc, hepatology t: **Role of SREBPs in liver diseases: a mini-review**. 2018, **6**(3):332.

177. Guo D, Hlavin Bell E, Mischel P, Chakravarti AJCpd: **Targeting SREBP-1-driven lipid metabolism to treat cancer**. 2014, **20**(15):2619-2626.

178. Menendez JA, Lupu R: **Fatty acid synthase and the lipogenic phenotype in cancer pathogenesis**. *Nat Rev Cancer* 2007, **7**(10):763-777.

179. Zhang F, Du G: **Dysregulated lipid metabolism in cancer**. *World journal of biological chemistry* 2012, **3**(8):167.

180. Eberlé D, Clément K, Meyre D, Sahbatou M, Vaxillaire M, Le Gall A, Ferré P, Basdevant A, Froguel P, Foufelle FJD: **SREBF-1 gene polymorphisms are associated with obesity and type 2 diabetes in French obese and diabetic cohorts**. 2004, **53**(8):2153-2157.

181. Felder T, Oberkofler H, Weitgasser R, Mackevics V, Krempler F, Paulweber B, Patsch WJIjoo: **The SREBF-1 locus is associated with type 2 diabetes and plasma adiponectin levels in a middle-aged Austrian population**. 2007, **31**(7):1099-1103.

182. Musso G, Bo S, Cassader M, De Michieli F, Gambino RJTAjocn: **Impact of sterol regulatory element-binding factor-1c polymorphism on incidence of nonalcoholic fatty liver disease and on the severity of liver disease and of glucose and lipid dysmetabolism**. 2013, **98**(4):895-906.

183. Bao J, Zhu L, Zhu Q, Su J, Liu M, Huang WJOl: **SREBP-1 is an independent prognostic marker and promotes invasion and migration in breast cancer**. 2016, **12**(4):2409-2416.

184. Martel PM, Bingham CM, McGraw CJ, Baker CL, Morganelli PM, Meng ML, Armstrong JM, Moncur JT, Kinlaw WBJEcr: **S14 protein in breast cancer cells: direct evidence of regulation by SREBP-1c, superinduction with progestin, and effects on cell growth**. 2006, **312**(3):278-288.

185. Zhu Z, Zhao X, Zhao L, Yang H, Liu L, Li J, Wu J, Yang F, Huang G, Liu JJO: **p54 nrb/NONO regulates lipid metabolism and breast cancer growth through SREBP-1A**. 2016, **35**(11):1399-1410.

186. Jie Z, Xie Z, Xu W, Zhao X, Jin G, Sun X, Huang B, Tang P, Wang G, Shen SJBeBA-MBoD: **SREBP-2 aggravates breast cancer associated osteolysis by promoting osteoclastogenesis and breast cancer metastasis**. 2019, **1865**(1):115-125.

187. Chen M, Zhang J, Sampieri K, Clohessy JG, Mendez L, Gonzalez-Billalabeitia E, Liu X-S, Lee Y-R, Fung J, Katon JMJNg: **An aberrant SREBP-dependent lipogenic program promotes metastatic prostate cancer**. 2018, **50**(2):206-218.

188. Huang W-C, Li X, Liu J, Lin J, Chung LWJMCR: **Activation of androgen receptor, lipogenesis, and oxidative stress converged by SREBP-1 is responsible for regulating growth and progression of prostate cancer cells**. 2012, **10**(1):133-142.

189. Li X, Wu JB, Li Q, Shigemura K, Chung LW, Huang W-CJO: **SREBP-2 promotes stem cell-like properties and metastasis by transcriptional activation of c-Myc in prostate cancer**. 2016, **7**(11):12869.

190. Wen Y-A, Xiong X, Zaytseva YY, Napier DL, Vallee E, Li AT, Wang C, Weiss HL, Evers BM, Gao TJCd *et al*: **Downregulation of SREBP inhibits tumor growth and initiation by altering cellular metabolism in colon cancer**. 2018, **9**(3):1-14.

191. Liu Y, Hua W, Li Y, Xian X, Zhao Z, Liu C, Zou J, Li J, Fang X, Zhu YJBP: **Berberine suppresses colon cancer cell proliferation by inhibiting the scap/srebp-1 signaling pathway-mediated lipogenesis**. 2020, **174**:113776.

192. Li W, Tai Y, Zhou J, Gu W, Bai Z, Zhou T, Zhong Z, McCue PA, Sang N, Ji JY *et al*: **Repression of endometrial tumor growth by targeting SREBP1 and lipogenesis**. *Cell Cycle* 2012, **11**(12):2348-2358.

193. Zhou C, Qian W, Ma J, Cheng L, Jiang Z, Yan B, Li J, Duan W, Sun L, Cao JJCP: **Resveratrol enhances the chemotherapeutic response and reverses the stemness induced by gemcitabine in pancreatic cancer cells via targeting SREBP 1**. 2019, **52**(1):e12514.

194. Li X, Wu JB, Chung LW, Huang W-CJO: **Anti-cancer efficacy of SREBP inhibitor, alone or in combination with docetaxel, in prostate cancer harboring p53 mutations**. 2015, **6**(38):41018.

195. Liu W, Furuta E, Shindo K, Watabe M, Xing F, Pandey PR, Okuda H, Pai SK, Murphy LL, Cao DJBcr *et al*: **Cacalol, a natural sesquiterpene, induces apoptosis in breast cancer cells by modulating Akt-SREBP-FAS signaling pathway**. 2011, **128**(1):57-68.

196. Wang C, Ji, J.Y., Tian, L., and Pestell, R.G. : **Transcriptional regulation of lipogenesis as a therapeutic target for cancer treatment**. In: *Nuclear Signaling Pathways and*

Targeting Transcription in Cancer. Edited by Kumar R. New York: Humana Press, New York, NY; 2014: 259-275.

197. Currie E, Schulze A, Zechner R, Walther TC, Farese Jr RV: **Cellular fatty acid metabolism and cancer**. *Cell metabolism* 2013, **18**(2):153-161.

198. Goldstein JL, Rawson RB, Brown MS: **Mutant mammalian cells as tools to delineate the sterol regulatory element-binding protein pathway for feedback regulation of lipid synthesis**. *Arch Biochem Biophys* 2002, **397**(2):139-148.

199. Osborne TF, Espenshade PJJG, development: **Evolutionary conservation and adaptation in the mechanism that regulates SREBP action: what a long, strange tRIP it's been**. 2009, **23**(22):2578-2591.

200. Sakai J, Nohturfft A, Cheng D, Ho Y, Brown MS, Goldstein JLJJoBC: **Identification of complexes between the COOH-terminal domains of sterol regulatory element-binding proteins (SREBPs) and SREBP cleavage-activating protein**. 1997, **272**(32):20213-20221.

201. Sato R, Yang J, Wang X, Evans MJ, Ho Y, Goldstein JL, Brown MSJJoBC: **Assignment of the membrane attachment, DNA binding, and transcriptional activation domains of sterol regulatory element-binding protein-1 (SREBP-1)**. 1994, **269**(25):17267-17273.

202. Wang X, Sato R, Brown MS, Hua X, Goldstein JLJC: **SREBP-1, a membrane-bound transcription factor released by sterol-regulated proteolysis**. 1994, **77**(1):53-62.

203. Yokoyama C, Wang X, Briggs MR, Admon A, Wu J, Hua X, Goldstein JL, Brown MSJC: **SREBP-1, a basic-helix-loop-helix-leucine zipper protein that controls transcription of the low density lipoprotein receptor gene**. 1993, **75**(1):187-197.

204. Hua X, Yokoyama C, Wu J, Briggs MR, Brown MS, Goldstein JL, Wang XJPotNAoS: **SREBP-2, a second basic-helix-loop-helix-leucine zipper protein that stimulates transcription by binding to a sterol regulatory element**. 1993, **90**(24):11603-11607.

205. Seegmiller AC, Dobrosotskaya I, Goldstein JL, Ho Y, Brown MS, Rawson RBJDc: **The SREBP pathway in Drosophila: regulation by palmitate, not sterols**. 2002, **2**(2):229-238.

206. Rawson RB, DeBose-Boyd R, Goldstein JL, Brown MS: **Failure to cleave sterol regulatory element-binding proteins (SREBPs) causes cholesterol auxotrophy in Chinese hamster ovary cells with genetic absence of SREBP cleavage-activating protein**. *J Biol Chem* 1999, **274**(40):28549-28556.

207. Rosenfeld JM, Osborne TF: **HLH106, a Drosophila sterol regulatory element-binding protein in a natural cholesterol auxotroph**. *J Biol Chem* 1998, **273**(26):16112-16121.

208. Perkins LA, Holderbaum L, Tao R, Hu Y, Sopko R, McCall K, Yang-Zhou D, Flockhart I, Binari R, Shim HS *et al*: **The Transgenic RNAi Project at Harvard Medical School: Resources and Validation**. *Genetics* 2015, **201**(3):843-852.

209. Xie X-J, Hsu F-N, Gao X, Xu W, Ni J-Q, Xing Y, Huang L, Hsiao H-C, Zheng H, Wang CJPB: **CDK8-cyclin C mediates nutritional regulation of developmental transitions through the ecdysone receptor in Drosophila**. 2015, **13**(7):e1002207.

210. Dobin A, Davis CA, Schlesinger F, Drenkow J, Zaleski C, Jha S, Batut P, Chaisson M, Gingeras TRJB: **STAR: ultrafast universal RNA-seq aligner**. 2013, **29**(1):15-21.

211. Liao Y, Smyth GK, Shi WJB: **featureCounts: an efficient general purpose program for assigning sequence reads to genomic features**. 2014, **30**(7):923-930.

212. Love MI, Huber W, Anders SJGb: **Moderated estimation of fold change and dispersion for RNA-seq data with DESeq2**. 2014, **15**(12):550.

213. Kolde R, Kolde MRJRP: **Package 'pheatmap'**. 2015, **1**(7):790.

214. Yu G, Wang LG, Han Y, He QY: **clusterProfiler: an R package for comparing biological themes among gene clusters**. *Omics : a journal of integrative biology* 2012, **16**(5):284-287.

215. Yu GJRpv: **Enrichplot: Visualization of functional enrichment result**. 2018, **1**(2).

216. O'Leary NA, Wright MW, Brister JR, Ciufo S, Haddad D, McVeigh R, Rajput B, Robbertse B, Smith-White B, Ako-Adjei DJNar: **Reference sequence (RefSeq) database at NCBI: current status, taxonomic expansion, and functional annotation**. 2016, **44**(D1):D733-D745.

217. Sievers F, Wilm A, Dineen D, Gibson TJ, Karplus K, Li W, Lopez R, McWilliam H, Remmert M, Söding JJMsb: **Fast, scalable generation of high‐quality protein multiple sequence alignments using Clustal Omega**. 2011, **7**(1):539.

218. Dosztanyi Z, Meszaros B, Simon I: **ANCHOR: web server for predicting protein binding regions in disordered proteins**. *Bioinformatics* 2009, **25**(20):2745-2746.

219. Mészáros B, Erdős G, Dosztányi ZJNar: **IUPred2A: context-dependent prediction of protein disorder as a function of redox state and protein binding**. 2018, **46**(W1):W329-W337.

220. Jaluria P, Konstantopoulos K, Betenbaugh M, Shiloach J: **A perspective on microarrays: current applications, pitfalls, and potential uses**. *Microbial cell factories* 2007, **6**:4.

221. Jewell JL, Russell RC, Guan K-LJNrMcb: **Amino acid signalling upstream of mTOR**. 2013, **14**(3):133-139.

222. Tokunaga C, Yoshino K-i, Yonezawa KJB, communications br: **mTOR integrates amino acid-and energy-sensing pathways**. 2004, **313**(2):443-446.

223. Avruch J, Hara K, Lin Y, Liu M, Long X, Ortiz-Vega S, Yonezawa KJO: **Insulin and amino-acid regulation of mTOR signaling and kinase activity through the Rheb GTPase**. 2006, **25**(48):6361-6372.

224. Long X, Ortiz-Vega S, Lin Y, Avruch JJJoBC: **Rheb binding to mammalian target of rapamycin (mTOR) is regulated by amino acid sufficiency**. 2005, **280**(25):23433-23436.

225. Dreyer HC, Drummond MJ, Pennings B, Fujita S, Glynn EL, Chinkes DL, Dhanani S, Volpi E, Rasmussen BBJAJoP-E, Metabolism: **Leucine-enriched essential amino acid and carbohydrate ingestion following resistance exercise enhances mTOR signaling and protein synthesis in human muscle**. 2008, **294**(2):E392-E400.

226. Feng D, Youn DY, Zhao X, Gao Y, Quinn 3rd WJ, Xiaoli AM, Sun Y, Birnbaum MJ, Pessin JE, Yang F: **mTORC1 down-regulates cyclin-dependent kinase 8 (CDK8) and cyclin C (CycC)**. *PloS one* 2015, **10**(6):e0126240.

227. Tang HW, Hu Y, Chen CL, Xia B, Zirin J, Yuan M, Asara JM, Rabinow L, Perrimon N: **The TORC1-Regulated CPA Complex Rewires an RNA Processing Network to Drive Autophagy and Metabolic Reprogramming**. *Cell metabolism* 2018, **27**(5):1040-1054 e1048.

228. Gao X, Xie XJ, Hsu FN, Li X, Liu M, Hemba-Waduge RU, Xu W, Ji JY: **CDK8 mediates the dietary effects on developmental transition in Drosophila**. *Dev Biol* 2018, **444**(2):62-70.

229. Ni JQ, Liu LP, Binari R, Hardy R, Shim HS, Cavallaro A, Booker M, Pfeiffer BD, Markstein M, Wang H *et al*: **A Drosophila resource of transgenic RNAi lines for neurogenetics**. *Genetics* 2009, **182**(4):1089-1100.

230. Germani F, Bergantinos C, Johnston LAJG: **Mosaic analysis in Drosophila**. 2018, **208**(2):473-490.

231. Sundqvist A, Bengoechea-Alonso MT, Ye X, Lukiyanchuk V, Jin J, Harper JW, Ericsson J: **Control of lipid metabolism by phosphorylation-dependent degradation of the SREBP family of transcription factors by SCF(Fbw7)**. *Cell metabolism* 2005, **1**(6):379-391.

232. Lee JE, Cranna NJ, Chahal AS, Quinn LM: **Genetic systems to investigate regulation of oncogenes and tumour suppressor genes in Drosophila**. *Cells* 2012, **1**(4):1182-1196.

233. Cooksey KE, Guckert JB, Williams SA, Callis PR: **Fluorometric determination of the neutral lipid content of microalgal cells using Nile Red**. *Journal of microbiological methods* 1987, **6**(6):333-345.

234. Li X, Li Y, Yang W, Xiao C, Fu S, Deng Q, Ding H, Wang Z, Liu G, Li X: **SREBP-1c overexpression induces triglycerides accumulation through increasing lipid synthesis and decreasing lipid oxidation and VLDL assembly in bovine hepatocytes**. *The Journal of steroid biochemistry and molecular biology* 2014, **143**:174-182.

235. Yang F, Vought BW, Satterlee JS, Walker AK, Jim Sun ZY, Watts JL, DeBeaumont R, Saito RM, Hyberts SG, Yang S *et al*: **An ARC/Mediator subunit required for SREBP control of cholesterol and lipid homeostasis**. *Nature* 2006, **442**(7103):700-704.

236. Xu W, Amire-Brahimi B, Xie XJ, Huang L, Ji JY: **All-atomic molecular dynamic studies of human CDK8: insight into the A-loop, point mutations and binding with its partner CycC**. *Computational biology and chemistry* 2014, **51**:1-11.

237. Schneider EV, Bottcher J, Blaesse M, Neumann L, Huber R, Maskos K: **The Structure of CDK8/CycC Implicates Specificity in the CDK/Cyclin Family and Reveals Interaction with a Deep Pocket Binder**. *Journal of molecular biology* 2011, **412**(2):251-266.

238. Parraga A, Bellsolell L, Ferre-D'Amare AR, Burley SK: **Co-crystal structure of sterol regulatory element binding protein 1a at 2.3 A resolution**. *Structure* 1998, **6**(5):661-672.

239. Raghow R, Dong Q, Elam MB: **Phosphorylation dependent proteostasis of sterol regulatory element binding proteins**. *Biochimica et biophysica acta Molecular and cell biology of lipids* 2019, **1864**(8):1145-1156.

240. Xiaoping Z, Fajun Y: **Regulation of SREBP-Mediated Gene Expression**. *Sheng Wu Wu Li Hsueh Bao* 2012, **28**(4):287-294.

241. Punga T, Bengoechea-Alonso MT, Ericsson JJJoBC: **Phosphorylation and ubiquitination of the transcription factor sterol regulatory element-binding protein-1 in response to DNA binding**. 2006, **281**(35):25278-25286.

242. Dong Q, Majumdar G, O'Meally RN, Cole RN, Elam MB, Raghow RJM, Biochemistry C: **Insulin-induced de novo lipid synthesis occurs mainly via mTOR-dependent regulation of proteostasis of SREBP-1c**. 2020, **463**(1-2):13-31.

243. Dong Q, Giorgianni F, Beranova-Giorgianni S, Deng X, O'Meally RN, Bridges D, Park EA, Cole RN, Elam MB, Raghow RJBr: **Glycogen synthase kinase-3-mediated phosphorylation of serine 73 targets sterol response element binding protein-1c (SREBP-1c) for proteasomal degradation**. 2016, **36**(1).

244. Kotzka J, Knebel B, Haas J, Kremer L, Jacob S, Hartwig S, Nitzgen U, Muller–Wieland DJPO: **Preventing phosphorylation of sterol regulatory element-binding protein 1a by MAP-kinases protects mice from fatty liver and visceral obesity**. 2012, **7**(2):e32609.

245. Li Y, Xu S, Mihaylova MM, Zheng B, Hou X, Jiang B, Park O, Luo Z, Lefai E, Shyy JY-JJCm: **AMPK phosphorylates and inhibits SREBP activity to attenuate hepatic steatosis and atherosclerosis in diet-induced insulin-resistant mice**. 2011, **13**(4):376-388.

246. Garami A, Zwartkruis FJ, Nobukuni T, Joaquin M, Roccio M, Stocker H, Kozma SC, Hafen E, Bos JL, Thomas G: **Insulin activation of Rheb, a mediator of mTOR/S6K/4E-BP signaling, is inhibited by TSC1 and 2**. *Molecular cell* 2003, **11**(6):1457-1466.

247. Chen R, Zou Y, Mao D, Sun D, Gao G, Shi J, Liu X, Zhu C, Yang M, Ye W: **The general amino acid control pathway regulates mTOR and autophagy during serum/glutamine starvation**. *Journal of Cell Biology* 2014, **206**(2):173-182.

248. Kim J, Guan K-L: **mTOR as a central hub of nutrient signalling and cell growth**. *Nature Cell Biology* 2019, **21**(1):63-71.

249. Ali M, Bukhari SA, Ali M, Lee H-W: **Upstream signalling of mTORC1 and its hyperactivation in type 2 diabetes (T2D)**. *BMB reports* 2017, **50**(12):601.

250. Blagosklonny MV: **Rapamycin-induced glucose intolerance: hunger or starvation diabetes**. *Cell Cycle* 2011, **10**(24):4217-4224.

251. Garcia-Bellido A, de Celis JF: **Developmental genetics of the venation pattern of Drosophila**. *Annual review of genetics* 1992, **26**(1):277-304.

252. Williams JA, Paddock SW, Vorwerk K, Carroll SB: **Organization of wing formation and induction of a wing-patterning gene at the dorsal/ventral compartment boundary**. *Nature* 1994, **368**(6469):299-305.

253. Klein T, Arias AM: **The vestigial gene product provides a molecular context for the interpretation of signals during the development of the wing in Drosophila**. *Development* 1999, **126**(5):913-925.

254. Muñoz-Nava LM, Alvarez HA, Chara O, Nahmad M: **Cell Recruitment Drives Growth of the Drosophila Wing by Overscaling the Vestigial Expression Pattern**. *Available at SSRN 3330882* 2019.

255. Kuuluvainen E, Hakala H, Havula E, Sahal Estime M, Ramet M, Hietakangas V, Makela TP: **Cyclin-dependent kinase 8 module expression profiling reveals requirement of mediator subunits 12 and 13 for transcription of Serpent-dependent innate immunity genes in Drosophila**. *The Journal of biological chemistry* 2014, **289**(23):16252-16261.

256. Cooper G: **Protein degradation**. *The Cell: A Molecular Approach* 2000.

257. Davis MA, Larimore EA, Fissel BM, Swanger J, Taatjes DJ, Clurman BE: **The SCF–Fbw7 ubiquitin ligase degrades MED13 and MED13L and regulates CDK8 module association with Mediator**. *Genes & development* 2013, **27**(2):151-156.

258. Zhao X, Feng D, Wang Q, Abdulla A, Xie X-J, Zhou J, Sun Y, Yang ES, Liu L-P, Vaitheesvaran BJTJoci: **Regulation of lipogenesis by cyclin-dependent kinase 8–mediated control of SREBP-1**. 2012, **122**(7):2417-2427.

259. Yang F, Vought BW, Satterlee JS, Walker AK, Sun Z-YJ, Watts JL, DeBeaumont R, Saito RM, Hyberts SG, Yang SJN: **An ARC/Mediator subunit required for SREBP control of cholesterol and lipid homeostasis**. 2006, **442**(7103):700-704.

APPENDIX A

FIGURES

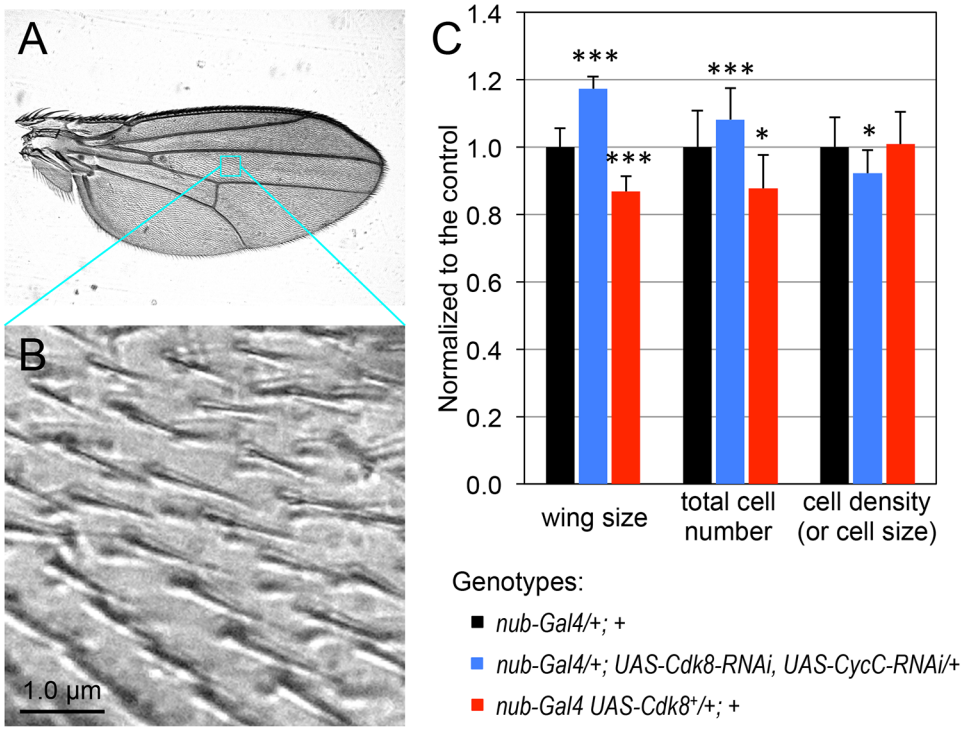

Fig. A.II.1 Effects of CDK8 on the size of wings, cell number, and cell sizes. (A) A normal wing; (B) high magnification of an L3-L4 intervein region showing the hairs in wing cells. (C) Quantification of wing sizes, total cell numbers, and hair density (reflecting cell sizes) in the control (black bars, genotype: "*nub-Gal4/+; +*"), CDK8- and CycC-depleted (blue, "*nub-Gal4/+; UAS-cdk8-RNAi UAS-cycC-RNAi/+*"), and CDK8-overexpressing (red, "*nub-Gal4 UAS-cdk8*$^{+}$*/+; +*") wings. One-sided *t*-tests were used to determine the statistical significance of the differences.

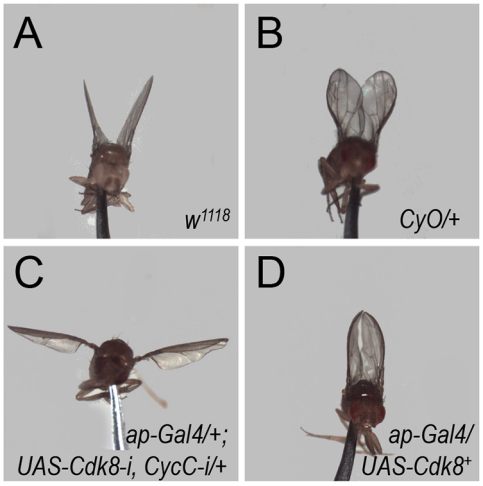

Fig. A.II.2 Effects of CDK8 on the wing morphology with *ap-Gal4*. Representative adult wings of (A) *w1118*; (B) *CyO/+;* (C) *ap-Gal4/+; UAS-Cdk8-RNAi CycC-RNAi/+;* (D) *ap-Gal4/UAS-Cdk8*$^{+}$

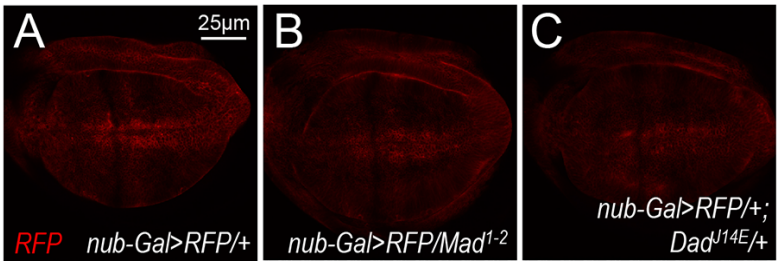

Fig. A.II.3 Effects of Dpp signaling pathway components on *nub-Gal4*. Representative confocal images of RFP signal of the wing pouch area of discs of the following genotypes: (A) *nub-Gal>RFP/+*; (B) *nub-Gal>RFP/Mad*$^{1-2}$; and (C) *nub-Gal>RFP/+; Dad*^{J14E}*/+*. At least five discs were examined for each genotype. All these images were taken at the same settings for fixations, staining, and confocal imaging.

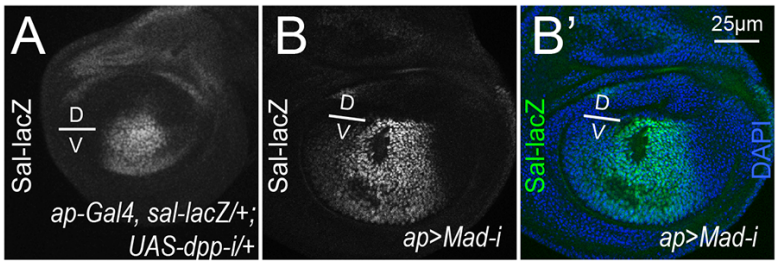

Fig. A.II.4 Validation of the *sal-lacZ* reporter. Representative confocal images of anti-β-Gal stainings of the wing pouch area of discs of the following genotypes: (A) *ap-Gal4, sal-lacZ/+; UAS-dpp-RNAi/+*; (B) *ap-Gal4, sal-lacZ/+; UAS-Mad-RNAi/+* (BL-31315); and (B') merge image of DAPI (blue) and anti-β-gal (green) channel of *ap-Gal4, sal-lacZ/+; UAS-Mad-RNAi/ +* (BL-31315). At least five discs were examined for each genotype.

A

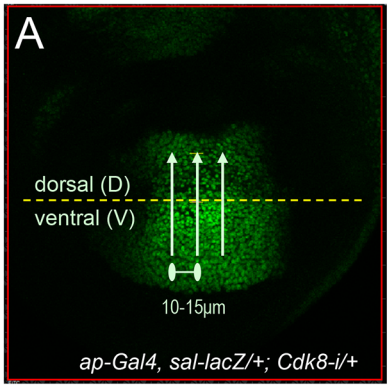

C

Name	Index Area (Alexa 488)	Length	Index Area /Length		Normalized
Ventral 1	36106.01	48.22	748.78	748.78	1.00
Dorsal 1	19730.02	40.73	484.41	748.78	0.65
Ventral 2	31048.35	39.81	779.91	748.78	1.04
Dorsal 2	20573.24	38.87	529.28	748.78	0.71
Ventral 3	25369.78	37.77	671.69	748.78	0.90
Dorsal 3	14461.69	37.93	381.27	748.78	0.51

D

Normalized ventral	Normalized dorsal	Average ventral	Average dorsal
1	0.65		
1.04	0.71	0.98	0.62
0.90	0.51		

B

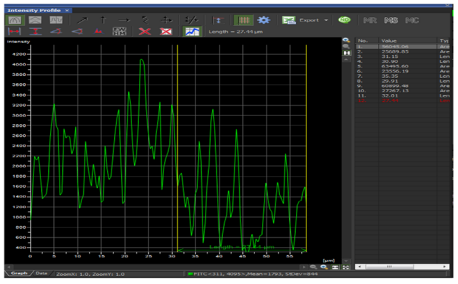

E

wing disc	Average ventral	Average dorsal	T test
#1	0.98	0.62	
#2	0.98	0.75	
#3	1.13	0.81	0.0032
#4	0.83	0.69	
#5	1.10	0.88	

Fig. A.II.5 Quantification of the Sal-lacZ expression. (A) Three lines were drawn across the dorsal-ventral compartment boundary within the wing pouch area to calculate the intensity index profile; genotype: *ap-Gal4, sal-lacZ/+; UAS-Cdk8-i/+*. (B) An example of the index profile of one line, measured area below the index profile, and its length. (C) Average and normalization of average intensity of the anti-β-Gal staining in the dorsal and ventral compartments of a wing disc. (D) Average of three lines. (E) Student's *t*-test was used to compare the Sal-lacZ expression levels in the dorsal and ventral compartments of five discs of the same genotype. See Materials and Methods for more details.

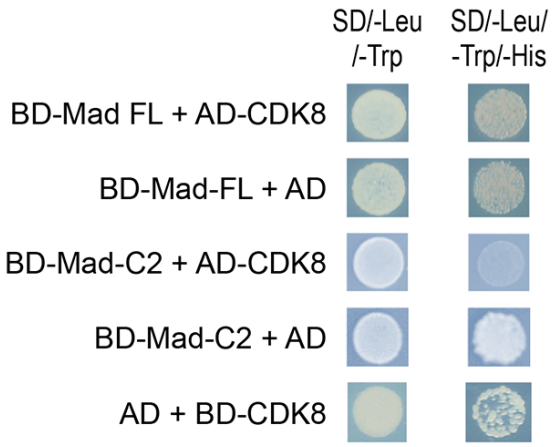

Fig. A.II.6 An alternative method to quantify the Sal-lacZ expression. (A) 20x20μm squares were drawn in both dorsal and ventral compartments; genotype: *ap-Gal4, sal-lacZ/+; UAS-Med15-i/+*). (B) Mean intensity of the anti-β-Gal staining of three different discs within the taken squares was given. Dorsal to ventral ratio of each disc was calculated. Student's *t*-test was used to compare the Sal-lacZ expression levels ratio between different genotypes (C), and plotted as column chart (D). See Materials and Methods for more details.

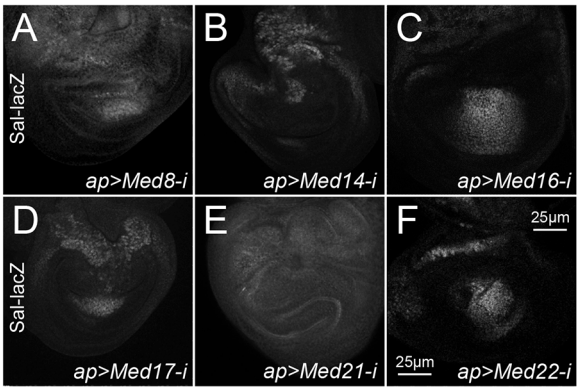

Fig. A.II.7 Effects of depleting subunits of the CKM and CDK9 on *ap-Gal4*, and effect of depleting Ap on *sal-lacZ*. Representative confocal images of GFP (green) and DAPI (blue) signal of the wing pouch area of discs of the following genotypes: (A) *ap-Gal>GFP/+*; (B) *ap-Gal4>GFP/+; UAS-Cdk8-i,CycC-i/+*; (D) *ap-Gal4>GFP/+; UAS-Cdk9-i/+*; (E) *ap-Gal4>GFP/+;UAS-Med12-i/+*; (F) *ap-Gal4>GFP/+;UAS-Med13-i/+*; (C) Confocal images of anti-β-Gal staining of wing discs of *ap-Gal4,sal-lacZ/+; UAS-ap-i/+*. At least five discs were examined for each genotype.

A

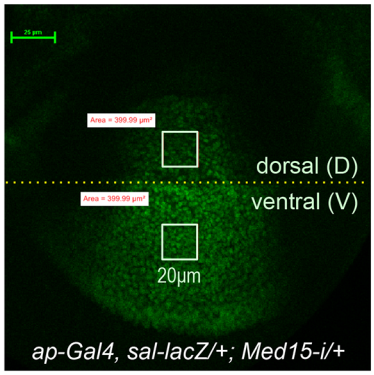

note: 20x20μm square was taken.

B

Med15-i	Mean Intensity	Dorsal to ventral Ratio
Ventral 1	805.03	0.445852414
Dorsal 1	408.49	
Ventral 2	890.93	0.589929152
Dorsal 2	798.01	
Ventral 3	944.09	0.796062198
Dorsal 3	537.82	

C

Name	Dorsal to ventral Ratio	t-test
Med1-i	0.975132926	
	0.993161627	
	0.978508217	
Cdk8-i, CycC-i	0.739999478	0.026216934
	0.913055316	
	0.867293488	
Med15-i	0.445852414	0.010869324
	0.589929152	
	0.796062198	

D

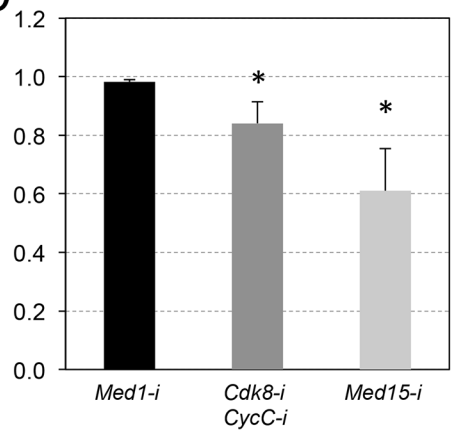

Square quantification of *ap-Gal4, sal-lacZ*

Fig. A.II.8 Depletion of CDK8 or CycC does not affect p-Mad level. Representative confocal images of anti-p-Mad staining of wing discs from the following genotypes: (A) *ap-Gal4, sal-lacZ/+* (control); (B) *ap-Gal4, sal-lacZ/+; UAS-Cdk8-i/+*; (C) *ap-Gal4, sal-lacZ/+; UAS-CycC-i*; and (D) *ap-Gal4, sal-lacZ/+; UAS-Cdk8-i CycC-i*. At least five discs were examined for each genotype. Scale bar in D: 25μm.

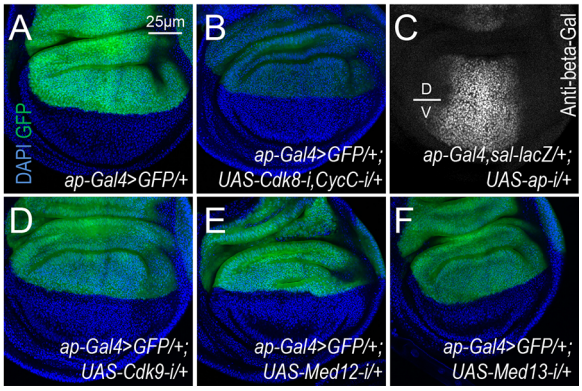

Fig. A.II.9 Additional results from the Y2H assay. Full-length (FL) Mad, Mad-C2 fragment or CDK8 proteins as the bait are able to auto-activate in this assay. Refer the figure legend in Fig. 5 and the Materials and Methods for more details.

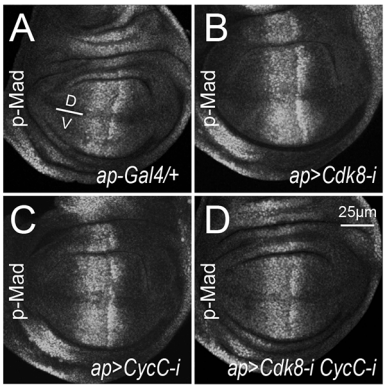

Fig. A.II.10 Depletion of dedicated Mediator subunits strongly disrupted wing disc morphology. Representative confocal images of anti-β-Gal staining of wing discs of the following genotypes: (A) *ap-Gal4, sal-lacZ/+; UAS-Med8-RNAi/+*; (B) *ap-Gal4, sal-lacZ/+; UAS-Med14-RNAi/+*; (C) *ap-Gal4, sal-lacZ/+; UAS-Med16-RNAi/+*; (D) *ap-Gal4, sal-lacZ/+; UAS-Med17-RNAi/+*; (E) *ap-Gal4, sal-lacZ/+; UAS-Med21-RNAi/+*; (F) in *ap-Gal4, sal-lacZ/+; UAS-Med22-RNAi/+*; and (G) *ap-Gal4/+; vgQE-lacZ/UAS-Med21-RNAi.* At least five discs were examined for each genotype. Scale bar in F: 25µm.

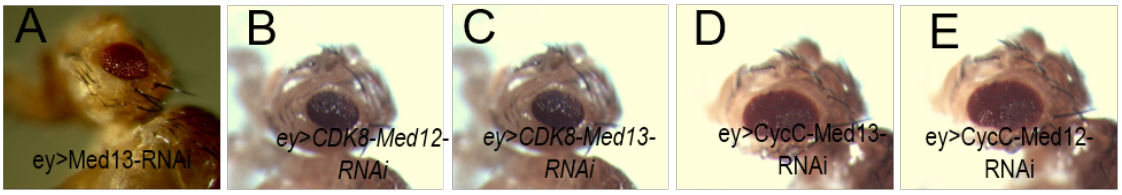

Fig A.III.1. Eye defects caused by depletion of different combinations of the CKM subunits. Adult female eyes of (A) *ey-Gal4/+; UAS-Med13-RNAi/+*; (B) *ey-Gal4/+; UAS-Cdk8-RNAi Med12-RNAi/+*; (C) *ey-Gal4/+; UAS-Cdk8-RNAi Med13-RNAi/+*; (D) *ey-Gal4/+; UAS-CycC-RNAi Med13-RNAi* (E) *ey-Gal4/+; UAS-CycC-RNAi Med12-RNAi/+*.

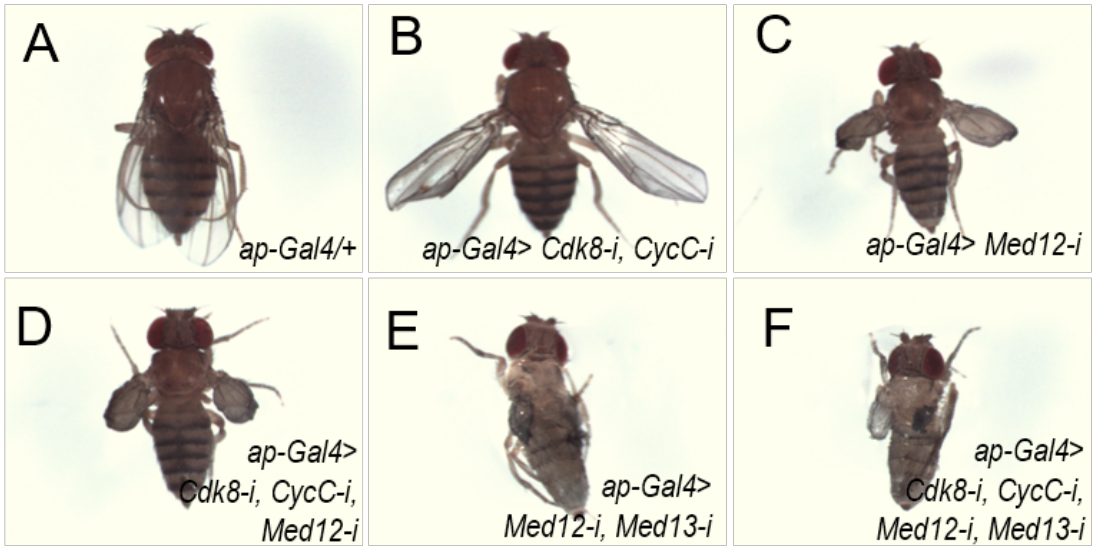

Fig A.III.2. Wing defects caused by depletion of different combinations of the CKM subunits.n Adult female eyes of (A) *ap-Gal4/+* (control); (B) *ap-Gal4/+; UAS-Cdk8-RNAi CycC-RNAi/+*; (C) *ap-Gal4/+; UAS-Med12-RNAi/+*; (D) *ap-Gal4/+; UAS-Cdk8-RNAi CycC-RNAi Med12-RNAi/+*; (E) *ap-Gal4/+; UAS-Med12-RNAi Med13-RNAi/+*; (F) *ap-Gal4/+; UAS-Cdk8-RNAi CycC-RNAi Med12-RNAi Med13-RNAi/+*.

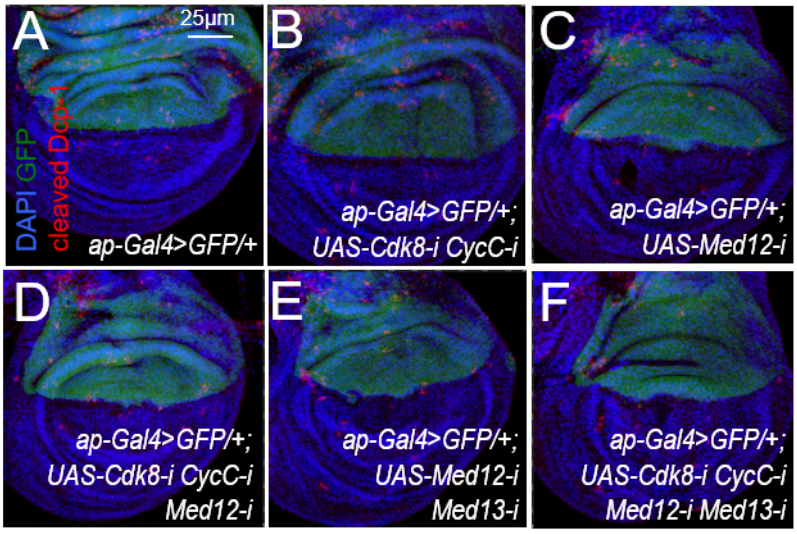

Fig A.III.3. Effects of depleting different combinations of the CKM subunits on the cell apoptosis. Representative confocal images of wing discs with anti-cleaved-Dcp1 (red) staining of the following genotypes: (A) *ap-Gal4/+;* (B) *ap-Gal4/+; UAS-Cdk8-RNAi CycC-RNAi/+*; (C) *ap-Gal4/+; UAS-Med12-RNAi*; (D) *ap-Gal4/+; UAS-Cdk8-RNAi CycC-RNAi UAS-Med12-RNAi/+*; (E) *ap-Gal4/+; UAS-Med12-RNAi Med13-RNAi/+*; (F) *ap-Gal4/+; UAS-Cdk8-RNAi CycC-RNAi UAS-Med12-RNAi Med13-RNAi/+*; (G) Quantification of the PH3 signal ratio comparing Doral and Ventral compartment. At least five wing discs were examined for each genotype. Scale bar in C: 25µm.

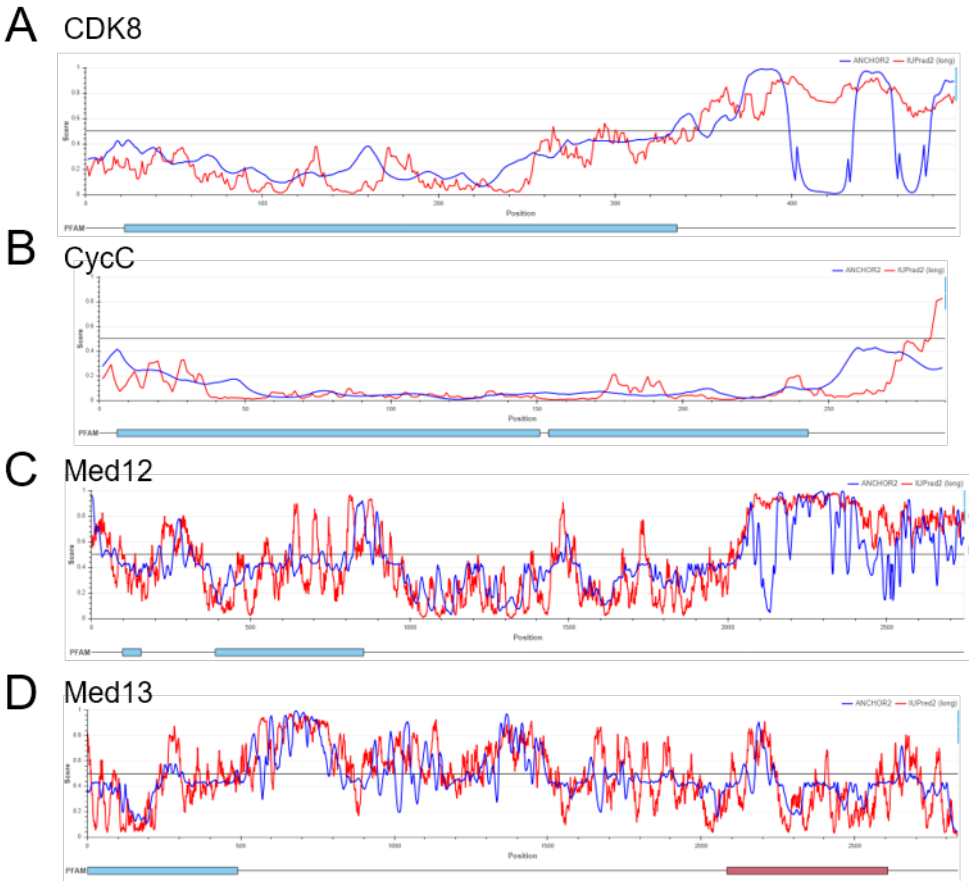

Fig A.III.4. Part of all the four CKM subunits are intrinsically disordered. Anchor2 and IUPred2 prediction results of *Drosophila* (A)CDK8; (B)CycC; (C)Med12; (D)Med13.

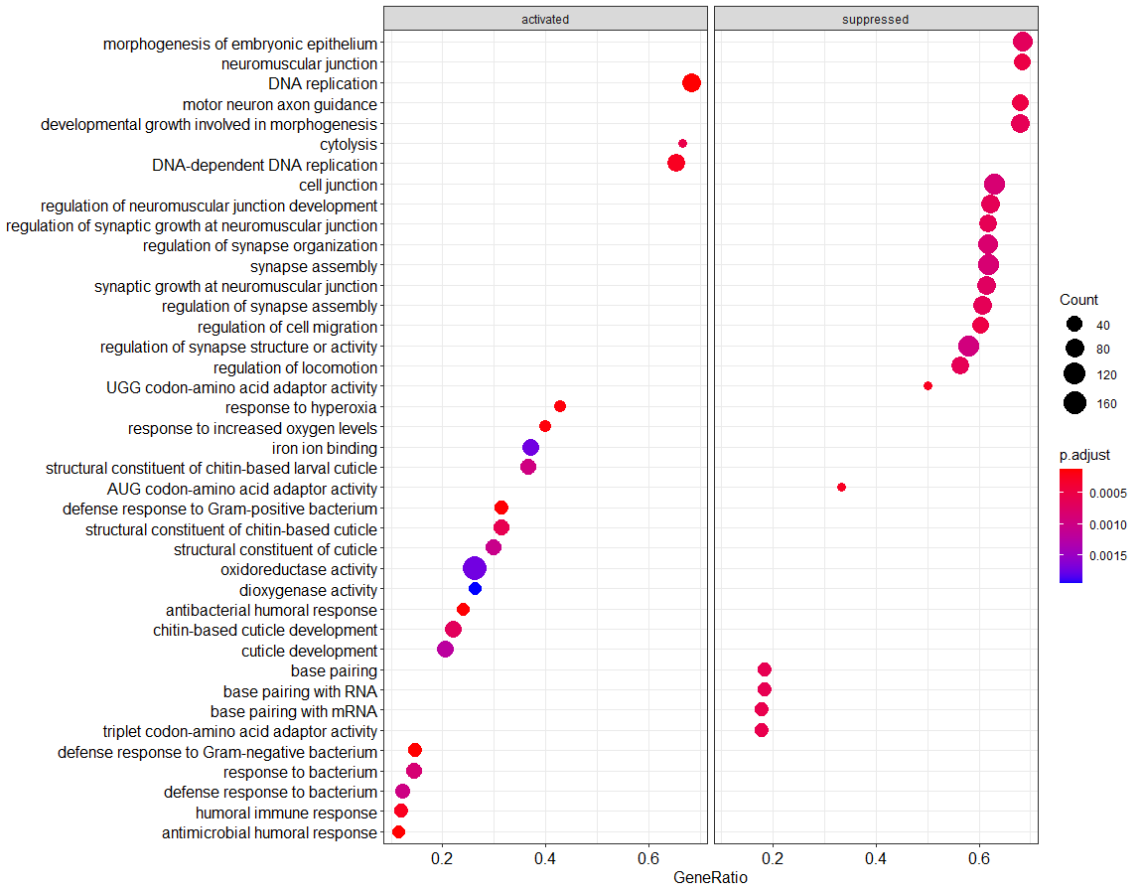

Fig A.IV.1. Dotplot of the top 40 Gene Ontology categories of significant altered genes in *cycc*^{Y5} *comparing with* w^{1118}.

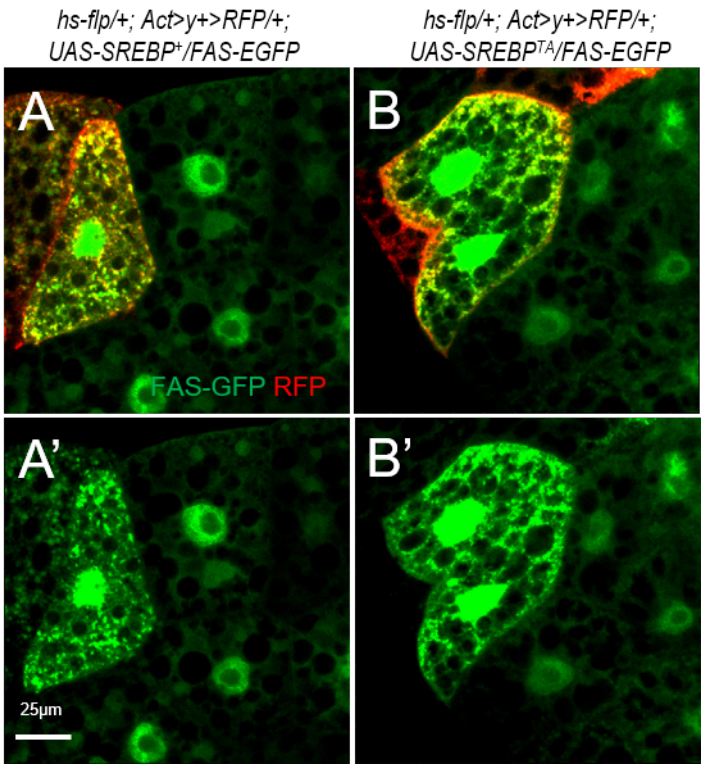

Fig A.IV.2. Phopho-mutant dSREBP protein is more potent in target transcription. Representative confocal merge channel image of FAS-EGFP (green), RFP (red) and DAPI (blue) in *Drosophila* larvae fat body of (A) *hs-flp/+; Act>y*$^{+}$*>RFP/+; UAS-SREBP*$^{+}$*/FAS-EGFP*; (B) *hs-flp/+; Act>y*$^{+}$*>RFP/+; UAS-SREBP*^{T390A}*/FAS-EGFP* and only FAS-EGFP (green) of (A') *hs-flp/+; Act>y*$^{+}$*>GFP/+; UAS-SREBP*$^{+}$*/FAS-EGFP*; (B') *hs-flp/+; Act>y*$^{+}$*>GFP/+; UAS-SREBP*^{T390A}*/FAS-EGFP.*

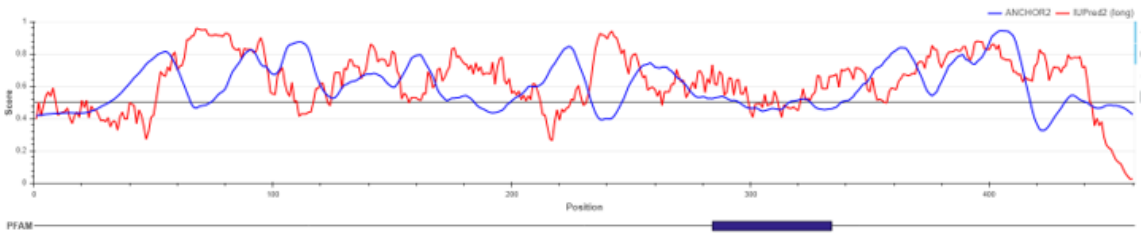

Fig A.IV.3. Anchor2 and IUPred2 prediction of the mature form dSREBP

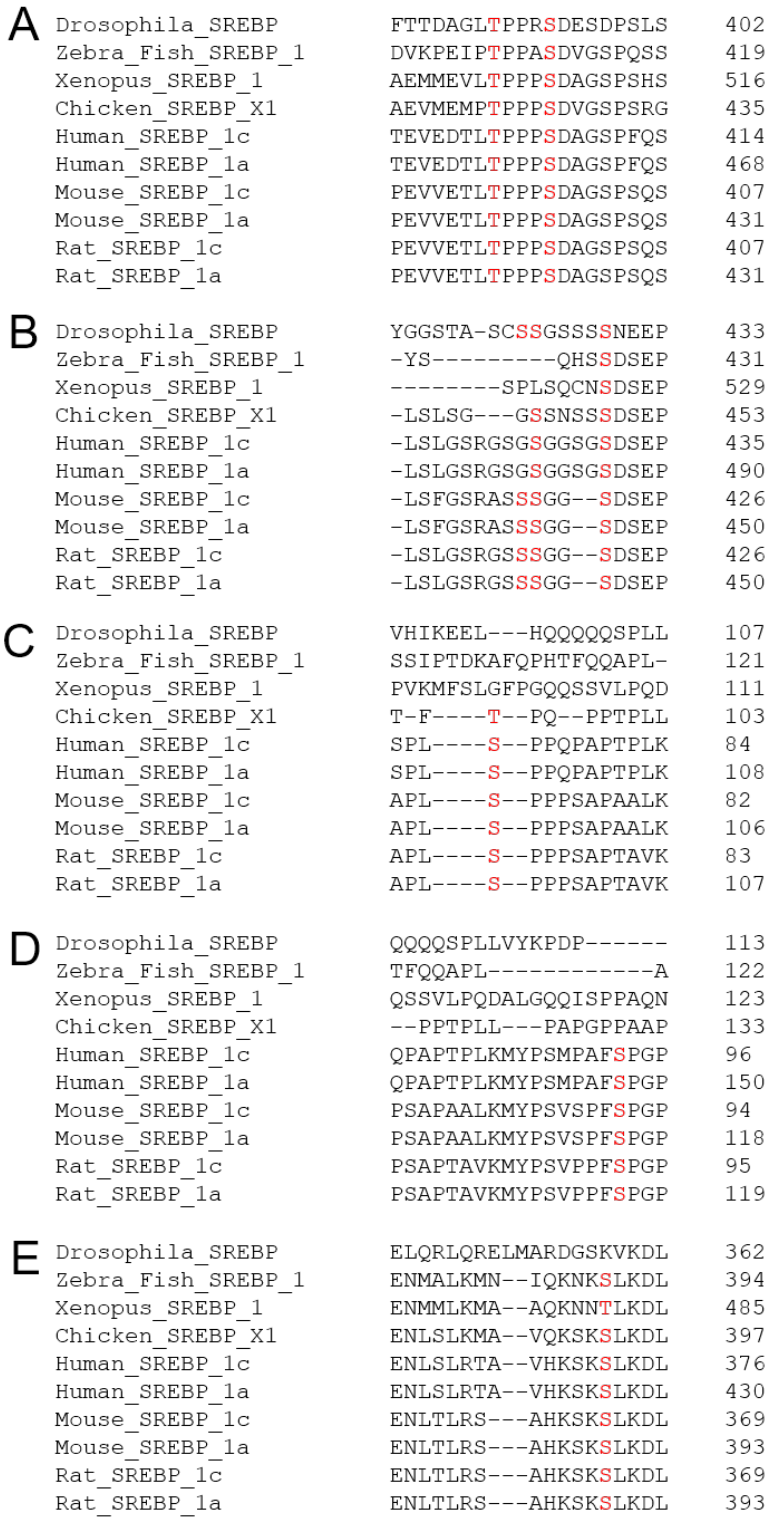

Fig A.IV.4. Sequence alignment around the potential phosphorylation sites of SREBP

APPENDIX B

TABLES

Table B.II.1. Results of 490 deficiency (*Df*) lines tested for potential dominant modification of vein phenotypes caused by altered levels of CDK8 or CycC.

Stock #	Deficiency lines	Cytogenetic breakpoints	*nub>CDK8+* backrgound	*nub>CDK8-RNAi* background	*nub>CycC-RNAi* background
27887	*Df(1)BSC843*	1A1;1A3	NE	NE	NE
901	*Df(1)svr*	1A1;1B9--10	weak suppressor	strong enhancer	enhancer
25058	*Df(1)BSC530*	1A5;1B12	NE	NE	lethal
3370	*Df(1)su(s)83*	1B10;1D6--E1	lethal	lethal	NE
9053	*Df(1)ED6443*	1B14;1E1	NE	NE	NE
26571	*Df(1)BSC719*	2A3;2B13	NE	NE	NE
26569	*Df(1)BSC717*	2F2;3A4	NE	NE	NE
8031	*Df(1)ED411*	3A3;3A8	NE	enhancer	enhancer
9348	*Df(1)ED6584*	3A8;3B1	NE	NE	NE
8948	*Df(1)ED6630*	3B1;3C5	NE	NE	NE
27886	*Df(1)BSC834*	3C11;3F3	enhancer	NE	weak suppressor
25059	*Df(1)BSC531*	3C3;3E2	enhancer	strong suppressor	strong suppressor
9169	*Df(1)ED6712*	3D3;3F1	enhancer	NE	NE
24145	*Df(1)ED6716*	3F3;4B4	NE	NE	NE
25414	*Df(1)BSC580*	4A5;4C13	NE	NE	NE
8956	*Df(1)ED6727*	4B6;4D5	NE	NE	NE
944	*Df(1)JC70*	4C15--16;5A1--2	NE	NE	NE
7708	*Df(1)Exel6234*	4F10;5A2	NE	suppressor	NE
25061	*Df(1)BSC533*	4F4;4F10	NE	NE	NE
8949	*Df(1)ED6802*	5A12;5D1	NE	NE	NE
7709	*Df(1)Exel6235*	5A2;5A6	enhancer	NE	NE
25114	*Df(1)BSC571*	5A4;5A10	NE	NE	NE
5281	*Df(1)dx81*	5C3--10;6C3--12	lethal	lethal	lethal
8947	*Df(1)ED6829*	5C7;5F3	suppressor	NE	NE
7713	*Df(1)Exel6239*	5F2;6B1--2	NE	NE	NE
7714	*Df(1)Exel6240*	6B2;6C4	NE	NE	NE
24375	*Df(1)BSC351*	6C11;6D7	NE	NE	NE
25063	*Df(1)BSC535*	6C2;6C8	enhancer	NE	NE
3196	*Df(1)Sxl-bt*	6E2;7A6	suppressor	strong enhancer	strong enhancer
8955	*Df(1)ED6906*	7A3;7B2	NE	weak enhancer	NE
25064	*Df(1)BSC536*	7B2;7C1	NE	suppressor	suppressor
6698	*Df(1)hl-a*	7B7;7E2	weak suppressor	NE	NE
25697	*Df(1)BSC622*	7C2;7D1	NE	NE	NE
949	*Df(1)C128*	7D1;7D5--6	enhancer	NE	strong enhancer
26514	*Df(1)BSC662*	7D6;7F1	NE	NE	suppressor
8033	*Df(1)ED6957*	8B6;8C13	NE	NE	enhancer
25065	*Df(1)BSC537*	8C4;8E4	NE	NE	NE
26564	*Df(1)BSC712*	8F1;9B1	suppressor	suppressor	suppressor
27586	*Df(1)BSC825*	7E1;8C4	NE	enhancer	NE
9153	*Df(1)ED7005*	9B1;9D3	NE	NE	NE
26853	*Df(1)BSC755*	9C4;9F5	NE	NE	NE
25068	*Df(1)BSC540*	9E8;10A3	NE	NE	suppressor
903	*Df(1)v-L3*	9F10;10A7--8	NE	NE	NE
6219	*Df(1)v-L1*	9F13;10A5	NE	enhancer	enhancer
25391	*Df(1)BSC572*	9F8;10A3	NE	NE	NE
23672	*Df(1)BSC287*	10A10;10B11	NE	NE	NE
26574	*Df(1)BSC722*	10B3;10E1	NE	NE	NE
9171	*Df(1)ED7147*	10D6;11A1	NE	NE	NE
9217	*Df(1)ED7161*	11A1;11B14	NE	NE	NE
8898	*Df(1)ED7170*	11B15;11E8	NE	NE	NE
26864	*Df(1)BSC767*	11E8;12A7	NE	enhancer	enhancer
8952	*Df(1)ED7217*	12A9;12C6	suppressor	NE	NE
24146	*Df(1)ED7225*	12C4;12E8	NE	NE	NE
9352	*Df(1)ED7229*	12E5;12F2	NE	NE	NE

Continued Table B.II.1

Stock #	Deficiency lines	Cytogenetic breakpoints	*nub>CDK8+* backrgound	*nub>CDK8-RNAi* background	*nub>CycC-RNAi* background
9218	*Df(1)ED7261*	12F2;12F5	enhancer	NE	NE
24336	*Df(1)BSC310*	12F5;13A10	NE	NE	NE
8035	*Df(1)ED7294*	13B1;13C3	NE	NE	NE
9219	*Df(1)ED7331*	13C3;13F1	NE	NE	NE
26566	*Df(1)BSC714*	13E14;14A8	NE	NE	suppressor
26855	*Df(1)BSC758*	14A6;14C1	NE	suppressor	suppressor
26869	*Df(1)BSC772*	14B9;14C4	lethal	strong suppressor	strong enhancer
23295	*Df(1)FDD-0024486*	14C4;14D1	NE	suppressor	NE
26858	*Df(1)BSC761*	14D1;14F1	NE	NE	NE
26857	*Df(1)BSC760*	14E1;14F2	NE	NE	NE
1158	*Df(1)rif*	15A1--2;15A4--5	NE	NE	NE
25416	*Df(1)BSC582*	15A1;15E2	NE	NE	NE
8954	*Df(1)ED7374*	15A1;15E3	suppressor	NE	NE
25417	*Df(1)BSC583*	15F1;16B10	NE	NE	NE
25733	*Df(1)BSC643*	15F9;16F1	NE	NE	NE
24429	*Df(1)BSC405*	16D5;16F6	NE	NE	pupa lethal
24376	*Df(1)BSC352*	16F7;17A8	NE	NE	suppressor
26568	*Df(1)BSC716*	17A3;17D6	NE	NE	NE
9350	*Df(1)ED7424*	17D1;18C1	NE	suppressor	NE
7768	*Df(1)Exel7468*	18B7;18C8	NE	NE	NE
23171	*Df(1)BSC275*	18C8;18D3	NE	NE	NE
9059	*Df(1)ED7620*	18D10;19A2	NE	NE	enhancer
25420	*Df(1)BSC586*	18F2;19D1	NE	NE	NE
25734	*Df(1)BSC644*	19C1;19E7	NE	NE	NE
26560	*Df(1)BSC708*	19E7;20A4	NE	NE	NE
7723	*Df(1)Exel6255*	20A1;20C1	NE	NE	NE
27585	*Df(1)BSC824*	20C1;20F3	NE	NE	NE
977	*Df(1)DCB1-35b*	19F1--2;20E--F	NE	weak suppressor	weak suppressor
4959	*Df(2L)C'*	h35;h38L	NE	NE	NE
24626	*Df(2L)ED50001*	21A1;21B1	NE	NE	NE
9353	*Df(2L)ED5878*	21B1;21B3	NE	weak enhancer	enhancer
8901	*Df(2L)ED19*	21B3;21B7	NE	strong enhancer	enhancer
24958	*Df(2L)BSC454*	21B7;21B8	suppressor	weak suppressor	NE
8672	*Df(2L)BSC106*	21B7;21C2	NE	NE	NE or weak enhancer
3548	*Df(2L)al*	21B8--C1;21C8--D1	NE	enhancer	weak suppressor
8673	*Df(2L)BSC107*	21C2;21E2	NE	strong enhancer	enhancer
3084	*Df(2L)ast2*	21D1--2;22B2--3	weak enhancer	NE	weak suppressor
8908	*Df(2L)ED94*	21E2;21E3	NE	NE	NE
24118	*Df(2L)ED105*	21E2;22A1	NE	suppressor	strong suppressor
7492	*Df(2L)Exel6005*	22A3;22B1	NE	weak enhancer	weak enhancer
26540	*Df(2L)BSC688*	22B1;22D6	NE	NE	NE
24959	*Df(2L)BSC455*	22D5;22E1	NE	NE	NE
9176	*Df(2L)ED136*	22F4;23A3	NE	NE	NE
7744	*Df(2L)Exel6277*	23A2;23B1	enhancer	NE	NE
1581	*Df(2L)JS31*	23A3--4;23D	strong suppressor	enhancer	enhancer
26544	*Df(2L)BSC692*	23B3;23B7	NE	NE	NE
9610	*Df(2L)BSC180*	23B7;23C3	NE	NE	NE
8904	*Df(2L)ED4651*	23B8;23F3	NE	NE	NE
6507	*Df(2L)drm-P2*	23F3--4;24A1--2	NE	NE	NE
23677	*Df(2L)BSC292*	23F6;24A2	NE	NE	NE
24123	*Df(2L)ED247*	24A2;24C3	NE	NE	NE
5330	*Df(2L)ed1*	24A2;24D4	NE	NE	strong suppressor
7495	*Df(2L)Exel6009*	24C3;24C8	NE	NE	enhancer
7790	*Df(2L)Exel8010*	24C8;24D4	suppressor	weak enhancer	NE
9600	*Df(2L)BSC165*	24D4;24D8	NE	NE	NE
23680	*Df(2L)BSC295*	24D4;24F3	strong suppressor	enhancer	NE
744	*Df(2L)M24F-B*	24E1--2;24F6--7	NE	NE	NE
9270	*Df(2L)ED250*	24F4;25A7	NE	NE	NE

Continued Table B.II.1

Stock #	Deficiency lines	Cytogenetic breakpoints	*nub>CDK8+* backrgound	*nub>CDK8-RNAi* background	*nub>CycC-RNAi* background
24124	*Df(2L)ED7853*	25A3;25B10	NE	NE	NE
1164	*Df(2L)tkv3*	25A4--5;25D5	weak enhancer	strong enhancer	strong enhancer
9605	*Df(2L)BSC172*	25B10;25C1	NE	NE	NE
8835	*Df(2L)BSC110*	25C1;25C4	NE	NE	NE
8674	*Df(2L)BSC109*	25C4;25C8	NE	NE	NE
7497	*Df(2L)Exel6011*	25C8;25D5	lethal	enhancer	NE or weak suppressor
7498	*Df(2L)Exel6012*	25D5;25E6	NE	strong suppressor	suppressor
9560	*Df(2L)BSC169*	25E5;25F3	weak enhancer	NE	enhancer
9343	*Df(2L)ED334*	25F2;26B2	NE	NE	NE
9341	*Df(2L)ED385*	26B1;26D7	NE	NE	NE
6338	*Df(2L)BSC6*	26D3--E1;26F4--7	NE	NE	NE
24378	*Df(2L)BSC354*	26D7;26E3	enhancer	NE	NE
9615	*Df(2L)BSC188*	26F1;27A2	NE	NE	NE
24126	*Df(2L)ED441*	27A1;27E1	strong suppressor	NE	NE
23676	*Df(2L)BSC291*	27D6;27F2	NE	NE	NE
9060	*Df(2L)ED489*	27E4;28B1	NE	NE	NE
9708	*Df(2L)BSC233*	27F3;28D2	NE	NE	NE
9502	*Df(2L)BSC142*	28C3;28D3	NE	NE	NE
7807	*Df(2L)Exel7034*	28E1;28F1	NE	NE	NE
9704	*Df(2L)BSC227*	28E8;29B1	NE	weak suppressor	suppressor
8836	*Df(2L)BSC111*	28F5;29B1	NE	NE	suppressor
24132	*Df(2L)ED629*	29B4;29E4	strong enhancer	NE	NE or weak enhancer
9631	*Df(2L)BSC204*	29D5;29F8	NE	NE	NE
8906	*Df(2L)ED678*	29F5;30B12	NE	NE	NE
24133	*Df(2L)ED690*	30B3;30E4	NE	NE	NE
6478	*Df(2L)BSC17*	30C3--5;30F1	weak suppressor	NE	lethal
9715	*Df(2L)BSC240*	30C7;30F2	NE	NE	NE
8469	*Df(2L)BSC50*	30F4--5;31B1--4	NE	NE	NE
26541	*Df(2L)BSC689*	30F5;31B1	NE	NE	NE
9503	*Df(2L)BSC143*	31B1;31D9	suppressor	NE	NE
1469	*Df(2L)J39*	31C--D;32D--E	NE	NE	NE
9635	*Df(2L)BSC208*	31D7;31D11	NE	NE	NE
9637	*Df(2L)BSC209*	31D7;31E1	NE	NE	NE
24135	*Df(2L)ED8142*	31E1;32A4	NE	NE	weak enhancer
9642	*Df(2L)BSC214*	31F5;32B4	NE	NE	NE
9641	*Df(2L)BSC213*	32B1;32C1	NE	NE	NE or weak suppressor
9505	*Df(2L)BSC145*	32C1;32C1	NE	NE	NE
9716	*Df(2L)BSC241*	32C1;32F2	suppressor	NE	NE
9718	*Df(2L)BSC244*	32F2;33B6	enhancer	strong suppressor	strong suppressor
7512	*Df(2L)Exel6030*	33A2--33B3	suppressor	enhancer	enhancer
24109	*Df(2L)ED761*	33A2;33E5	NE	weak suppressor	suppressor
8907	*Df(2L)ED775*	33B8;34A3	NE	NE	NE
23662	*Df(2L)BSC277*	34A1;34B2	NE	NE	weak enhancer
6999	*Df(2L)BSC30*	34A3;34B7--9	weak enhancer	NE	NE
26865	*Df(2L)BSC768*	34A9;34B8	lethal	lethal	lethal
27383	*Df(2L)BSC812*	34B11;34E1	NE	NE	suppressor
9594	*Df(2L)BSC159*	34B4;34C4	strong suppressor	NE	suppressor
23152	*Df(2L)BSC252*	34D1;34F1	enhancer	NE	NE
9061	*Df(2L)ED793*	34E4;35B4	NE	weak enhancer	weak enhancer
6963	*Df(2L)ED3*	35B2;35D1	NE	NE	NE
8946	*Df(2L)ED1050*	35B8;35D4	NE	NE	NE or weak suppressor
1491	*Df(2L)r10*	35D1;36A6--7	weak enhancer	NE	NE or weak enhancer
26542	*Df(2L)BSC690*	35D4;35D4	NE	NE	NE
7521	*Df(2L)Exel6038*	35D6;35E2	NE	suppressor	suppressor
23663	*Df(2L)BSC278*	35E1;35F1	NE	NE	NE

Continued Table B.II.1

Stock #	Deficiency lines	Cytogenetic breakpoints	*nub>CDK8+* backrgound	*nub>CDK8-RNAi* background	*nub>CycC-RNAi* background
27353	*Df(2L)BSC781*	35F1;36A1	NE	enhancer	strong enhancer
24113	*Df(2L)ED1102*	35F12;36A10	NE	NE	NE
24114	*Df(2L)ED1161*	36A10;36C9	NE	NE	NE
3180	*Df(2L)H20*	36A8--9;36E1--2	NE	enhancer	enhancer
9507	*Df(2L)BSC148*	36C8;36E3	NE	NE	NE
7839	*Df(2L)Exel7070*	36E2;36E6	suppressor	NE	NE
23156	*Df(2L)BSC256*	36E3;36F2	NE	NE	NE
7840	*Df(2L)Exel8038*	36E5;36F5	enhancer	enhancer	enhancer
9508	*Df(2L)BSC149*	36F5;36F10	NE	NE	NE
8935	*Df(2L)ED1203*	36F7;37C5	NE	NE	NE
24116	*Df(2L)ED1272*	37C5;38A2	NE	NE	weak enhancer
8679	*Df(2L)ED1303*	37E5;38C6	NE	NE	NE
167	*Df(2L)TW161*	38A6--B1;40A4--B1	NE	NE	NE
9269	*Df(2L)ED1315*	38B4;38F5	NE	NE	NE
9682	*Df(2L)ED1378*	38F1;39D2	NE	NE	NE
9266	*Df(2L)ED1473*	39B4;40A5	NE	weak suppressor	NE
9510	*Df(2L)BSC151*	40A5;40E5	NE	NE	suppressor
741	*Df(2R)M41A10*	41A;41A	NE	weak enhancer	NE
25705	*Df(2R)BSC630*	41D3;41F11	NE	NE	NE
749	*In(2R)bw[VDe2L]Cy[R]*	42A2;42A3	NE	suppressor	enhancer
8045	*Df(2R)ED1612*	42A13;42E6	NE	enhancer	NE
9683	*Df(2R)ED1484*	42A2;42A14	weak suppressor	NE	NE
9062	*Df(2R)ED1673*	42E1;43D3	NE	NE	NE
8931	*Df(2R)ED1715*	43A4;43F1	NE	NE	NE
8941	*Df(2R)ED1725*	43E4;44B5	weak enhancer	strong enhancer	NE
24335	*Df(2R)BSC267*	44A4;44C4	weak enhancer	NE	NE or weak suppressor
9157	*Df(2R)ED1770*	44D5;45B4	enhancer	strong enhancer	enhancer
9063	*Df(2R)ED1791*	44F7;45F1	NE	NE	NE
23665	*Df(2R)BSC280*	45C4;45F4	NE	NE	strong enhancer
9410	*Df(2R)BSC132*	45F6;46B4	NE	NE	enhancer
23682	*Df(2R)BSC298*	46B2;46C7	NE	weak enhancer	NE
1702	*Df(2R)X1*	46C;47A1	suppressor	NE	NE
9539	*Df(2R)BSC152*	46C1;46D6	NE	NE	NE
23686	*Df(2R)BSC303*	46E1;46F3	NE	NE	NE
23666	*Df(2R)BSC281*	46F1;47A9	NE	NE	NE
25428	*Df(2R)BSC595*	47A3;47F1	suppressor	weak suppressor	NE
8910	*Df(2R)ED2219*	47D6;48B6	weak enhancer	NE	NE
8912	*Df(2R)ED2247*	48A3;48D5	NE	strong enhancer	enhancer
9626	*Df(2R)BSC199*	48C5;48E4	enhancer	NE	NE
26551	*Df(2R)BSC699*	48D7;48E6	NE	NE	NE
24929	*Df(2R)BSC425*	48F1;49A1	NE	NE	NE
7543	*Df(2R)Exel6061*	48F1;49A6	enhancer	NE	NE
1642	*Df(2R)vg135*	49A;49E1--2	NE	NE	NE
23688	*Df(2R)BSC305*	49A4;49A10	NE	NE	NE
24989	*Df(2R)BSC485*	49B10;49E6	suppressor	strong suppressor	strong suppressor
7869	*Df(2R)Exel7121*	49B5;49B12	weak suppressor	NE	NE
442	*Df(2R)CX1*	49C1--4;50C23--D2	strong suppressor	strong suppressor	strong suppressor
7544	*Df(2R)Exel6062*	49E6;49F1	NE	NE	NE or weak enhancer
7871	*Df(2R)Exel8057*	49F1;49F10	suppressor	NE	NE
23169	*Df(2R)BSC273*	49F4;50A13	NE	NE	suppressor
23170	*Df(2R)BSC274*	50A7;50B4	NE	NE	NE
23690	*Df(2R)BSC307*	50B6;50C18	NE	suppressor	suppressor
24385	*Df(2R)BSC361*	50C3;50F1	NE	NE	NE
24407	*Df(2R)BSC383*	50C6;50D2	NE	suppressor	suppressor
7875	*Df(2R)Exel7130*	50D4;50E4	NE	NE	NE
7876	*Df(2R)Exel7131*	50E4;50F6	NE	NE	NE
8913	*Df(2R)ED2354*	50E6;51B1	NE	suppressor	NE
7749	*Df(2R)Exel6284*	51B1;51C2	NE	NE	enhancer

Continued Table B.II.1

Stock #	Deficiency lines	Cytogenetic breakpoints	*nub>CDK8+* backrgound	*nub>CDK8-RNAi* background	*nub>CycC-RNAi* background
24933	*Df(2R)BSC429*	51C2;51D1	NE	NE	weak enhancer
25741	*Df(2R)BSC651*	51C5;51E2	NE	NE	NE
9064	*Df(2R)ED2426*	51E2;52B1	NE	NE	NE
8914	*Df(2R)ED2436*	51F11;52D11	NE	NE	NE
8915	*Df(2R)ED2457*	52D11;52E7	lethal	NE	weak enhancer
7885	*Df(2R)Exel9060*	52E11;52F1	strong suppressor	NE	NE
3521	*Df(2R)Jp6*	52E3--5;52F	NE	NE	NE
7545	*Df(2R)Exel6063*	52F6;53C4	suppressor	suppressor	NE
25078	*Df(2R)BSC550*	53C1;53C6	NE	NE	NE or weak suppressor
7546	*Df(2R)Exel6064*	53C11;53D11	strong enhancer	suppressor	strong suppressor
7888	*Df(2R)Exel7144*	53C8;53D2	weak suppressor	NE	NE
9278	*Df(2R)ED2747*	53D11;53F8	NE	NE	NE
24356	*Df(2R)BSC331*	53D14;54A1	NE	NE	NE
7548	*Df(2R)Exel6066*	53F8;54B6	enhancer	NE	NE
24379	*Df(2R)BSC355*	54B16;54C3	NE	NE	NE
9596	*Df(2R)BSC161*	54B2;54B17	NE	NE	NE
7890	*Df(2R)Exel7149*	54C10;54D5	weak suppressor	NE	NE
24371	*Df(2R)BSC347*	54D2;54E9	NE	NE	NE
6780	*Df(2R)14H10W-35*	54E5--7;55B5--7	enhancer	strong enhancer	strong enhancer
9066	*Df(2R)ED3610*	54F1;55C8	NE	NE	suppressor
8918	*Df(2R)ED3683*	55C2;56C4	NE	NE	NE
7551	*Df(2R)Exel6069*	56B5;56C11	suppressor	NE	suppressor
9423	*Df(2R)BSC135*	56C11;56D5	NE	NE	NE
9067	*Df(2R)ED3728*	56D10;56E2	NE	NE	NE
6647	*Df(2R)BSC22*	56D7--E3;56F9--12	NE	NE	NE
27354	*Df(2R)BSC782*	56D8;56D14	NE	NE	NE
25678	*Df(2R)BSC594*	56E1;56F9	NE	suppressor	suppressor
7896	*Df(2R)Exel7162*	56F11;56F16	NE	enhancer	enhancer
6609	*Df(2R)BSC19*	56F12--14;57A4	weak suppressor	NE	weak suppressor
26553	*Df(2R)BSC701*	56F15;57A9	NE	NE	NE
26554	*Df(2R)BSC702*	57A2;57B3	NE	NE	NE
9267	*Df(2R)ED3791*	57B1;57D4	NE	NE	NE
3469	*Df(2R)PK1*	57C5;57F5--6	weak enhancer	enhancer	strong enhancer
27582	*Df(2R)BSC821*	57D10;57E6	NE	NE	enhancer
26516	*Df(2R)BSC664*	57D12;58A3	NE	suppressor	NE
25430	*Df(2R)BSC597*	58A2;58F1	suppressor	strong enhancer	enhancer
7903	*Df(2R)Exel7173*	58D4;58E5	NE	strong enhancer	enhancer
25431	*Df(2R)BSC598*	58F3;59A1	NE	NE	weak suppressor
27359	*Df(2R)BSC787*	58F4;59B1	NE	NE	NE
3909	*Df(2R)59AD*	59A1--3;59D1--4	NE	strong enhancer	strong enhancer
25432	*Df(2R)BSC599*	59B1;59B3	NE	suppressor	suppressor
27356	*Df(2R)BSC784*	59B4;59B6	NE	enhancer	enhancer
26866	*Df(2R)BSC769*	59B7;59D9	NE	NE	NE or weak suppressor
26513	*Df(2R)BSC661*	59D8;59F5	weak suppressor	NE	NE
9424	*Df(2R)BSC136*	59F5;60B6	suppressor	suppressor	strong suppressor
24380	*Df(2R)BSC356*	60B8;60C4	NE	strong enhancer	NE
27352	*Df(2R)BSC780*	60C2;60D14	strong suppressor	strong enhancer	strong enhancer
7561	*Df(2R)Exel6082*	60C4--60C7	suppressor	enhancer	enhancer
25436	*Df(2R)BSC603*	60C7--60D1	strong suppressor	enhancer	enhancer
25437	*Df(2R)BSC604*	60D4;60E11	NE	NE	suppressor
25441	*Df(2R)BSC608*	60E11;60F2	NE	NE	NE
2471	*Df(2R)M60E*	60E2--3;60E11--12	weak suppressor	NE	enhancer
2528	*Df(2R)gsb*	60E9--10;60F1--2	NE	NE	NE

Continued Table B.II.1

Stock #	Deficiency lines	Cytogenetic breakpoints	*nub>CDK8+* backrgound	*nub>CDK8-RNAi* background	*nub>CycC-RNAi* background
4961	*Df(2R)Kr10*	60F1;60F5	NE	lethal	NE
24758	*Df(2R)ED50004*	60F5;60F5	NE	suppressor	suppressor
24627	*Df(3L)ED50002*	61A1;61B1	NE	NE or suppressor	NE
8047	*Df(3L)ED201*	61B1;61C1	NE	NE	NE
24386	*Df(3L)BSC362*	61C1;61C7	NE	suppressor	NE
8049	*Df(3L)ED4191*	61C3;62A2	NE	NE	NE
23674	*Df(3L)BSC289*	61F6;62A9	enhancer	NE	NE or weak suppressor
9693	*Df(3L)BSC181*	62A11;62B7	strong enhancer	NE	NE or weak suppressor
27372	*Df(3L)BSC800*	62A9;62A9	NE	NE	NE
5411	*Df(3L)Aprt-32*	62B1;62E3	strong enhancer	NE	enhancer
8096	*Df(3L)ED4287*	62B4;62E5	strong enhancer	NE	NE
8976	*Df(3L)BSC119*	62E7;62F5	NE	enhancer	weak enhancer
6755	*Df(3L)BSC23*	62E8;63B5--6	NE	NE	NE
3650	*Df(3L)M21*	62F;63D	strong suppressor	suppressor	suppressor
7571	*Df(3L)Exel6092*	62F5;63A3	NE	NE	NE
26523	*Df(3L)BSC671*	63A2;63B11	NE	NE	weak enhancer
26524	*Df(3L)BSC672*	63A7;63B12	weak suppressor	NE or weak enhancer	NE
8058	*Df(3L)ED4293*	63C1;63C1	NE	NE	NE
8059	*Df(3L)ED208*	63C1;63F5	NE	NE	NE
7573	*Df(3L)Exel6094*	63D2;63E1	NE	enhancer	enhancer
7574	*Df(3L)Exel6095*	63E1;63E3	weak suppressor	suppressor	NE
24392	*Df(3L)BSC368*	63F1;64A4	NE	NE	NE
7577	*Df(3L)Exel6098*	63F2;63F7	weak suppressor	suppressor	NE
8060	*Df(3L)ED4341*	63F6;64B9	NE	NE	NE
8061	*Df(3L)ED210*	64B9;64C13	NE	NE	NE
3096	*Df(3L)ZN47*	64C;65C	strong enhancer	NE	NE
24395	*Df(3L)BSC371*	64C1;64E1	suppressor	NE or weak suppressor	NE
7585	*Df(3L)Exel6106*	64D6;64E2	NE	NE	enhancer
7586	*Df(3L)Exel6107*	64E5;64F5	NE	NE	NE
24914	*Df(3L)BSC410*	64E7;65B3	NE	NE	NE
24915	*Df(3L)BSC411*	65A2;65C1	NE	NE	NE
7588	*Df(3L)Exel6109*	65C3;65D3	enhancer	NE	NE
6867	*Df(3L)BSC27*	65D4--5;65E4--6	NE	NE	NE
9701	*Df(3L)BSC224*	65D5;65E6	suppressor	NE	NE
6964	*Df(3L)BSC33*	65E10--F1;65F2--6	NE	NE	NE
8974	*Df(3L)BSC117*	65E9;65F5	suppressor	NE	suppressor
7929	*Df(3L)Exel8104*	65F7;66A4	NE	NE	NE
7745	*Df(3L)Exel6279*	66A17;66B5	weak enhancer	enhancer	NE
24399	*Df(3L)BSC375*	66A3;66A19	NE	weak enhancer	NE or weak enhancer
24412	*Df(3L)BSC388*	66A8;66B11	suppressor	NE	suppressor
7591	*Df(3L)Exel6112*	66B5;66C8	NE	NE	NE
24413	*Df(3L)BSC389*	66C12;66D8	suppressor	enhancer	enhancer
27576	*Df(3L)BSC815*	66C3;66D4	weak suppressor	NE	NE or weak enhancer
8066	*Df(3L)ED4421*	66D12;67B3	NE	weak suppressor	suppressor
27577	*Df(3L)BSC816*	66D9;66D12	weak suppressor	enhancer	strong enhancer
7079	*Df(3L)BSC35*	66F1--2;67B2--3	suppressor	suppressor	weak suppressor
997	*Df(3L)AC1*	67A2;67D11--13	strong enhancer	enhancer	enhancer
8970	*Df(3L)BSC113*	67B1;67B5	NE	NE	NE
8975	*Df(3L)BSC118*	67B11;67C5	NE	NE	suppressor
24415	*Df(3L)BSC391*	67B7;67C5	NE	enhancer	enhancer
24416	*Df(3L)BSC392*	67C4;67D1	suppressor	NE or weak enhancer	NE
26525	*Df(3L)BSC673*	67C7;67D10	suppressor	enhancer	weak enhancer
9355	*Df(3L)ED4457*	67E2;68A7	NE	NE	NE
8068	*Df(3L)ED4470*	68A6;68E1	NE	NE	NE
8069	*Df(3L)ED4475*	68C13;69B4	suppressor	NE	NE
26828	*Df(3L)BSC730*	68F7;69E6	weak suppressor	weak suppressor	NE
8072	*Df(3L)ED4486*	69C4;69F6	NE	suppressor	suppressor

Continued Table B.II.1

Stock #	Deficiency lines	Cytogenetic breakpoints	*nub>CDK8+* backrgound	*nub>CDK8-RNAi* background	*nub>CycC-RNAi* background
6457	*Df(3L)BSC12*	69F6--70A1;70A1--2	NE	suppressor	weak suppressor
8097	*Df(3L)ED4502*	70A3;70C10	NE	NE	NE
8073	*Df(3L)ED4543*	70C6;70F4	NE	NE	NE
8074	*Df(3L)ED217*	70F4;71E1	NE	enhancer	enhancer
24946	*Df(3L)BSC442*	71D2;71E3	weak suppressor	NE	NE
27888	*Df(3L)BSC845*	71D3;72A1	suppressor	NE	NE
27346	*Df(3L)BSC774*	71F1;72D10	suppressor	NE	NE
24947	*Df(3L)BSC443*	72B1;72E4	suppressor	NE	pupal lethal
8078	*Df(3L)ED4606*	72D4;73C4	NE	NE	NE
8098	*Df(3L)ED4674*	73B5;73E5	strong enhancer	enhancer	enhancer
8099	*Df(3L)ED4685*	73D5;74E2	NE	NE	NE
8100	*Df(3L)ED4710*	74D1;75B11	NE	NE	weak suppressor
27347	*Df(3L)BSC775*	75A2;75E4	NE	NE	NE
9697	*Df(3L)BSC220*	75F1;76A1	weak suppressor	weak enhancer	NE
8087	*Df(3L)ED229*	76A1;76E1	strong suppressor	suppressor	NE
6646	*Df(3L)BSC20*	76A7--B1;76B4--5	suppressor	NE	suppressor
7943	*Df(3L)Exel9008*	76B3--4;76B9	NE	strong suppressor	NE
7944	*Df(3L)Exel9009*	76B5;76B9	suppressor	suppressor	NE
7945	*Df(3L)Exel9011*	76B8;76B9	suppressor	weak enhancer	enhancer
8088	*Df(3L)ED4858*	76D3;77C1	NE	NE	weak enhancer
27369	*Df(3L)BSC797*	77C3;78A1	NE	NE	NE
24953	*Df(3L)BSC449*	77F2;78C2	weak suppressor	NE	NE
25116	*Df(3L)BSC553*	78A2;78C2	suppressor	NE	weak suppressor
24923	*Df(3L)BSC419*	78C2;78D8	NE	enhancer	enhancer
8101	*Df(3L)ED4978*	78D5;79A2	NE	NE	NE
9700	*Df(3L)BSC223*	79A3;79B3	suppressor	NE	NE
24955	*Df(3L)BSC451*	79B2;79F5	NE	NE	NE
8089	*Df(3L)ED230*	79C2;80A4	NE	NE	enhancer
7617	*Df(3L)Exel6138*	79D3;79E3	NE	enhancer	NE
8102	*Df(3L)ED5017*	80A4;80C2	NE	NE	NE
7002	*Df(3L)1-16*	80F;80F	enhancer	NE	suppressor
9226	*Df(3R)ED5100*	81F6;82E7	NE	weak suppressor	NE
2596	*Df(3L)6B-29+Df(3R)6B-29*	81Fa;81Fa	suppressor	enhancer	enhancer
2597	*Df(3R)10-65*	81Fa;81Fa	suppressor	NE	NE
8967	*Df(3R)ED5147*	82E7;83A1	NE	enhancer	NE
8965	*Df(3R)ED5156*	82F8;83A4	NE	NE	NE
7623	*Df(3R)Exel6144*	83A6-83A6	strong suppressor	enhancer	enhancer
25077	*Df(3R)BSC549*	83A6;83B6	NE	enhancer	strong enhancer
8103	*Df(3R)ED5177*	83B4;83B6	NE	enhancer	enhancer
7443	*Df(3R)BSC47*	83B7--C1;83C6--D1	suppressor	NE	NE
7952	*Df(3R)Exel7283*	83B7;83C2	suppressor	weak enhancer	NE
24968	*Df(3R)BSC464*	83B7;83E1	NE	NE	NE
1990	*Df(3R)Tpl10*	83C1--2;84B1--2	enhancer	NE	weak suppressor
7624	*Df(3R)Exel6145*	83C1;83C4	strong enhancer	suppressor	enhancer
26533	*Df(3R)BSC681*	83E2;83E5	NE	NE	NE
26836	*Df(3R)BSC738*	83E5;84A1	weak suppressor	NE	enhancer
24971	*Df(3R)BSC467*	83F1;84B2	suppressor	NE	NE
1842	*Df(3R)Antp17*	84A5;84D9	NE	NE	NE
25724	*Df(3R)BSC633*	84B2;84C3	NE	NE	weak suppressor
8685	*Df(3R)ED7665*	84B4;84E11	NE	NE	NE
24970	*Df(3R)BSC466*	84E1;85A10	strong enhancer	enhancer	NE or weak enhancer
9077	*Df(3R)ED5330*	85A5;85D1	weak enhancer	strong enhancer	strong enhancer
7631	*Df(3R)Exel6152*	85C11;85D2	suppressor	NE	NE
9204	*Df(3R)ED5339*	85D1;85D11	NE	weak suppressor	NE
24980	*Df(3R)BSC476*	85D16;85D24	NE	NE	NE
7731	*Df(3R)Exel6264*	85D24;85E5	enhancer	NE	NE
25011	*Df(3R)BSC507*	85D6;85D15	NE	NE	suppressor

Continued Table B.II.1

Stock #	Deficiency lines	Cytogenetic breakpoints	*nub>CDK8+* backrgound	*nub>CDK8-RNAi* background	*nub>CycC-RNAi* background
9078	*Df(3R)ED5438*	85E5;85F8	weak enhancer	NE	NE
7633	*Df(3R)Exel6154*	85E9;85F1	weak suppressor	enhancer	NE
7634	*Df(3R)Exel6155*	85F1;85F10	NE	NE	NE
9082	*Df(3R)ED5474*	85F11;86B1	NE	suppressor	suppressor
9215	*Df(3R)ED5495*	85F16;86C7	enhancer	suppressor	suppressor
25696	*Df(3R)BSC621*	85F5;85F14	NE	NE	NE
7636	*Df(3R)Exel6157*	86B1;86B2--86B3	lethal	weak enhancer	NE
25126	*Df(3R)BSC568*	86C7;86D7	NE	NE	NE
8957	*Df(3R)ED5514*	86C7;86E11	strong enhancer	NE	NE
24973	*Df(3R)BSC469*	86D8;87A2	suppressor	NE	weak enhancer
7965	*Df(3R)Exel7310*	86E18;87A1	suppressor	strong enhancer	enhancer
8029	*Df(3R)ED5577*	86F9;87B13	NE	NE	weak enhancer
24990	*Df(3R)BSC486*	87B10;87E9	suppressor	NE	enhancer
7931	*Df(3R)Exel7315*	87B8;87B9	NE	enhancer	NE
7973	*Df(3R)Exel8157*	87D8;87D10	NE	strong suppressor	suppressor
8921	*Df(3R)ED5623*	87E3;88A4	NE	weak enhancer	NE
7649	*Df(3R)Exel6170*	87F10;87F14	strong enhancer	suppressor	enhancer
7976	*Df(3R)Exel8159*	88A4;88B1	suppressor	enhancer	enhancer
9090	*Df(3R)ED5644*	88A4;88C9	suppressor	weak enhancer	NE
7734	*Df(3R)Exel6267*	88B1;88C2	weak suppressor	weak enhancer	NE
23714	*Df(3R)ED10555*	88C9;88D8	NE	NE	NE
7742	*Df(3R)Exel6275*	88D1;88D7	NE	NE	NE
24137	*Df(3R)ED5664*	88D1;88E3	strong suppressor	NE	NE
9152	*Df(3R)ED5705*	88E12;89A5	NE	NE	NE
26848	*Df(3R)BSC750*	88E2;88E5	NE	enhancer	NE
26839	*Df(3R)BSC741*	88E8;88F1	suppressor	weak suppressor	NE
25019	*Df(3R)BSC515*	88F6;89A8	enhancer	enhancer	enhancer
7983	*Df(3R)Exel7328*	89A12;89B6	NE	NE	NE
26580	*Df(3R)BSC728*	89A8;89B2	suppressor	NE	NE
9482	*Df(3R)ED10642*	89B17;89D5	NE	weak suppressor	NE
7737	*Df(3R)Exel6270*	89B18;89D8	NE	NE	NE or weak enhancer
3678	*Df(3R)sbd45*	89B4;89B10	NE	NE	NE
1467	*Df(3R)P115*	89B7--8;89E7	suppressor	NE	NE
9481	*Df(3R)ED10639*	89B7;89B18	NE	suppressor	suppressor
3486	*Df(3R)Ubx109*	89D1--2;89E1--2	NE	NE	NE
7655	*Df(3R)Exel6176*	89E11;89F1	strong suppressor	weak enhancer	weak enhancer
8104	*Df(3R)ED5780*	89E11;90C1	NE	NE	weak enhancer
26846	*Df(3R)BSC748*	89E5;89E11	strong suppressor	enhancer	enhancer
27362	*Df(3R)BSC790*	90B6;90E2	NE	suppressor	suppressor
25740	*Df(3R)BSC650*	90C6;91A2	suppressor	NE	weak suppresor
7657	*Df(3R)Exel6178*	90F4;91A5	suppressor	enhancer	enhancer
9208	*Df(3R)ED5815*	90F4;91B8	weak suppressor	NE	NE
6962	*Df(3R)ED2*	91A5;91F1	NE	NE	enhancer
7659	*Df(3R)Exel6180*	91B5;91C5	NE	weak enhancer	strong enhancer
24139	*Df(3R)ED5938*	91D4;92A11	strong enhancer	NE	letahl
8964	*Df(3R)ED6025*	92A11;92E2	NE	NE	NE
25021	*Df(3R)BSC517*	92C1;92F13	NE	NE	NE
9501	*Df(3R)BSC141*	92F2;93A1	NE	suppressor	NE
7413	*Df(3R)BSC43*	92F7--93A1;93B3--6	NE	NE	NE
27580	*Df(3R)BSC819*	93A2;93B8	enhancer	NE	NE
7739	*Df(3R)Exel6272*	93A4;93B13	NE	NE	NE
9487	*Df(3R)ED10845*	93B9;93D4	NE	NE	NE
26529	*Df(3R)BSC677*	93D1;93F14	lethal	lethal	NE
8923	*Df(3R)ED6085*	93F14;94B5	enhancer	NE	weak suppressor
8684	*Df(3R)ED6096*	94B5;94E7	NE	NE	enhancer
25694	*Df(3R)BSC619*	94D10;94E13	NE	NE	NE
9497	*Df(3R)BSC137*	94F1;95A4	NE	NE	NE
24993	*Df(3R)BSC489*	94F3;95D1	NE	NE	NE

Continued Table B.II.1

Stock #	Deficiency lines	Cytogenetic breakpoints	*nub>CDK8+* backrgound	*nub>CDK8-RNAi* background	*nub>CycC-RNAi* background
7675	*Df(3R)Exel6196*	95C12;95D8	NE	NE	NE
9347	*Df(3R)ED6187*	95D10;96A7	weak enhancer	weak enhancer	NE
Stock #	Deficiency lines	Cytogenetic breakpoints	*nub>CDK8+* backrgound	*nub>CDK8-RNAi* background	*nub>CycC-RNAi* background
7676	*Df(3R)Exel6197*	95D8;95E1	NE	enhancer	NE
9211	*Df(3R)ED6220*	96A7;96C3	NE	suppressor	weak suppressor
24965	*Df(3R)BSC461*	96B15;96D1	NE	NE	weak suppressor
7680	*Df(3R)Exel6201*	96C2;96C4	NE	NE	NE
27404	*Df(3R)FDD-0317950*	96C8;96D1	suppressor	NE	NE
7681	*Df(3R)Exel6202*	96D1;96D1	NE	NE	NE or weak enhancer
7682	*Df(3R)Exel6203*	96E2;96E6	weak enhancer	NE	NE
24909	*Df(3R)BSC321*	96E6;96E9	NE	NE	NE
9500	*Df(3R)BSC140*	96F1;96F10	NE	NE	NE
8105	*Df(3R)ED6232*	96F10;97D2	NE	NE	enhancer
9210	*Df(3R)ED6255*	97D2;97F1	weak suppressor	NE	NE
25001	*Df(3R)BSC497*	97E6;98B5	NE	NE	NE
25390	*Df(3R)BSC567*	98B6;98E5	NE	lethal	lethal
7688	*Df(3R)Exel6210*	98E1;98F5	weak suppressor	NE	NE
27378	*Df(3R)BSC806*	98F1;98F10	NE	NE	NE
25005	*Df(3R)BSC501*	98F10;99B9	NE	NE	NE
3547	*Df(3R)L127*	99B5--6;99F1	weak suppressor	enhancer	enhancer
25075	*Df(3R)BSC547*	99B5;99C2	NE	NE	NE
7691	*Df(3R)Exel6213*	99C5;99D1	NE	enhancer	enhancer
25695	*Df(3R)BSC620*	99C5;99D3	suppressor	NE	enhancer
2352	*Df(3R)X3F*	99D1--2;99E1	suppressor	enhancer	enhancer
25006	*Df(3R)BSC502*	99D3;99D8	NE	NE	NE
7692	*Df(3R)Exel6214*	99D5;99E2	NE	lethal	weak enhancer
2234	*Df(3R)R133*	99E1--5;3Rt	NE	NE	NE
25007	*Df(3R)BSC503*	99E3;99F6	enhancer	NE	NE
25008	*Df(3R)BSC504*	99F4;100A2	NE	NE	NE
7997	*Df(3R)Exel7378*	99F8;100A5	NE	NE	NE
2155	*Df(3R)A113*	100A;3Rt	suppressor	strong enhancer	enhancer
7918	*Df(3R)Exel8194*	100A4;100A7	suppressor	weak enhancer	enhancer
24142	*Df(3R)ED6346*	100A5;100B1	NE	NE	NE
26847	*Df(3R)BSC749*	100B1--100C1	suppressor	NE	enhancer
27365	*Df(3R)BSC793*	100B5;100C4	NE	NE	NE
24143	*Df(3R)ED6361*	100C7;100E3	NE	NE	NE
24516	*Df(3R)ED50003*	100E1;100F5	enhancer	NE	NE
9433	*Df(4)M101-62f*	101E;102B	NE	weak suppressor	NE
9421	*Df(4)ED6364*	101F1;102A6	NE	NE	NE
9422	*Df(4)ED6369*	102A1;102C1	NE	NE	NE
9579	*Df(4)ED6380*	102B7;102D5	NE	enhancer	NE

NE, no effects.

Table B.IV.1. Primers for subcloning

Primer sequence (5' to 3')	Primer name
CACCATGGACTACGATTTCAAGAT	CDK8-N-5.1
CTACGGAAACCCCATCACATTGA	CDK8-N-3.1
CACCATGGACACGACACTGATGAAC	dSREBP-5.10
CTAGGCCCGACTACCTGTGCTTG	dSREBP-3.11
CACCATGCAGTCGTATCCGCAACCCTT	dSREBP-5.12
CTACTCCCTCTGCAGGCGCTG	dSREBP-3.12
CACCATGGACAAGATTAACGAGTTGAA	dSREBP-5.13
GAGTCCGAGGCGAGAGTG	dSREBP-3.10
CTACTGCTGATGCAGTTCCTCCT	dSREBP-3.21
CACCATGCAGATGTACAACATGCTGCT	dSREBP-5.22
CTACTGGGGCAAAGGAGCAGAAG	dSREBP-3.22
CACCATGACGGCGGTGTATCCCCCATC	dSREBP-5.23
CTAGACATCCTCCGCTTTGAACA	dSREBP-3.31
CTACGTCGGCGCCAGGTCCATGT	dSREBP-3.32
CTATTGCGGCTGCTGATCCACGG	dSREBP-3.33
GCGCCAGGTCCATGTCGTTGAGGGCGGCGGCCGCCGCGGCCGAGTGCAGGTCGGCGTCGAAC	dSREBP-mut-5.1
GTTCGACGCCGACCTGCACTCGGCCGCGGCGGCCGCCGCCCTCAACGACATGGACCTGGCGC	dSREBP-mut-3.1
ACGGATGCCGGACTGGCGCCGCCACGCAGCGAT	dSREBP-TA-5.1
ATCGCTGCGTGGCGGCGCCAGTCCGGCATCCGT	dSREBP-TA-3.1